

General Disclaimer

One or more of the Following Statements may affect this Document

- This document has been reproduced from the best copy furnished by the organizational source. It is being released in the interest of making available as much information as possible.
- This document may contain data, which exceeds the sheet parameters. It was furnished in this condition by the organizational source and is the best copy available.
- This document may contain tone-on-tone or color graphs, charts and/or pictures, which have been reproduced in black and white.
- This document is paginated as submitted by the original source.
- Portions of this document are not fully legible due to the historical nature of some of the material. However, it is the best reproduction available from the original submission.

FINAL TECHNICAL REPORT
VOLUME II
DIGIMEM
OPTICAL MASS MEMORY
INVESTIGATIONS

CONTRACT NUMBER NAS8-30564
(NASA-CR-150360) DIGIMEM, OPTICAL MASS
MEMORY INVESTIGATIONS, VOLUME 2 Final
Report (Harris Corp., Melbourne, Fla.)
175 p HC A08/MF A01

N79-25774

CSCI 09B

Unclas

G3/60

26865

JUNE 1977



FOR
GEORGE C. MARSHALL SPACE FLIGHT CENTER
NATIONAL AERONAUTICS AND SPACE ADMINISTRATION
MARSHALL SPACE FLIGHT CENTER, ALABAMA 38512

BY
ELECTRO-OPTICS DEPARTMENT

89678



HARRIS
COMMUNICATIONS AND
INFORMATION HANDLING

HARRIS CORPORATION Electronic Systems Division
P.O. Box 37, Melbourne, Florida 32901 305/727-4000

**FINAL TECHNICAL REPORT
VOLUME II**

DIGIMEM

**OPTICAL MASS MEMORY
INVESTIGATIONS**

CONTRACT NUMBER NAS8-30564

JUNE 1977

FOR

**GEORGE C. MARSHALL SPACE FLIGHT CENTER
NATIONAL AERONAUTICS AND SPACE ADMINISTRATION
MARSHALL SPACE FLIGHT CENTER, ALABAMA 38512**

BY

ELECTRO-OPTICS DEPARTMENT



TABLE OF CONTENTS

<u>Section</u>		<u>Page</u>
	SUMMARY	
	FOREWORD	
	ACKNOWLEDGEMENTS	
I	INTRODUCTION AND BACKGROUND	1-2
	1.1 A TRANSITION	1-2
	1.2 DIGIMEM: AN OVERVIEW	1-3
II	REQUIREMENTS FOR ARCHIVAL STORAGE AND RETRIEVAL ...	2-2
	2.1 COST AND PERFORMANCE FACTORS	2-3
	2.1.1 Storage Material Cost and Packing Density	2-3
	2.1.2 Storage Space Requirements	2-4
	2.1.3 Maintenance of Data Quality	2-4
	2.1.4 Supplying Users With Data From the Archival Base	2-6
	2.1.5 Browse Capability	2-6
	2.1.6 Data Input/Output Rates	2-7
	2.2 TECHNOLOGICAL DEVELOPMENTS	2-8
	2.3 COMMENTS AND RECOMMENDATIONS	2-9
	2.4 REFERENCES	2-11
III	DIGIMEM BREADBOARD RECORDER/REPRODUCER	3-2
	3.1 BREADBOARD SYSTEM CONCEPTS	3-2
	3.2 IMPACTS OF BASELINE SPECIFICATIONS	3-5
	3.3 SPECIAL COMPONENTS/SUBSYSTEMS	3-11
	3.3.1 Electronic Subsystems	3-11
	3.3.2 Mechanical Subsystems	3-21
	3.3.3 Optical Subsystems	3-29



TABLE OF CONTENTS (Continued)

<u>Section</u>	<u>Page</u>
3.4 BREADBOARD EXPERIMENTS	3-42
3.4.1 The Film Transport	3-42
3.4.2 Data Wander Correction and Tracking	3-45
3.4.3 Key Optical Components	3-46
3.5 RECORDING EXPERIMENTS	3-49
3.5.1 Film Curl	3-49
3.5.2 Microscopic Spot Shifting	3-50
3.5.3 Bleaching of the Sensitizing Dye in SO-173 Film	3-53
3.5.4 Spot Recording	3-55
3.6 READOUT EXPERIMENTS	3-61
3.7 REPLICATION EXPERIMENTS	3-67
3.8 COMPARISON OF BREADBOARD RESULTS TO DESIGN GOALS	3-70
3.9 REFERENCES	3-72
IV TRANSPARENT ELECTROPHOTOGRAPHIC FILM STUDY	4-2
4.1 INTRODUCTION	4-2
4.2 GENERAL DESCRIPTION AND CONSTRUCTION	4-3
4.3 INFORMATION STORAGE MECHANISM AND PROCESSING	4-4
4.4 EXPERIMENTAL EVALUATION	4-10
4.4.1 Experimental Apparatus	4-10
4.4.2 Experimental Procedure	4-12
4.4.3 Sensitometry	4-15
4.4.4 Diffraction Efficiency	4-15
4.4.5 Frequency Response	4-26
4.4.6 Storage Density	4-26
4.4.7 Contact Printing	4-36



HARRIS

ELECTRO-OPTICS

iii

TABLE OF CONTENTS (Continued)

<u>Section</u>		<u>Page</u>
	4.5 DISCUSSION, COMMENTS, AND CONCLUSIONS	4-39
	4.6 REFERENCES	4-41
V	DATA BASE MANAGEMENT CONSIDERATIONS	5-2
	5.1 GENERAL CONSIDERATIONS	5-2
	5.1.1 Data Storage	5-3
	5.1.2 Data Displays and Recorders	5-4
	5.1.3 Data Processing	5-5
	5.2 PRELIMINARY DATA BASE MANAGEMENT/END-USER SURVEY	5-6
	5.2.1 Summary of Survey Data	5-6
	5.2.2 Specific Example: Goddard Space Flight Center ..	5-8
	5.2.3 Conclusions	5-11
VI	CONCLUSIONS AND RECOMMENDATIONS	6-2
APPENDICES		
A	THE WRITE CONTROL ELECTRONICS	A-1/2
B	THE READOUT CONTROL ELECTRONICS	B-1/2



HARRIS

ELECTRO-OPTICS

iv

LIST OF ILLUSTRATIONS

<u>Figure</u>		<u>Page</u>
3-1	The Breadboard Block Diagram	3-3
3-2	The Acousto-Optic Page Composer	3-7
3-3	The Breadboard Film Format	3-8
3-4	The Breadboard Data Format	3-10
3-5	The Write Control Electronics	3-13
3-6	The Readout Control Electronics	3-19
3-7	Depth-of-Focus as a Function of Spot Diameter (For Recording With 632.8 nm Laser Light)	3-23
3-8	The Floppy Disk Film Transport	3-25
3-9	Air Bearing Schematic (Side View)	3-26
3-10	The Tracking Subsystem	3-28
3-11	The DIGIMEM Breadboard (Top View)	3-30
3-12	The DIGIMEM Breadboard (Side View)	3-31
3-13	Aerial Spot Intensity as a Function of Spot Diameter	3-36
3-14	The Readout Optics Configuration	3-41
3-15	SO-173 Base Sensitizing Dye Density as a Function of Soaking Time in 0.5 Percent Clorox Solution	3-54
3-16	Kodak 649F Microfiche Transport Spot Recordings (2.0 μ m Spot Centers)	3-56
3-17	Conventionally Processed Spot Recordings on SO-173 Film (3.5 μ m Spot Centers)	3-58
3-18	Spot Size as a Function of Exposure on SO-173 Film (For 2 μ s Exposures and an Aerial Spot Diameter of 3.5 μ m)	3-59
3-19	Reversal-Processed Spot Recordings on SO-173 Film (3.5 μ m Spot Centers)	3-62
3-20	The Electronically Agile Photodetector Array	3-64
3-21	Oscilloscope Readout of Recorded DIGIMEM Spots From the Electronically Agile Photodetector Array	3-65
3-22	The DIGIMEM Breadboard System	3-66



HARRIS

ELECTRO-OPTICS

v

LIST OF ILLUSTRATIONS (Continued)

<u>Figure</u>		<u>Page</u>
3-23	Master and Replicated Copies of DIGIMEM Recordings	3-68
3-24	The Effects of Dirt and Air Pockets on Replicated DIGIMEM Recordings	3-69
4-1	Construction of a Transparent Electrophotographic (TEP) Film	4-5
4-2	The Basic Steps of Image Formation on a Negative-Working TEP Film	4-7
4-3	Mach-Zehnder Interferometer Used for Recording Holograms on TEP Film	4-11
4-4	Liquid Parallel-Plate Processing Cell Used for Electro- development of TEP Films	4-13
4-5	Schematic Representation of TEP Development for Positive and Negative Imaging Modes (Square-Wave Exposure Assumed)	4-14
4-6	Amplitude Transmittance T_A as a Function of Exposure E for TEP P5-003	4-16
4-7	Amplitude Transmittance T_A as a Function of Exposure E for TEP P4-005	4-17
4-8	Density D as a Function of Exposure E for TEP P5-003 (D-Log E Curve)	4-18
4-9	Density D as a Function of Exposure E for TEP P4-005 (D-Log E Curve)	4-19
4-10	Diffraction Efficiency DE as a Function of Exposure E for TEP P5-003	4-21
4-11	Diffraction Efficiency DE as a Function of Exposure E for P4-005	4-22
4-12	Diffraction Efficiency DE as a Function of Exposure E for TEP P5-003	4-23
4-13	Diffraction Efficiency DE as a Function of Exposure E for TEP P4-005	4-24
4-14	Maximum Diffraction Efficiency as a Function of Spatial Frequency for TEP P5-003	4-27



LIST OF ILLUSTRATIONS (Continued)

<u>Figure</u>		<u>Page</u>
4-15	Maximum Diffraction Efficiency as a Function of Spatial Frequency for TEP P4-005	4-28
4-16	Diffraction Efficiency DE and Signal-to-Noise Ratio SNR as Functions of Exposure E for Unfixed TEP P5-003 With K=2	4-30
4-17	Diffraction Efficiency DE and Signal-to-Noise Ratio SNR as Functions of Exposure E for Unfixed TEP P5-003 With K=10 ...	4-31
4-18	Diffraction Efficiency DE and Signal-to-Noise Ratio SNR as Functions of Exposure E for Unfixed TEP P5-003 With K=25 ...	4-32
4-19	Diffraction Efficiency DE and Signal-to-Noise Ratio SNR as Function of Exposure E for Unfixed TEP P4-005 With K=2	4-33
4-20	Diffraction Efficiency DE and Signal-to-Noise Ratio SNR as Functions of Exposure E for Unfixed TEP P4-005 With K=10 ...	4-34
4-21	Diffraction Efficiency DE and Signal-to-Noise Ratio SNR as Functions of Exposure E for Unfixed TEP P4-005 With K=25 ...	4-35
4-22	Diffraction Efficiency DE and Signal-to-Noise SNR as Functions of Exposure E for TEP P4-005 After Fixation With K=10	4-37
4-23	Diffraction Efficiency DE and Signal-to-Noise SNR as Functions of Exposure for TEP P4-005 With Index Matching With K=10 ..	4-38
A-1	The Write Control Electronics, Part 1	A-2
A-2	The Write Control Electronics, Part 2	A-3
A-3	The Write Control Electronics, Part 3	A-4
B-1	The Readout Control Electronics, Part 1	B-2
B-2	The Readout Control Electronics, Part 2	B-3
B-3	The Readout Control Electronics, Part 3	B-4
B-4	The Readout Control Electronics, Part 4	B-5



HARRIS

ELECTRO-OPTICS

vii

LIST OF TABLES

<u>Table</u>		<u>Page</u>
3-1	Selected Reduction Lens Candidates	3-34
3-2	Selected Eastman Kodak Photographic Films for Spot Recording	3-38
3-3	Percent Distortion of SO-173 Emulsion and Film Base for Various Development and Environmental Conditions	3-52
3-4	Reversal Process 2460	3-60
3-5	Summary of DIGIMEM Breadboard Results	3-71
4-1	Performance Consistency Data for Scott Graphics TEP Film	4-25
5-1	Summary of Data Base Management/End-User Survey Activity ..	5-7
5-2	NASA Goddard SFC Near-Term Mass Storage System Requirements	5-12



HARRIS

ELECTRO-OPTICS

SUMMARY

The DIGIMEM phase of the Optical Mass Memory Investigations Program addressed problems related to the analysis, design, and implementation of a direct digital optical recorder/reproducer. The objective of the present study was a delineation of advantages, disadvantages and limitations of optical spot recording as a means of high-density information storage and retrieval. The goal of this effort is the development of an operational archival mass storage system to support one or more key NASA missions.

The primary activity of the DIGIMEM program phase was the design, fabrication, and test and evaluation of a breadboard digital optical recorder/reproducer. Starting with technology and subsystems perfected during the HOLOMEM program phase, we evaluated a fully operational optical spot recording breadboard that met or exceeded all program goals. Specific accomplishments worthy of note are:

- Recording and reading out eight binary data channels simultaneously with an electronically agile photodetector array
- Recording and reading out at a rate of 1 Mb/s
- Recording and reading out at an information storage density of 50 Mb/in²
- Recording and reading out in both human-read and machine-read formats
- Demonstrating 72 hours of continuous, unattended readout
- Recording on a commercial photographic film without special handling or processing
- Replication of complete unit records in a single step

In addition, we performed a thorough evaluation of several high resolution electrophotographic recording films and completed a preliminary data base management/end-user requirements survey.

The DIGIMEM program phase demonstrates the feasibility of bringing to operational status in the early 1980's an archival optical mass memory system based on direct digital optical spot recording. Current technology, appropriately engineered, is sufficient to achieve this goal. No research breakthrough need be scheduled.

The DIGIMEM approach provides an attractive approach for the development of large mass stores with capacities in the 10^{12} to 10^{15} bit range. We recommend that the DIGIMEM effort be continued with an emphasis on critical component design, system architecture, and data base management.



HARRIS

ELECTRO-OPTICS

FOREWORD

This report was prepared by the Electro-Optics Department of the Electronic Systems Division of Harris Corporation. It documents technical effort on the DIGIMEM phase of NASA Contract NAS8-30564, entitled "Optical Mass Memory Investigations," between 14 May 1976 and 29 June 1977. Mr. G. A. Bailey, Marshall Space Flight Center, was the project engineer and COTR.

The principal investigator and program manager for this program phase was Dr. R. G. Zech. B. R. Reddersen was systems engineer. Task leaders were D. C. Bailey, J. E. Holmes, G. A. Neal, and L. M. Ralston. Important design and experimental contributions were made by D. E. Trimble. Data base management support was provided by W. Huckleby and J. Spikes, Engineering Software Systems Department.

Contributors to this report are L. M. Ralston, B. R. Reddersen, Dr. H. N. Roberts, and Dr. R. G. Zech. Dr. Zech is the technical editor, and is responsible for the content and format of the report.

Technical direction and research and development personnel were provided by the Optical Processing and Storage Section (Dr. H. N. Roberts, Section Head). Program monitoring was the responsibility of the Program/Systems Management Section (R. H. Nelson, Section Head). The Electro-Optics Department is under the general direction of Dr. A. Vander Lugt.

The publication date of this report is June 1977.



HARRIS

ELECTRO-OPTICS

ACKNOWLEDGEMENTS

We are pleased to acknowledge the advice, cooperation, and insight provided by the following:

- Mr. G. A. Bailey, Dr. B. Moore, and Mr. E. J. Reinbolt
NASA Marshall Space Flight Center
Huntsville, AL
- Mr. H. Alsberg, Mr. C. Catoe, and Mr. H. Ernst
NASA Headquarters
Washington, D.C.
- Mr. John Sos
Goddard Space Flight Center
Greenbelt, MD
- Mr. C. Krpec
Johnson Space Center
Houston, TX
- Mr. A. H. Watkins, and Staff
EROS Data Center
Sioux Falls, SD
- Dr. J. F. Dirks and Mr. J. Paulin
Scott Graphics Incorporated
Holyoke, MA
- Mr. F. E. Dailey, Jr.
Image Technology and Application
Wilbraham, MA



HARRIS

ELECTRO-OPTICS

1

SECTION I

INTRODUCTION AND BACKGROUND



SECTION I

INTRODUCTION AND BACKGROUND

This final technical report summarizes analysis, design and breadboard test and evaluation activities directed toward the development of a direct digital optical recorder/reproducer (optical spot recorder). The ultimate goal of this activity is the evaluation of a new generation of archival mass storage system. The key subsystem is to be the high-speed, high-density direct digital optical recorder/reproducer whose feasibility was demonstrated during this program phase. The overall system concept is referred to as DIGIMEM throughout this volume and Volume IV of the report.

The report consists of five sections. Section I is a general introduction. Section II is a brief technology overview and problem definition. Section III is a summary of analysis, design and test and evaluation activities in support of the development of a high-density direct digital optical recorder/reproducer. Section IV is a presentation of the properties and experimental characteristics of an electrophotographic recording media with significant potential for optical spot recording. Section V is a discussion of data base management considerations, including the results of an end-user survey. Finally, Section VI is a synopsis of program results, conclusions, and recommendations.

1.1 A TRANSITION

In Volume I of this report we described research and development work directed toward the creation of a high-speed, high-density holographic recorder/reproducer, or HOLOMEM. We noted there that the new approach represented an important concept transition for the evolution of read/write mass memory for space applications; that is, a change from a no moving parts, block-oriented volume hologram memory to a some moving parts, tape or fiche-oriented one dimensional planar hologram memory. In this volume of the report we document a notable technology and an end-application transition. The new technical approach is direct digital optical spot recording and the new application is a



ground-based archival mass storage system. The near-term goal is the development of a high-speed, high-density direct digital optical recorder/reproducer, or DIGIMEM.

A fair question at this point is: Why such a radical change? The negative part of the answer is simple. First, the state of the art of holographic recorder/reproducers does not permit the design, fabrication, and insertion of this type of system in space. Weight, volume, and power requirements are currently incompatible with most space missions, including Space Shuttle. Reliability is another problem area. The need for a high performance read/write recording material is a further consideration. Second, at this time no critical application can be identified. On-board feature extraction for remote sensing data is an attractive application, if a holographic memory can be formatted for high-speed parallel processing. However, the need is not urgent. The positive part of the answer is equally simple. First, existing technology is sufficient for the near term development to operational status of a very high-capacity archival mass storage system. No R&D breakthroughs need be scheduled. Being ground-based, the constraints on volume, weight and power consumption of a space application are removed. The recording material problem becomes moot since there are several well-qualified read-only archival storage media. Second, there is a demonstrated need for a high-density, high-capacity mass storage system. The applications profile include: the storage of remote sensing data; historical records; mission support data for deep space probes; weather, ocean and atmosphere records; and so forth. Potential end-users of mass storage systems are: NASA; NOAA; The Department of Defense (e.g., the Defense Mapping Agency); Departments of the Interior (e.g., USGS and the EROS Data Center), Agriculture (e.g., Forestry Service), Treasury (e.g., the IRS), and HEW (e.g., the Social Security Administration); the Library of Congress; the National Archives; and the larger private insurance and banking corporations.

1.2 DIGIMEM: AN OVERVIEW

DIGIMEM is a systems concept for the development of a high-density, high-capacity archival optical mass storage system. The baseline technology is a high-speed, high-density direct digital optical recorder/reproducer. Depending on the end-user, the



HARRIS

ELECTRO-OPTICS

1-4

system concept could include a wideband downlink recorder, computer interfaces, soft copy displays (e.g., high resolution CRT), a browse capability, hard copy generators (e.g., laser recorder, laser facsimile or acoustic travelling wave scanner), remote terminals and so forth. The actual system configuration will be determined by the ultimate end-user, who for the present and in Volume III of this report is assumed to be a generator, processor, and user of remote sensing data. Systems considerations are considered in detail in Volume III. Here the emphasis is on the DIGIMEM direct digital optical recorder/reproducer.

The performance of a fully operational DIGIMEM can be estimated from the results of the optical spot recorder breadboard experiments reported in Section III of this volume. Basically, we designed and fabricated a floppy disc laser spot recorder that achieved the following: 8-channel byte-oriented parallel record and readout; 1 Mb/s record and readout rates; 50 Mb/in² information storage density on a commercial photographic film; human and machine record and read formats; and 72 hours of continuous unattended operation. The present study has demonstrated the feasibility of implementing a direct digital optical recorder/reproducer, using currently available technology, with the following performance: 128-channel parallel record and readout; 10-20 Mb/s record and readout rates; and 150 Mb/in² information storage density. The combination of this level of storage and retrieval performance with appropriate unit record transports, computer interfaces and data base management provides a realistic basis for the overall development of an archival optical mass storage system.

We expand and develop this background throughout the remaining sections of this volume and Volume III.



HARRIS

ELECTRO-OPTICS

2-1

SECTION II

REQUIREMENTS FOR ARCHIVAL STORAGE AND RETRIEVAL



HARRIS

ELECTRO-OPTICS

2-2

SECTION II

REQUIREMENTS FOR ARCHIVAL STORAGE AND RETRIEVAL

Data which must be archivally stored are accumulating at ever increasing rates. Data processing is used in some applications to reduce the amount of data which must be stored, while preserving all essential information contained in the arriving data. However, the rate at which data will be received at ground stations in the future is expected to exceed considerably the rate at which data compaction ratios can be improved through the use of various data processing algorithms. Therefore, the requirements for large capacity data storage systems will continue for several decades.

High-density direct digital optical data storage offers notable improvements over magnetic tapes and cylinders, as we will subsequently show. We concentrate our attention in this section on very high capacity archival data storage (10^{13} to 10^{17} bit capacities). Emerging memory technologies based on magnetic bubbles, MOS devices, electron-beam accessed MOS devices, and charge-coupled devices are not considered candidates for such high capacity archival storage systems.¹⁻⁴ Magnetic bubble memories are expected to bridge the capacity/access time gap between core memory and moving surface magnetic on-line memories (disks and tapes) by providing millisecond access times with up to 10^9 bit capacities.^{1, 2} Semiconductor (MOS³, CCD³ and BEAMOS⁴) memories with capacities above 10^{10} bits are not considered economically feasible; however, as main frame core memories, they offer nanosecond to microsecond access times with capacities projected for the 10^7 to 10^9 bit range.

Magnetic disk memories with capacities of 10^9 bits are in use today; however, expansion of magnetic disk technology in a cost-effective way above 10^{10} bit capacities is not considered feasible in the foreseeable future. Disks will continue to be heavily used as on-line memory units, particularly as a staging or buffer memory between an active mass storage system and a CPU.^{5, 6}



Half-inch magnetic tape is the mainstay for large data block storage in all medium and large computer facilities. Over 100,000 half-inch magnetic tape transport units are currently in user facilities.⁷ Any mass archival memory system will find the broadest base of users in the most cost-effective manner if it can supply data to users on magnetic tapes compatible with their respective tape readers. A high density optical system for an archival data store can be readily configured to provide data to users on conventional magnetic tapes.

2.1 COST AND PERFORMANCE FACTORS

The costs associated with accumulating and maintaining a high capacity, high quality archival data base are strongly affected by: 1) storage material costs, 2) storage space requirements, 3) rate of data deterioration (or frequency of respooling and rerecording required), 4) the cost of generating copies for distribution to users, and 5) environmental (energy) costs. Other important factors which must be considered include 6) the archival properties of the storage media, 7) providing a convenient means for users to browse through the data base, 8) generating copies of segments of the data base without degrading the original data, and 9) providing for increased data throughput rates, possibly with a range of rates. These factors are considered below in more detail in comparing high density optical and magnetic data storage.

2.1.1 Storage Material Cost and Packing Density

The cost per bit for the storage material is determined by the cost per unit of the material and the number of bits which can be stored per unit area. Magnetic tapes in the Ampex TBM^R format⁸ permit a data area density of 2.3×10^5 bits/cm². For 1 mil tape, the volume density is 9.2×10^7 bits/cm³. Significant increases above these levels on magnetic tape are not anticipated. With direct-spot recording on, for example, photographic film, a data area density of 5×10^7 bits/cm² has been achieved in the video recorder prototype developed by the Digital Recording Corporation in association



with Battelle Pacific Northwest Laboratories. We allow an extra design margin and use 10^7 bits/cm² on a 2 mil film (such as Kodak 1414) to obtain a volume density of 2×10^9 bits/cm³.

The costs of both magnetic tape and photographic film are generally considered on an area basis. Representative figures are \$0.20/ft² for certified magnetic tape and \$0.80/ft² for quality photographic film. However, with film we can achieve a $10^7/2.3 \times 10^5 = 43X$ area packing density advantage. Thus, we can project approximately a 10-fold cost advantage with film.

Another important feature of photographic film related to area packing density is the rate at which film must be translated past a read station to achieve a selected readout rate. For equal film and tape widths (≈ 35 mm each), the film can move 43 times slower, or data can be transferred 43 times faster, or somewhere in between. The impact of a slower film translation rate on the design of a transport unit can be quite favorable.

2.1.2 Storage Space Requirements

We assume that similar mechanical overhead ratios are required for configuring a practical storage and retrieval facility for film and tape. Based on the previous volume density figures, film will require 22 times less volume than tape for the same data base size. Conversely, 22 times as much data could be stored in a given facility. The cost savings which can be projected for storage space with an optical archival store using film are considerable. The combined impact of material costs and storage volume costs is more than two orders of magnitude in operating cost savings.

2.1.3 Maintenance of Data Quality

In existing archival data storage facilities which use magnetic tape, tape and tape transport manufacturers typically recommend that each stored reel of tape be periodically respooled at the proper tension and cleaned; these procedures can be required



as often as once a year. The two main reasons why these procedures are recommended are as follows: ⁷

1. Tape is wound with a preferred tension. Over extended periods of time, the winding tension decreases as the film undergoes visco-elastic relaxation, thereby reducing the tension between adjacent tape layers. If an improperly tensioned tape reel is mounted on a tape transport, the normal accelerations it experiences can allow interlayer slippage to occur. Such tape slipping can damage the tape and cause notable increases in errors.
2. The tape base material contains plasticizers. Over extended periods these components can migrate to the surface where they form a tacky, viscous layer. This layer can coat read heads and cause them to retain any loose particles which they might subsequently encounter. These particles can scratch the tape surface and cause increases in errors.

Reduction in tension and plasticizer migration will also occur in a reel of photographic film. However, since film speeds can be much slower, much lower accelerations can be used to prevent film slipping even at reduced tension. Furthermore, the film base is thicker than the tape base, thereby rendering the film less susceptible to visco-elastic relaxation. The layer of plasticizer that can form on the film surface is transparent and has no impact on the film reading function, since the film does not contact any component in the read station.

Film is not degraded by magnetic fields or by other EMI. In a reasonable environment (50° to 70° F and 15 to 40 percent RH) many films have truly archival properties, as defined by ANSI standards PH 1.28-1969, PH 1.25-1965, and PH 1.41-1971. ¹⁰

Photographic film can be stored for many years in a reasonable environment with little or no handling (very little labor required) with high assurance of data recovery.



2.1.4 Supplying Users With Data From the Archival Base

The true value of an archival data store can be assessed by examining how responsive such a system is in supplying high quality data to qualified requestors in a highly usable form and in a timely manner. In addition, the process of extracting data from the archival base should have a minimal impact on the archived data.

Most users will prefer that the digital data they request be supplied on conventional magnetic tape which is compatible with the equipment they already use. However, the process of reading data from a primary tape onto a secondary tape to be shipped to a user has a deteriorating effect on the primary tape from the data base. It has been reported that after six to seven such reads from high density tapes, the quality of the data on the primary tape decreases to intolerable levels for certain users. This reduction in quality is largely a result of read head contact with the surface of the tape. Since there is no read head contact with photographic film, this problem would not arise.

The cost of copies supplied to users is projected to be approximately equal for the two approaches, but film can be accessed and copied many more times without degrading the primary data.

2.1.5 Browse Capability

Another measure of the value of an archival data base can be made by assessing how readily a user can determine where data which is most useful to him is located. Numerous indexing schemes can be implemented to aid users in their search for information. We are assuming that the bulk of the archived data is imagery (visible, IR, UV, radar, etc.). Data which a user requests based on indexing keys, without benefit of a visual inspection, may be of little or no value because it was not what he thought it would be. Time and materials expenditures could be largely avoided if users were provided with the opportunity to browse visually through the imagery before they issue a request for the digitized form of the imagery. A display of an image, even at reduced resolution, can provide considerable guidance to a user in his search through a large file.



With photographic film, it is feasible to incorporate microreduced analog imagery directly with the digitized data for subsequent recall using a viewer. Alternatively, a completely separate file of microreduced imagery can be generated with cross-indexing to the corresponding digital data; this scheme can be implemented in conjunction with either a film or tape data base.

The management and efficient utilization of the archival data base could be notably improved with the incorporation of a browse capability for users. The incorporation of such a feature should not limit access by others to the data base; multiple access ports which can be used simultaneously might be required. The alternative means for producing the microreduced imagery and the related viewing equipment should be part of any high-density, high-capacity optical storage system development program.

2.1.6 Data Input/Output Rates

The increasing quantity of data which must be stored is arriving at ever-increasing rates. Multiple channel techniques for recording and reading data optically on reel-to-reel film at rates as high as 750 Mb/s have been demonstrated.^{11, 12} Certain aspects of these techniques could be adapted to special configurations of a high density direct spot optical recorder to achieve record and readout rates well above 100 Mb/s. The prospects of recording digital data at high densities directly onto film at such rates from a satellite or other remote sensor are good.

An advantage of an optical system is that it can operate at readout rates that can be considerably different from the record rate. The intensity of the laser output can be adjusted in correspondence to the readout rate to provide an essentially constant signal level to all photodetectors. Thus, data which may have been recorded at very high rates from a remote sensor can be transferred to a CPU or other processing equipment at rates compatible with such hardware.

With magnetic tape, a change in the readout rate produces a corresponding change in the amplitude of the signal that the read head detects. This feature results from



the fact that a fixed magnetic flux difference $\Delta\phi$ occurs between 0's and 1's on the tape and the signal amplitude the read head detects is proportional to $\Delta\phi/\Delta t = v(\Delta\phi/\Delta x)$. Δt is the time required for the tape to traverse the fixed distance Δx over which a fixed head senses a signal, and $v = \Delta x/\Delta t$ is the tape speed. Thus, the signal amplitude varies with tape speed, and there is no way to compensate this effect analogous to increasing or decreasing a light intensity level. Increasing the gain on a preamplifier at the read head can compensate for a loss of signal but generally results in a lowered SNR, which degrades the bit error rate.

2.2 TECHNOLOGICAL DEVELOPMENTS

Since 1970, certain devices and techniques which are important elements of a high density optical recording system have been developed or improved. These technological advances have significantly enhanced the prospects for developing an optical archival mass storage system. Specific examples of these advances are listed below:

- Compact and efficient acousto-optic modulator arrays (page composers) capable of record rates in the 0-750 Mb/s range with up to 136 elements⁽¹²⁾
- Large solid-state photodetector arrays which can be used for extremely fast electronic position tracking for readout
- Improvements in techniques for precision control of film position with air-bearings^{12, 13}
- Improvements in servo-controlled beam position correction devices (acousto-optic, piezoelectric, electro-optics, and galvanometers) for lateral beam position control
- Advances in error-correction coding and decoding theory and hardware



- Demonstration of a unique multiple lens, high resolution mechanical scanner which incorporates simple lenses on a moving structure and permits the recording and reading of 10^4 to 10^5 spots per scan line⁹
- Demonstration of a digital data recording and playback system for video signals with $1 \times 2 \mu\text{m}$ spot centers on photographic plates¹³
- Demonstration of optical video recording and playback units for video signals using FM signals with $\sim 1 \mu\text{m}$ centers between zero-crossings and $2 \mu\text{m}$ centers between tracks¹³

These device and technique improvements and system demonstrations are positive indications that high density optical recording offers important new capabilities for mass archival data storage systems.

2.3 COMMENTS AND RECOMMENDATIONS

The challenge of combining these new devices and techniques with the more conventional optical, mechanical, and electronic technologies to produce an acceptable system is a considerable one. In particular, we stated prior to the DIGIMEM contract phase that the following key milestones were necessary to achieve a cost-effective and operationally successful system:

1. Demonstration of an axial film position control mechanism capable of holding moving reel-to-reel film within depth-of-focus tolerances for recording and reading spots on 2 to $5 \mu\text{m}$ centers (demonstrated only for plates and film disks to date)
2. Demonstration of a lateral film position control or capture mechanism capable of tracking data recorded on 2 to $5 \mu\text{m}$ track centers over the full scan length on moving flexible film (demonstrated only for plates and film disk to date)



HARRIS

ELECTRO-OPTICS

2-10

3. Demonstration of a multiple channel readout technique which permits data recovery from moving film with acceptable bit-error rates (no measurements of BER in demonstrations to date with video signals)
4. Demonstration of a breadboard system capable of recording and reading multiple channel data recorded at packing densities in the 4×10^6 to 2.5×10^7 bit/cm² range at equivalent data rates of 1 to 10 Mb/s
5. Demonstration of a scanner concept designed for recording multiple channel data on film (only single channels recorded to date)
6. Selection of a film and compatible automatic film processor which can reliably provide optimally developed reel film essentially free of scratches and other defects.
7. Demonstration of a floppy disc, fiche or reel-to-reel film transport mechanism which allows hundreds of access and readout cycles without degrading the quality of the retrieved data while permitting rapid file search and the required speed and position control.

As will be shown in Section III, the present DIGIMEM breadboard demonstrates the near-term feasibility of achieving these goals in an operational archival mass storage system. Consequently, there is ample justification for progressing toward an engineering model with full record and readout capabilities for a film size and format representative of those projected for use in an optical mass archival store. The successful demonstration of an engineering model should be followed by the development of a preproduction prototype and a fully operational optical archival mass storage system. A complete outline of our proposed development plan is discussed in Volume III of this report.



2.4 REFERENCES

1. Bobeck, A. H., P. I. Bonyhard, and J. E. Geusic, "Magnetic Bubbles - An Emerging New Memory Technology," Proc. IEEE, Vol. 63, No. 8, August 1975, pp. 1176-1195.
2. Cohen, M. S., and H. Chang, "The Frontiers of Magnetic Bubble Technology," Proc. IEEE, Vol. 63, No. 8, August 1975, pp. 1196-1206.
3. Hodges, D. A., "A Review and Projection of Semiconductor Components for Digital Storage," Proc. IEEE, Vol. 68, No. 8, August 1975, pp. 1136-1147.
4. Hughes, W. C., C. Q. Lemmond, H. G. Pasles, G. W. Ellis, G. E. Possin, and R. H. Wilson, "A Semiconductor Nonvolatile Electron Beam Accessed Mass Memory," Proc. IEEE, Vol. 68, No. 8, August 1975, pp. 1230-1240.
5. Harris, J. P., R. S. Rhode, and N. K. Arter, "The IBM 3850 Mass Storage System: Design Aspects," Proc. IEEE, Vol. 68, No. 8, August 1975, pp. 1171-1176.
6. Johnson, C. T., "The IBM 3850: A Mass Storage System with Disk Characteristics," Proc. IEEE, Vol. 68, No. 8, August 1975, pp. 1166-1170.
7. Rodriguez, J. A., "An Analysis of Tape Drive Technology," Proc. IEEE, Vol. 68, No. 8, August 1975, pp. 1153-1159.
8. Wildman, M., "Terabit Memory Systems: A Design History," Proc. IEEE, Vol. 68, No. 8, August 1975, pp. 1160-1165.
9. Russell, J. T., and R. A. Walker, "Optical Digital Recording," Optical Engineering, Vol. 15, No. 1, January-February 1976, pp. 20-23.
10. Pamphlet No. P-108, "Storage and Preservation of Microfilms," Eastman Kodak Co., 1972.
11. Bardos, A. M., "Wideband Holographic Recorder," Applied Optics, Vol. 13, No. 4, April 1974, pp. 832-840.



HARRIS

2-12

ELECTRO-OPTICS

12. Bardos, A. M., R. H. Nelson, H. N. Roberts, and C. A. Shuman, "Electro-Optic Components for Wideband Recording and Reproduction," Electro-Optics/International Laser Conference and Exposition, November 1975, Anaheim, California, Paper 11-1.
13. Adler, R., "An Optical Video Disc Player for NTSC Receivers," Transactions BRT, August 1974, pp. 230-234.



HARRIS

ELECTRO-OPTICS

3-1

SECTION III

DIGIMEM BREADBOARD RECORDER/REPRODUCER



HARRIS

ELECTRO-OPTICS

SECTION III

DIGIMEM BREADBOARD RECORDER/REPRODUCER

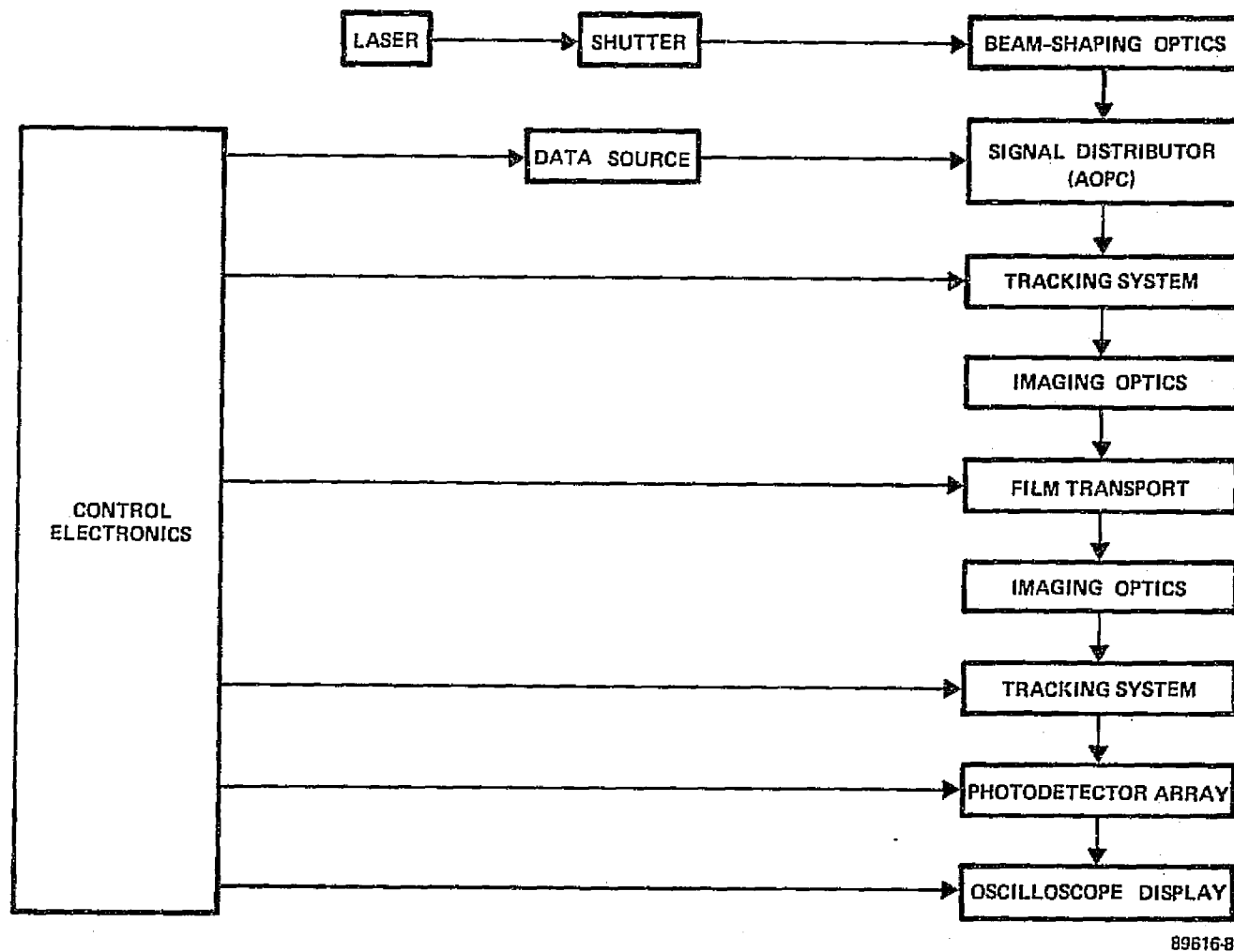
Direct digital optical spot recording provides a number of improvements over other proposed mass memory technologies. In addition to the advantage of recording on archival storage media such as photographic film, this concept provides very high information storage without requiring ultrahigh precision recording and readout tolerances. Where 128-bit 1.0 mm x 10 μ m Fourier-transform holograms on 15 μ m centers in a typical holographic mass memory system yield a local area information storage density of 0.85×10^6 b/cm², optical spots on 2.5 μ m centers provide an equivalent storage density of 16×10^6 b/cm², a gain of almost 20 times. In addition, by recording not one spot, but an array of spots in each data burst, recording and readout rates higher than 1 Mb/sec are possible. With random access time and economic considerations of key importance to many mass memory users, optical spot recording can be shown to have distinct advantages over other approaches to mass data storage. An objective of this Volume and Volume III of the final report is to demonstrate these advantages.

3.1 BREADBOARD SYSTEM CONCEPTS

To provide a framework for discussing breadboard implementation of the optical digital spot recorder/reproducer (to be called DIGIMEM throughout the remainder of this report), the block diagram of Figure 3-1 is useful. As part of the initial design of an optical spot recorder/reproducer, the primary components selected for the recording mode of operation are the signal distributor, the imaging optics, and the film transport. Because of the need for achieving high data recording rates, the optical signal distributor must provide an array of spots for each burst of (electronic) data. If, instead, the signal input had only one input channel, the film transport velocity would have to increase proportionately to achieve the same record rate. The laser and beam-shaping optics provide illumination for this signal distributor, and the imaging optics

DIGIMEM

BREADBOARD BLOCK DIAGRAM



89616-8

FIGURE 3-1. THE BREADBOARD BLOCK DIAGRAM

HARRIS
ELECTRO-OPTICS





HARRIS

ELECTRO-OPTICS

3-4

image the optical data from the signal distributor onto the film in the film transport. An additional block added to the recording part of the system, the tracking subsystem, is a movable mirror placed in the optical path to allow changing the location of the recorded spots on the film.

For readout, key components shown in the block diagram are an illumination system for the film transport and imaging optics to image the recorded data onto a photodetector array. The illumination system, which can be thought of as an illuminated signal distributor which is always "on" in all channels and which is focussed onto the film with the input imaging optics, is fairly straightforward in concept, as is the imaging optical system. The photodetector array block is considerably more complicated, primarily because of the phenomenon of "data wander."

In any mass memory system, magnetic or optical, there will be a problem in aligning the data in readout exactly as it was positioned during recording. This data wander can be the result of recording material expansion or contraction, mechanical tolerance limitations on film-positioning devices, and, when recordings from one system are to be played back in another system, overall system tolerance limitations. In the present concept, where spots on 2-5 μm center spacings have been proposed to provide high packing density, a practical mechanical alignment tolerance limit of $\pm 12.5 \mu\text{m}$ makes it obvious that any feasible system design must accommodate and compensate for this data wander. In the DIGIMEM concept, this is accomplished in two locations. In the output tracking subsystem, a rotating mirror assembly (described in detail in Paragraph 3.3.2 of this report) is responsible for keeping the imaged data located on the photodetector array. The photodetector array itself is designed to "find" the data bits as they wander over the array and send out a stable output signal for display on an oscilloscope. The result is that despite data wander in the film transport the display signal is stable (i.e., the recorded data are successfully recovered).



The next step in defining a breadboard system which will accurately determine the feasibility of multiple-channel optical digital recording systems is to establish design goals for an initial concept. These goals should be sufficiently demanding so that a true simulation of practical system requirements is achievable while avoiding the expense of building beyond the needs of a feasibility investigation. The first consideration was to build a system that recorded on flexible photographic film, rather than glass plates. Although a concept based on glass photographic plates would have been easier to implement because of much greater mechanical stability, the expense, bulk and fragility of glass plates did not provide a practical basis for a breadboard investigation. Next a decision was made to record (and read out) two or more channels in parallel to investigate the problems of block recording and readout which eventually arise in high data transfer rate mass memories. The data transfer rate for this implementation, 1 Mb/s during recording and readout, was selected to allow testing of the data wander tracking concepts with only moderate electronic data processing rates. For these experiments, demonstrating electronic data wander correction was determined to be more important than achieving the highest possible data rate. Finally, an information packing density goal of greater than 4×10^6 bits/cm² was selected, corresponding to spots recorded on 2-5 μ m centers. This last specification is necessary to provide the desired high capacity, low cost, and small volume optical mass memory system. These specifications provided the framework for the design work reported in the remainder of this section.

3.2 IMPACTS OF BASELINE SPECIFICATIONS

With the breadboard goals specified, the next step in the design process is to provide detailed guidelines for the overall DIGIMEM system concept. In all the analyses which follow, these guidelines will show an emphasis on demonstrating concept feasibility with the most cost-effective approach; existing equipment was utilized wherever possible, as long as it accurately simulated the problems expected to be encountered in a practical engineering model of an optical spot recorder/reproducer.



The first functional block of the breadboard system to be selected in detail must be the signal distributor, since its shape and dimensions will have a major effect on the rest of the system. The specifications which this block must meet are that it provide two or more data channels for recording in a parallel format and that it be capable of a 1 Mb/s data recording rate. With an acousto-optic page composer of the type shown in Figure 3-2, both of these specifications can be easily accommodated. Acousto-optic page composers are well-developed components already fabricated and operating with 128 parallel data channels and a total data rate of up to 750 Mb/s. In the DIGIMEM concept, an existing TeO_2 32-channel acousto-optic page composer (AOPC) was selected for use in the breadboard. To achieve a user recording rate of 1 Mb/s, eight data channels from the AOPC were designated as user data, and the decision was made to switch the entire page composer on and off at a 125 kHz rate to arrive at a rate of $8 \text{ bits/data burst} \times 125 \times 10^3 \text{ data bursts/second} = 10^6 \text{ bits/second}$. The 8-bit, or byte, format is directly compatible with existing electronic computers. The use of an acousto-optic page composer provides the flexibility to meet future demands for larger parallel format sizes or higher data rates with a minimum of engineering development.

With the signal distributor format chosen, it is possible to specify the film transport design. Because of the expense and complexity of x-y (fiche) and reel-to-reel (tape) film transport, a floppy-disk transport with conventional 4- by 5-inch film rotated about a hole punched in its center was selected. In previous mass memory investigations (see Volume I, Section III), floppy-disk film transports had demonstrated depth-of-focus tolerances using two air bearings (with 0.5 inch diameter openings) sufficient to record spots of less than $2 \mu\text{m}$ diameter on flexible film, which meets one specification for the transport. The general recording format, illustrated in Figure 3-3, shows that each data burst recorded on the film will be recorded parallel to the previous one as the film rotates. Since the data wander effect discussed earlier appears here as a decentering of the film rotation hole during readout, the data will appear to slide radially in and out from the center. By recording in this format, each "band" of data actually consists of eight data

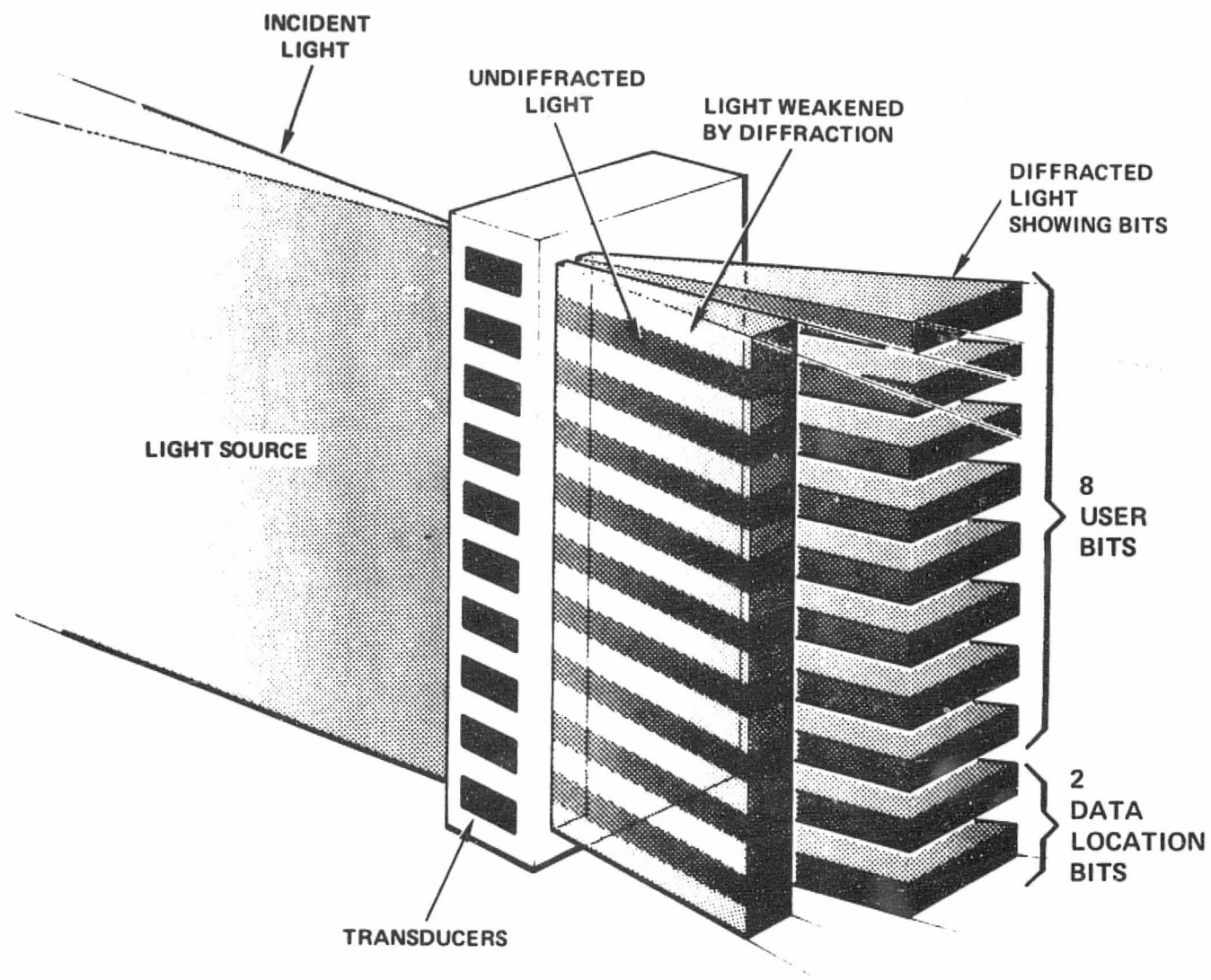


HARRIS

ELECTRO-OPTICS

3-7

ACOUSTO-OPTIC PAGE COMPOSER



88589 2B

FIGURE 3-2. THE ACOUSTO-OPTIC PAGE COMPOSER

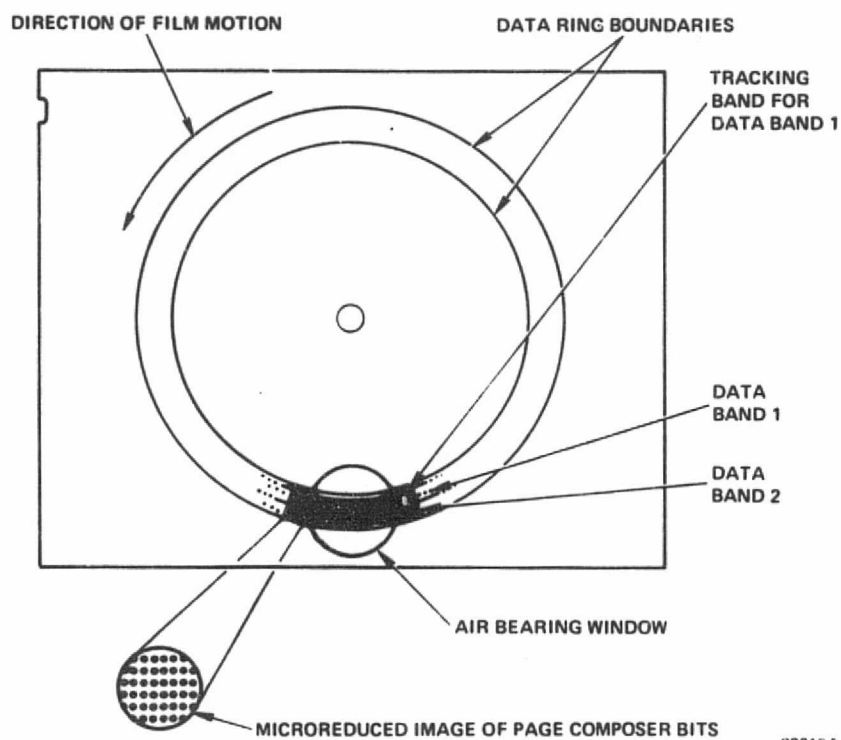
ORIGINAL PAGE IS
OF POOR QUALITY



HARRIS

ELECTRO-OPTICS

DIGIMEM BREADBOARD FILM FORMAT



89616 5

FIGURE 3-3. THE BREADBOARD FILM FORMAT



channel "tracks" which maintain approximately constant radial distance from the center of the transport. This makes spatial location of the data on a photodetector array much easier than if the data bursts were recorded end to end, another possible format. A more detailed description of the actual design features of the film transport is given in Paragraph 3.3.2.1.

Reading out the recorded spot information requires imaging the data so that it falls within the active length of the photodetector array. Since data wander can amount to several data bandwidths (greater than $8 \text{ spots} \times 2 \mu\text{m/spot} = 16 \mu\text{m}$ of wander with the smallest spot spacing), the trade-off is between having a large photodetector array (which can be unreliable, as well as expensive) and finding a means to compensate for coarse data wander so that only fine data wander movement must be tracked by the photodetector array. To implement the second alternative, an extra band, positioned next to each data band, is recorded on the film; this is shown in Figure 3-3 and in enlarged form in Figure 3-4. This band can be detected externally by a position detector in readout, which produces a voltage output proportional to the centering error of the output data pattern. This voltage output, when used as the input to a rotating mirror device, makes it possible to adjust the angle of the readout signal beam so that the coarse data wander is corrected. Details of the actual coarse tracking subsystem appear in Paragraph 3.3.2.2.

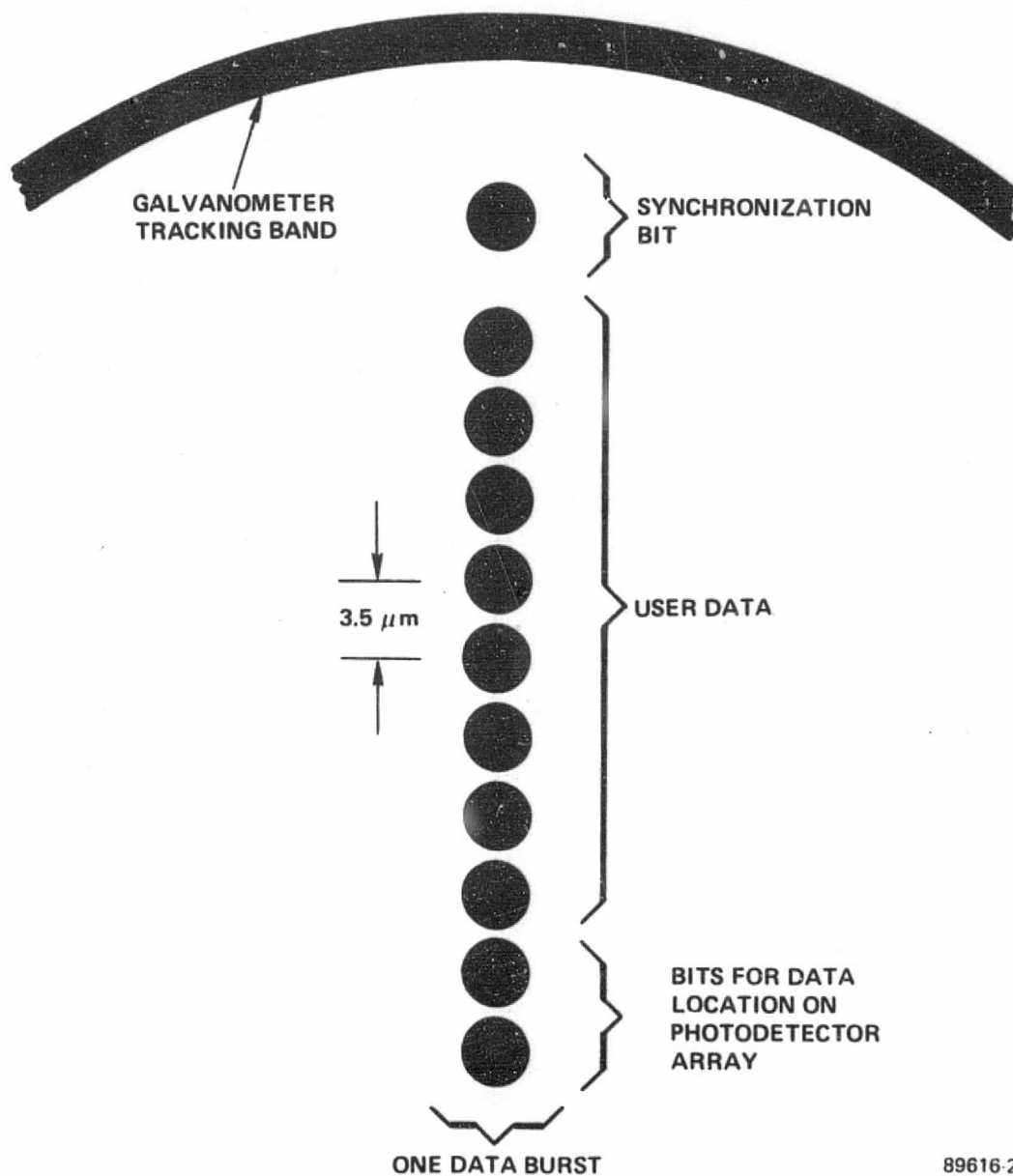
Once the data is displayed on the photodetector array, several additional considerations become important. If the detector array cannot read out several times as one data word sweeps past it (thus oversampling each data word in the film motion direction to allow proper selection of the peak signal), then an additional synchronization bit (shown in Figure 3-4) must be recorded with the data. This bit, part of the AOPC signal distributor data, is read out by a separate discrete detector and used as the "start scan" signal for the detector array. As a final format consideration, since the detector array must accommodate fine data wander, some kind of reference must be provided in the data pattern and must always be present to enable the control systems to locate the user data on the photodetector array. In the DIGIMEM concept, to be discussed further



HARRIS

ELECTRO-OPTICS

DIGIMEM BREADBOARD DATA FORMAT



89616-2

FIGURE 3-4. THE BREADBOARD DATA FORMAT



in Paragraph 3.3.1.2, the two data location bits of Figure 3-4 provide this reference. They are part of the AOPC input data pattern and are "on" for each data burst.

These basic design considerations, derived from the baseline specifications for the DIGIMEM breadboard, constitute only the fundamental framework for designing the system. More detailed analysis required for building a workable system around this framework follows.

3.3 SPECIAL COMPONENTS/SUBSYSTEMS

3.3.1 Electronic Subsystems

3.3.1.1 The Recording Electronics

The basic requirement for the recording electronics is that a user recording rate of 1 Mb/s be achieved with sufficient annotation and control so that a user readout rate of 1 Mb/s is possible. The first consideration is the data format and its impact on the kinds of information which the acousto-optic page composer, the signal input device for this breadboard, must produce for recording. Clearly the eight user bits of data must come from the AOPC along with the two data location bits required for locating the data in readout. In addition, to enable the photodetector array used in readout to trigger its data burst readout scan at the proper moment, a separate synchronization bit must also be recorded with the data and be switched on and off with the rest of the data. Together with the data, a separate track for the tracking subsystem (Paragraph 3.3.2.2) must also be recorded. All systems must be compatible with the 125 kHz data burst cycle rate and the 2.5 rev/s maximum required rotational film speed (derived in Paragraph 3.3.2.1).

To provide a programmable data source for the AOPC, two 4-bit x 512 Harris HMI-7621-5 PROM's were used in a serial manner to load eight channels simultaneously with each clock pulse to the PROM's. To allow optimum data synchronization in readout and the



HARRIS

ELECTRO-OPTICS

3-12

selection of any data sequence from the PROM in the recording mode, an additional feature of the PROM data is a recognition code programmed at the beginning of each new block of information. This pattern consists of four bytes of data with four "ones" and four "zeroes" as pictured below:

1	1	1	1	1	0	0	1	...
1	1	1	1	1	0	0	1	...
1	1	1	1	1	0	0	1	...
1	1	1	1	1	1	1	1	...
0	0	0	0	1	0	0	1	...
0	0	0	0	1	0	0	1	...
0	0	0	0	1	0	0	1	...
0	0	0	0	1	0	0	1	...

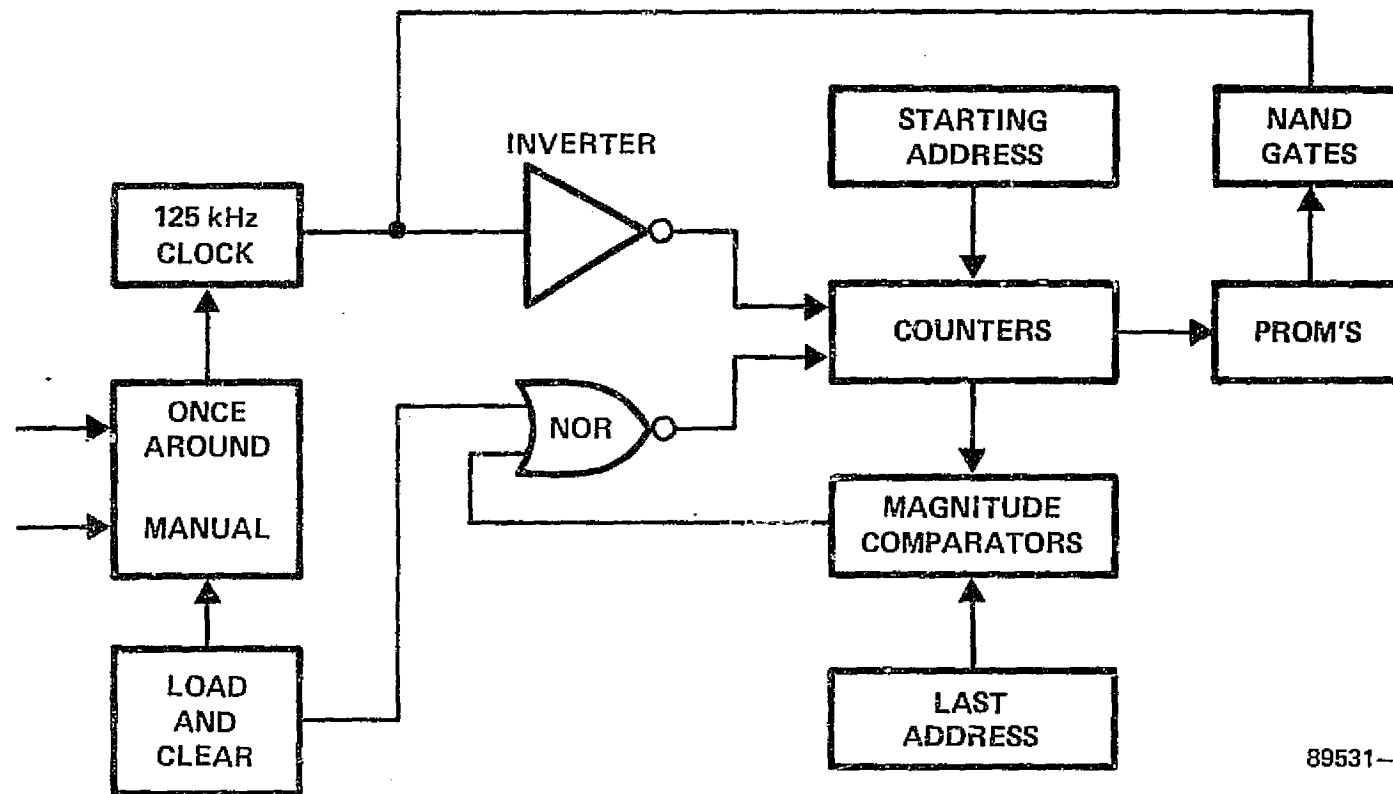
Recognition
Code

Data

For the other data, the byte sync signal and the data location bits are hard wired into the AOPC channels in an "on" position so that they always flash on for each burst of the user data. The tracking band is recorded with a separate laser so that it can be shuttered separately and left on continuously even when the AOPC is switched off.

In use, the system operates as shown in Figure 3-5. Initially the data location code is entered manually to select which block of information is desired as the recording "message." The load and clear switches are then activated to enter the beginning address of the message into the counters. With this address in the counters, the first word is channeled to one side of the magnitude comparators, as well as being decoded in the PROM's as the input to the NAND gates. Manually-programmable switches also load the last address number of the message into the other half of the magnitude comparators at this time; this makes it possible to program the system to stop the data at any desired point. As a final step, the load and clear switches disable the system clock at this time. The system is now ready to begin recording.

The film transport motor is now preset manually to a voltage corresponding to the required film speed and started. Next, the "once-around" disc movement



89531-3

FIGURE 3-5. THE WRITE CONTROL ELECTRONICS

ELECTRO-OPTICS

HARRIS





HARRIS

ELECTRO-OPTICS

3-14

subsystem begins feeding data to the control system. This "once-around" actually consists of a reflective spot on the film and an infrared emitter-plus-detector module used to detect the film's passing across the spot. This "once-around" signal is used during recording to signal the exact location of the start of the recording and during readout to provide the location of the beginning of data to the photodetector array subsystem.

To record data, the recording sequence is triggered manually, and the tracking beam shutter opens; this shutter is preset to remain open for one revolution of the floppy disc in the transport. A second shutter, the data recording beam shutter, is also opened at this time. Following this, when the first "once-around" signal is detected on the transport, the system clock is enabled and the next positive-going edge of the clock triggers the start of data. The first word of data is now shifted out of the NAND gates and into the AOPC, resulting in a pulse of light where a logical "one" has been programmed into the PROM. At this point the next message address is compared to the requested last address in the magnitude comparators. If these addresses are not equal, the PROM now decodes the next word of the message and presents it to the NAND gates. This next word, like the previous one, is clocked out to the AOPC on the next positive-going edge of the clock. This cycle is then repeated until the message address and the last address are found to be equal at the magnitude comparators; when that occurs, the counters are reset back to their original starting address and the recording cycle repeats. The data recording recycles continuously until the recording beam shutter (programmed manually but switched off electronically) blocks the light input to the AOPC. The tracking beam shutter closes next, and the recording cycle is complete.

The transport is shut off at this point and the film removed for processing. After the film has been developed, it is placed back in the system for readout.

Detailed circuit diagrams for the recording electronics are provided in Appendix A of this report.



3.3.1.2 Photodetection and Readout

To read out the recorded data, a linear array of detectors is required for the imaging readout technique selected. To permit electronic shifting of the data sensing detectors as the output light pattern shifts along the linear array, it is clear that several detectors must be assigned to each bit (or spot) of information to guarantee reliable readout of the data. In the present system, the oversampling factor was set equal to 4 in the design stage to allow good resolution of the spots without requiring a large photodetector array (PDA). With 10 data spots to be detected on the detector array, this means that the array, at a minimum, must have $10 \times 4 = 40$ detector elements. To accommodate fine data wander on the detector array, a minimum ± 3 data spot field was added to the array length, for a total of $6 \times 4 = 24$ additional detectors. The total minimum length of the array is therefore 64 detectors.

The next criterion for a readout device is the detector sensitivity, which in turn is dictated by the light available in the system. On the breadboard, a Model 125 Spectra-Physics helium-neon laser (with an output power of 50 mW at 632.8 nm) is the light source. From this, together with the design parameters already specified, the amount of light available at the photodetector array can be calculated. If the number of spots to be detected on the array is N , the oversampling factor (or number of detectors per bit of information) is S , the spatial duty cycle of the spots on the film is T_2 , the system optical efficiency is T_1 , and the input laser power is P_i , then the amount of power available at the PDA per detector is given by:

$$P_o = \frac{P_i T_1 T_2}{NS} \quad (3.1)$$

For an integrating system, where a detector integrates light over a period of time before its output is sampled, the "exposure time" of the detectors must be included in the analysis. If this time is t_e , then the intensity, I_d , at the PDA plane is given by:

$$I_d = P_o t_e = \frac{P_i T_1 T_2 t_e}{NS} \quad (3.2)$$



HARRIS

3-16

ELECTRO-OPTICS

In the present concept, $P_i = 50 \text{ mW}$, $N = 10$, and $S = 4$. If we assume a 5 percent system optical efficiency, a 50 percent duty cycle on the recorded spots at the film plane, and a $2 \mu\text{s}$ exposure time during recording, $T_1 = 10^{-2}$, $T_2 = 5 \times 10^{-1}$, and $t_e = 2 \times 10^{-6}$ seconds. Then we have that

$$P_o = 28.5 \mu\text{W} \text{ and } I_d = 57 \text{ pJ}.$$

This, then, is the specification for the minimum sensitivity of the detector elements.

The final consideration before selecting an array is data transfer rate. In the DIGIMEM breadboard, the data bursts are recorded and read out at a 125 kHz data rate. This means that all 64 elements of any array must be read out in $8 \mu\text{s}$ or less and that the detector readout rate be in excess of $64 \times 125 \text{ kHz} = 8 \text{ MHz}$. As an additional design constraint, it was specified that the readout devices operate at these data rates with an error rate of one part in 10^4 . Three devices which meet these requirements are the fiber-optic array, the charge-coupled device (CCD) array, and the self-scanned photodiode array.

The first of these detector technologies, that of the fiber-optic array, is the most versatile in terms of data rate and sensitivity. Arrays have been fabricated that operate with up to 128 discrete elements and at data rates in excess of 500 MHz; detectors with threshold requirements at less than $0.1 \mu\text{W}$ operating at the required data rates are commercially available. The problem with such a device is that each of the 64 fibers would require a separate photodetector, filter and amplifier, plus a complex arrangement of 64 delay lines to serialize the data into one comparator. (An only slightly simpler alternative to 64 separate delay lines would be to have a separate comparator on each of the 64 data channels.) The net cost of such an array, including materials and labor, was estimated to be more than \$30,000. While acceptable as a prototype cost in a development effort, this was felt to be beyond the scope of the present research program.



HARRIS

ELECTRO-OPTICS

3-17

The second approach, the recently-developed CCD array, appeared very promising. The array provides significantly higher detector-to-detector isolation than the self-scanned array technology discussed below, and it is capable of higher data rates than the self-scanned array. It functions by the creation of electron-hole pairs in the p-type silicon surface when light is incident. The charge in the even-numbered detector elements is then transferred to one shift register, and the charge in the odd-numbered elements to a second shift register. Following that, the two shift register outputs are routed to a multiplexer and then to a charge amplifier, which is normally reset at the end of each element. Because the smallest commercially-available CCD array has 256 elements, however, a 64-element array version of this CCD is created by dividing down the reset pulses to the charge amplifier. This then makes it possible to add the charges from several photosites to effectively reduce the number of photoelements being shifted out of the array. This does not change the number of photosites read out, however, so the required data rate for the device is $256 \times 125 \text{ kHz} = 32 \text{ MHz}$. Unfortunately, this is beyond the useful operating range of the device, and the CCD must be rejected as long as the study is restricted to commercially-available devices.

Self-scanned photodiode arrays are the final possibility under consideration, and in this case arrays are available in a number of array lengths from 16 elements up to 1872 elements. For the present program, because of its exact match with the required number of elements the RL-64A array from Reticon was the optimum choice. It can be operated at data rates in excess of 10 MHz with 16 dB dynamic range according to earlier experimental evaluations of Reticon technology. In addition, the detector saturation exposure is $1.3 \mu\text{W-s/cm}^2$, which means that for detectors 2 mils wide and 2 mils long the amount of light necessary for saturation is 33 pJ. Since it meets all the required specifications and is available at a total cost of less than \$1000 including support electronics, it was selected as the photodetector array for the DIGIMEM breadboard.

Because of the selection of a device which cannot be operated at a data rate much higher than the required data rate, it is necessary to provide the photodetector



HARRIS

array with a signal to trigger the array's start-of-scan pulse. To do this in practice, the breadboard has been configured so that an eleventh AOPC channel is flashed "on" every time a data burst is recorded; in readout, this spot is illuminated with all the others, but it is detected by a separate silicon photodiode operating in the photovoltaic mode (manufactured by Meret, Incorporated) with a rise time of less than 100 ns. The signal from this detector provides a synchronization input to the readout control electronics, and is called "byte sync."

Preparation for readout requires, first of all, that the recording be loaded into the film transport and the transport be switched on. At this point the read beam laser shutter is opened and full power switched into the read path; this involves rotating a variable attenuator and flipping a mirror in place in front of the illuminating optics, and is described in detail in Paragraph 3.3.3.3. The tracking beam shutter is opened next, and the tracking galvanometer is activated. If multiple bands were to be recorded, the dc offset voltage for the band selection galvanometer (described in Paragraph 3.3.2.2 and shown in Figure 3-10 as $GALVO_1$) would be set to align the readout beam with the band to be read; $GALVO_2$, the tracking galvanometer, will correct for any large errors in data positioning. At this point the "once-around" signal and the byte sync signals are providing synchronization data to the readout electronics. Preparation for readout is now completed.

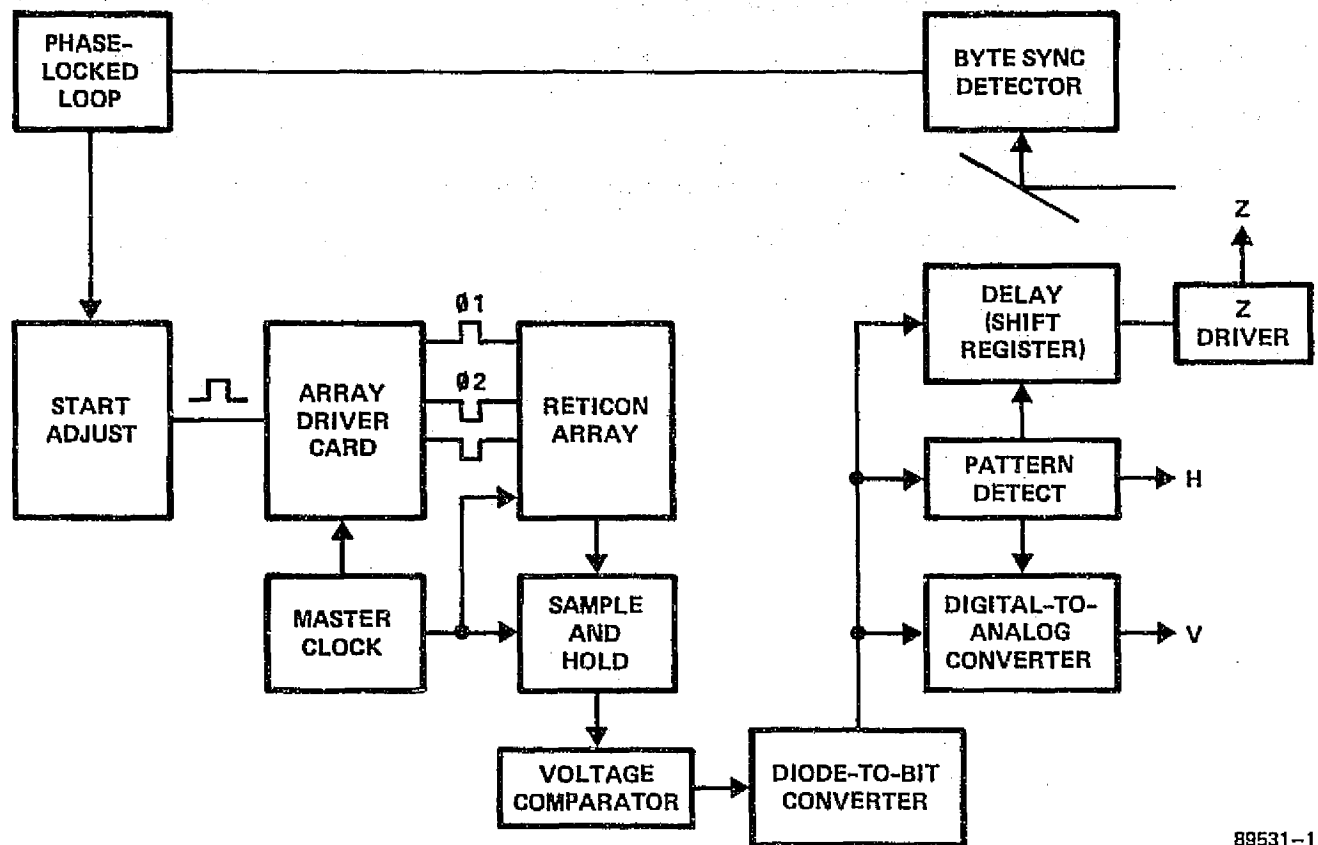
To read out the data, the circuit of Figure 3-6 is started at this point. After the "once-around" signal is detected by the read electronics, the system clock is enabled and the byte sync's sinusoidal data channeled to the phase-locked loop. The device locks the readout frequency into the actual data burst frequency, as detected by the byte sync detector, and transforms the byte sync's analog signal into a square-wave digital signal. This phase-locked loop signal then is routed to a manually-programmable delay device, the start adjust, to allow precise alignment of the readout start signal and the time at which the peak signal illuminates the detector array. When this delay



HARRIS

ELECTRO-OPTICS

3-19



89531-1

FIGURE 3-6. THE READOUT CONTROL ELECTRONICS



has been established, the array driver card triggers a start pulse from its master clock and the data is clocked out at the required 8 MHz rate. This completes the detection of the data.

To recognize the data, the data is run through a sample-and-hold/comparator circuit which transforms the analog signals into digital data as initial preparation for display. Once the two data wander bits are detected (as eight photodiodes reading out as logical "ones"), the data is justified by the diode-to-bit converter. This section transforms the diode data into bit data by combining the data from each four diodes following the data wander location bits into one bit. Next, the system searches for identification patterns, as described previously, on the recording electronics. The series of four bytes each consists of four ones and four zeroes. When the first set of identification patterns is detected, the electronics converts the digital data into analog display data for an oscilloscope readout. A horizontal trigger derived from the clock signal provides time base synchronization for the display, and a Z-axis modulation circuit subtracts out all data except the peak of the pulse to be displayed. The resulting display is identical to the actual spot data visible under the microscope when observing the recorded data patterns on the film records.

One problem with the readout electronics remains regarding visual observation of the display. While an electronic device can easily recognize the rapidly changing bit information, a human observer cannot process visual data at 1 Mb/s. To allow the readout to proceed at the required data rate and still provide a meaningful visual display of the data, several additional features were added to the readout electronics. The first is a manual "override" of the "once-around" signal. Readout now continues endlessly. In this situation, the electronics trigger the oscilloscope display in the readout mode by the pattern detection circuitry and allow continual updating of the display as each new pattern and message is detected. If, in addition to this, only one block of data is recorded and repeated around the circumference of the disc, then the updating of the display will appear only as a slight flicker of the single message recorded. The eye then has time to detect and recognize the rapidly changing data.



The detailed circuit diagrams for the readout electronics appear in Appendix B of this report.

3.3.2 Mechanical Subsystems

3.3.2.1 The Film Transport

The floppy disc film transport designed and fabricated for the DIGIMEM program phase had to satisfy several design constraints relating to the requirements of optical spot recording. First of all, to allow the use of commercially-available standard 4 inch by 5 inch photographic film formats, the device had to be designed to rotate a rectangular sheet of that size to avoid the expense and handling necessary to cut the film to a circular disc format (we have since learned that it is possible to obtain die-stamped circular film discs on a special order basis from Eastman Kodak). A second requirement was that the film transport maintain the optical depth-of-focus needed for the recording and readout of spots at diameters as small as $2\ \mu\text{m}$. It was also desirable to maintain this depth-of-focus with a noncontact device to minimize film scratching. As a final specification, the transport must also be capable of rotating at a speed compatible with the required recording and readout rates. These specifications then can be used for an initial design analysis of the transport.

The first significant design consideration for the transport is the depth-of-focus problem. In the present system, because the Gaussian beam of a helium-neon laser is used as the light source, a logical model for analyzing this is that of Gaussian beam propagation. For this model, the minimum spot diameter of a focused beam is $2\ w_0$, and the enlarged spot diameter of the beam at a distance z along the optical axis is $2\ w$. The relationship between $w(z)$ and w_0 is:



$$w = w_o \left[1 + \left(\frac{\lambda z}{\pi w_o^2} \right)^2 \right]^{1/2} \quad (3.3)$$

where λ is the wavelength of the Gaussian beam. Since in this application the spot diameter $2 w_o$ and the allowable enlarged spot diameter $2 w$ (corresponding to an axial film drift of z) are usually specified, the following form of the above equation is more useful:

$$z = \left(\frac{\pi w_o^2}{\lambda} \right) \left[\left(\frac{w}{w_o} \right)^2 - 1 \right]^{1/2} \quad (3.4)$$

Figure 3-7 shows the required z value as a function of spot diameter for $\lambda = 632.8$ nm, the helium-neon laser wavelength, and 10 percent, 20 percent and 50 percent spot growths. In the present system, if $2 \mu\text{m}$ diameter spots are recorded on film, with 50 percent allowable growth, the spot spacing could be set at $3.5 \mu\text{m}$ and still have $0.5 \mu\text{m}$ of "dead space" between adjacent spots. This then would correspond to a required depth-of-focus of about $\pm 5.6 \mu\text{m}$.

To meet the film rotation requirements, the transport must maintain a film speed corresponding to the 1 Mb/s data transfer rate. Since there are 8 user bits per data burst, the film must rotate fast enough to record or read 125×10^3 data bursts/sec. With the worst-case requiring a $5 \mu\text{m}$ center-to-center spacing between data bursts, this corresponds to a film speed of:

$$V_f = 125 \times 10^3 \times 5 \times 10^{-4} \frac{\text{cm}}{\text{sec}} = 62.5 \frac{\text{cm}}{\text{sec}} .$$

If the fixed recording head is located 40 cm from the center of the disc, approximately centered between the nearest film edge and the motor shaft, the circumference is $2 \cdot \pi \cdot 40 \text{ cm} \cong 251 \text{ cm}$. The required rotational speed is then only 2.5 rev/sec, or approximately



HARRIS

ELECTRO-OPTICS

3-

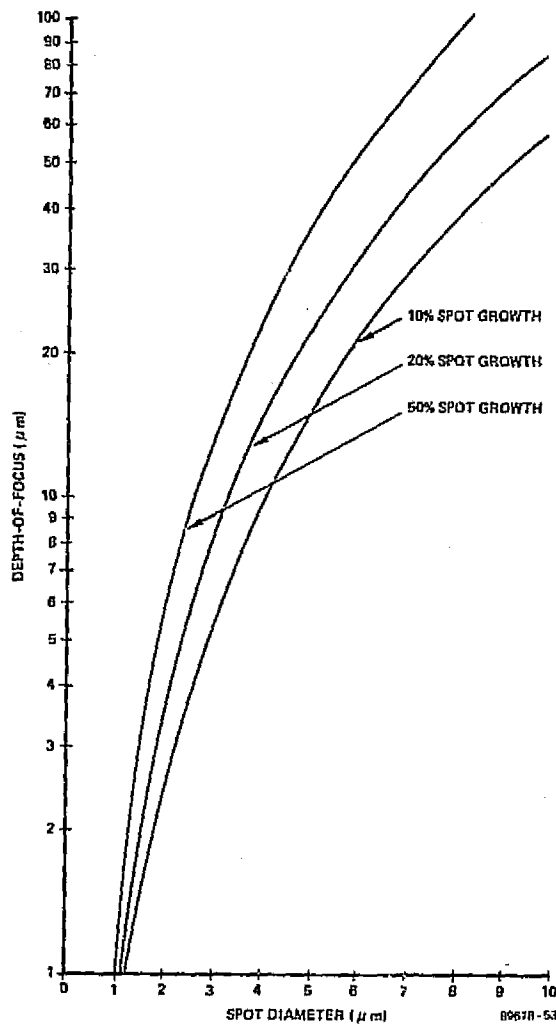


FIGURE 3-7. DEPTH-OF-FOCUS AS A FUNCTION OF SPOT DIAMETER
(FOR RECORDING WITH 632.8 nm LASER LIGHT)



150 rpm. (Note that if DIGIMEM employed single-spot rather than multiple-spot recording, the required film speed would be $8 \times 150 \text{ rpm} = 1200 \text{ rpm}$, a much more demanding specification if speed linearity is to be maintained). The motor used in the transport must also maintain this 150 rpm speed to an accuracy of $\pm 10\%$ to minimize the complexity of the data burst synchronization system in the readout mode.

The result of combining these specifications appears in Figure 3-8. An Inland T1342 torque motor rotation assembly with $\pm 3\%$ rms rotational speed accuracy at rotational speeds in excess of 3000 rpm (with no load) is mounted in a vibration-free housing to an aluminum plate, and the film is mounted on a post with a mounting hub screwed in place over it. The film itself has a hole punched in its geometric center and fits over the mounting post with an accuracy of $\pm 2 \times 10^{-5}$ inches. To provide the film stability required by depth-of-focus considerations, two 3M grade 15 Tegrilas air bearings were placed on either side of the film plane. Their size and shape were designed as shown in Figure 3-9 to allow the use of conventional 10X microscope objectives as the imaging optics for recording and readout. The actual clear aperture of the air bearings is held to 0.125 inch to maximize the percentage of air bearing area on the film. (Similar air bearings have maintained a depth-of-focus of $\pm 6 \mu\text{m}$ in previous laboratory testing.) Mechanical spacers set a spacing of 0.012 inch between the bearings to accommodate both 4-mil and 7-mil film bases, and individual needle valves match the pressures of the two air bearings. Finally, because it has a removable cover plate, the film transport provides an easy means of loading and unloading the film in total darkness.

The transport subsystem, as just specified, meets all requirements for the DIGIMEM breadboard concept. The experimental evaluation of this device is discussed in Paragraph 3.4.1.



HARRIS

ELECTRO-OPTICS

3-25

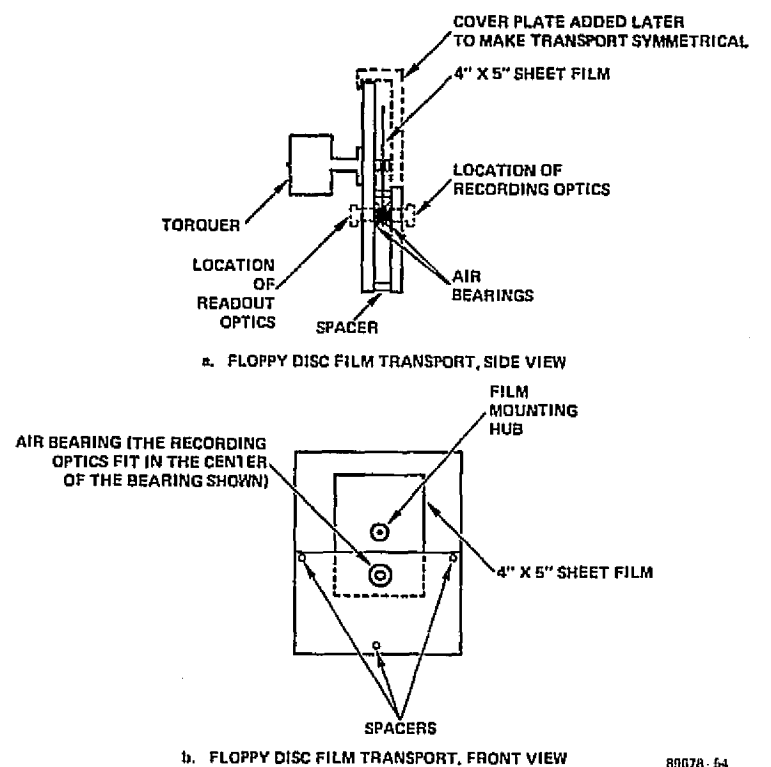


FIGURE 3-8. THE FLOPPY DISK FILM TRANSPORT



HARRIS

3-26

ELECTRO-OPTICS

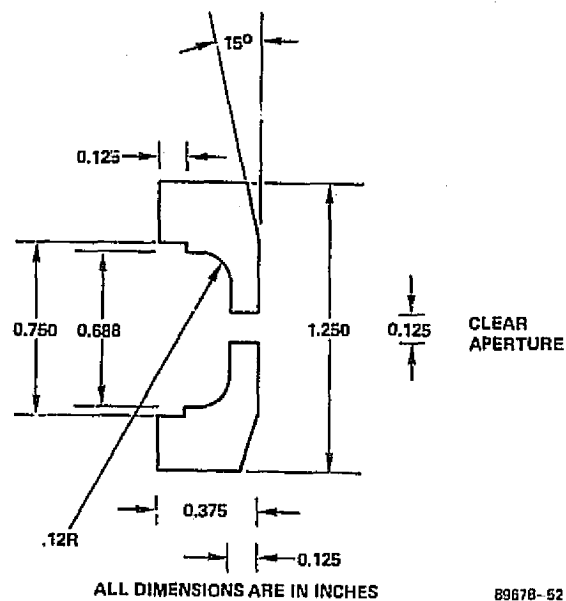


FIGURE 3-9. AIR BEARING SCHEMATIC (SIDE VIEW)



HARRIS

ELECTRO-OPTICS

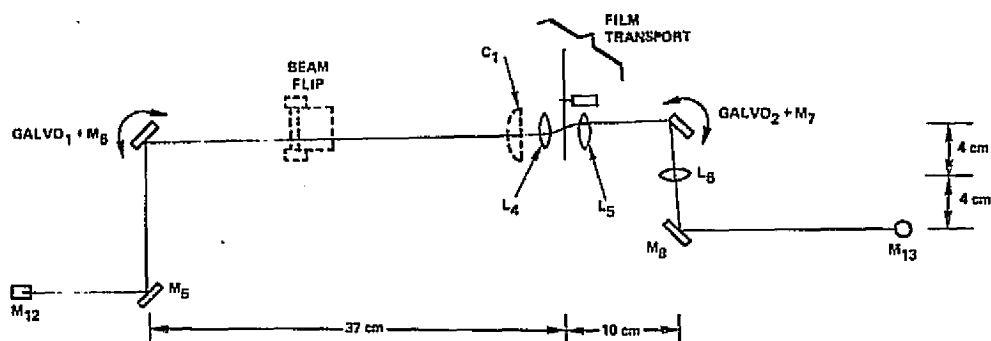
3-

3.3.2.2 The Tracking Subsystem

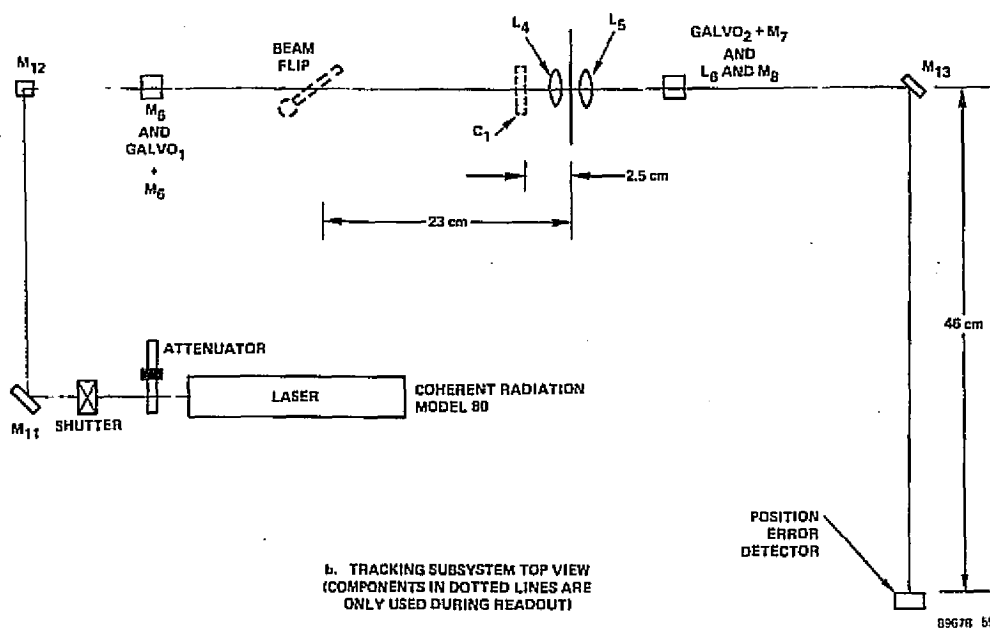
The tracking subsystem has two major components, and is shown in Figure 3-10. The first of these is the G-300 PDT galvanometer, capable of in excess of 30° peak-to-peak angular movement at frequencies in excess of 40 Hz with linearity to better than 0.1 percent. The G-300 PDT galvanometer, as driven by the CCX-100 servo controller, has been thoroughly studied and the results have been collected and discussed in Volume I (HOLOMEM) of this report. These are the galvanometers pictured in Figure 3-10. The other major component is a United Detector Technology PIN-SC/10 Silicon position detector in an MBA Information Systems circuit with an output of 22 volts per inch of beam motion on the detector surface. In use, it was found to perform reliably and without any need for adjustment.

As outlined earlier in this report, the role of GALVO₁ in the record mode is for accurate positioning of the recording beam on lens L_4 , the 10X microscope objective used to image the acousto-optic page composer onto the photographic film. To a lesser extent in the present concept, it also provides a capability of recording a number of bands on the film by changing the voltage input to the galvanometer in discreet steps. For each band of data to be recorded, there is also a tracking band recorded on the film as well. This band is always "ON" and is produced by a dedicated laser and attenuator used only for recording this tracking band.

In the read mode, a beam-flip mirror and the cylinder lens C (with a 50 mm EFL and 25 mm clear aperture) are added to the system for illumination of the entire field of the recorded band of spots, including the data spots and the tracking band. This illumination has an unfiltered laser beam as its input, and the effect of the $C_1 + L_4$ combination is to focus a line of light over the rotating parallel data bursts. Lens L_5 , a 10X microscope objective, and L_6 then provide imaging of the tracking band and the data to the appropriate detectors. With the long lever arm of the readout optics, a ± 0.001 -inch movement of the spots on the film is magnified as much as a thousand times (determined



a. TRACKING SUBSYSTEM SIDE VIEW
(COMPONENTS IN DOTTED LINES ARE
ONLY USED DURING READOUT)



b. TRACKING SUBSYSTEM TOP VIEW
(COMPONENTS IN DOTTED LINES ARE
ONLY USED DURING READOUT)

FIGURE 3-10. THE TRACKING SUBSYSTEM



experimentally because an exact imaging situation between the film plane and the position detector does not exist in the breadboard). This position detector provides an error signal on the order of 0 to 10 volts for typical wander values. This signal is used as the input to the CCX-100 servo controller for GALVO₂, which in turn swings the mirror on GALVO₂ to correct for the data wander. Since large-scale data wander of the kind which the tracking system must compensate is a low-frequency effect (less than 10 Hz, typically), the G-300 PDT galvanometers can easily follow the coarse data wander.

3.3.3 Optical Subsystems

3.3.3.1 The Recording Configuration

The recording optical system has two primary design goals: efficient illumination of the acousto-optic page composer and diffraction-limited imaging of the AOPC data onto the film in the film transport. To accomplish the first goal, a 32-element TeO₂ AOPC developed as part of the HOLOMEM contract phase was installed in the breadboard configuration shown in Figures 3-11 and 3-12. The recording beam is provided by the large laser at the bottom of the first figure, a Spectra-Physics Model 125 helium-neon laser with an output power of 50 mW. After reflecting off the mirror M₁ and passing through a shutter used to switch the recording beam on and off during recording, the beam passes through a half-wave plate. The half-wave plate rotates the linear polarization angle of the laser beam so that the light exiting from the half-wave plate is polarized at an angle of 45° to the plane of the paper (and optical bench) in Figure 3-11. This is required to ensure that the light incident on the AOPC matches the 45° polarization angle required by the fast-shear mode TeO₂ acousto-optic crystal and thus to obtain maximum diffraction efficiency. Following this, the beam passes through an adjustable beamsplitter (later to be used to pick off the laser beam in readout) and an optical attenuator where the exposure level is set for recording. The beam then reflects

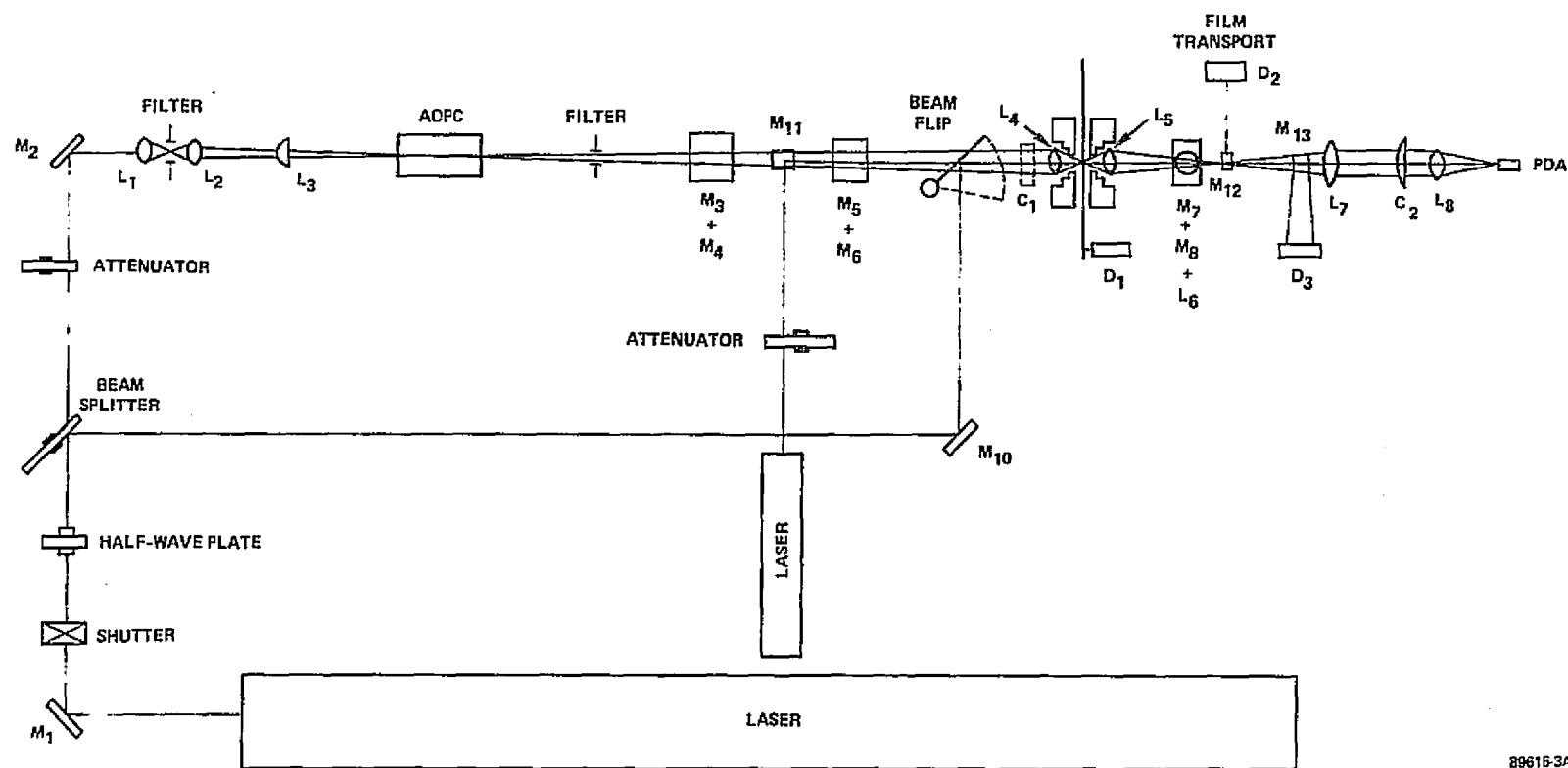
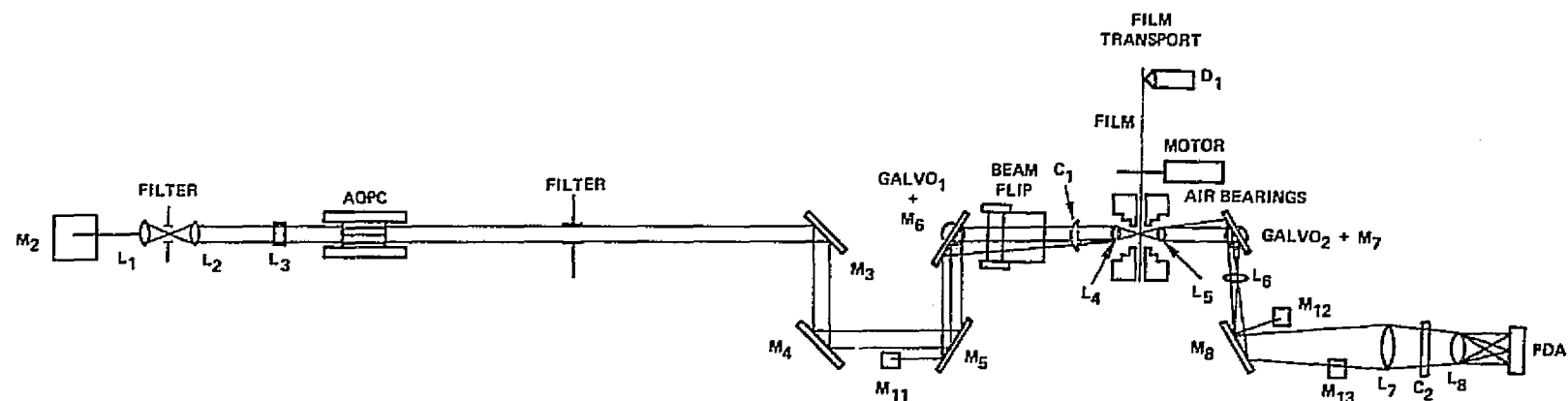


FIGURE 3-11. THE DIGIMEM BREADBOARD (TOP VIEW)

89616-3A



B9616 4A

FIGURE 3-12. THE DIGIMEM BREADBOARD (SIDE VIEW)





off M_2 , is expanded by L_1 (a 16 mm EFL, $f/2$, 10x microscope objective) and shaped by L_2 (a 100 mm EFL, 2-inch aperture spherical lens) and L_3 (a 2-inch aperture, 150 mm EFL cylindrical lens) to form a line focus on the AOPC. This line is sufficiently large to illuminate the eight data channels, the two data location channels and the byte sync bit. The illumination beam is actually longer than the required field of ~ 15 channels times 250 μm spacing from one AOPC channel to the next, or 3.75 mm; even allowing for spatial separation of the byte sync from the other channels to enable a separate mirror to pick off the byte sync signal in readout, this guarantees uniform illumination of the page composer.

The second design goal, that of optimally imaging the AOPC data onto the film, is far more demanding than the AOPC illumination requirement. Ideally, the lens L_4 should resolve 2-5 μm diameter spots at single-Rayleigh resolution. This then dictates the $f/\#$ of the lens performing this reduction, and an approximate formula for calculating this relationship is that the required $f/\#$ for a spot diameter $2w_o$ at wavelength λ is:

$$f/\# = \frac{w_o}{\lambda} \quad (3.5)$$

For $2w_o = 2$ to 5 μm , the required range of $f/\#$ s is from $f/1.6$ to $f/4.0$. Second, the lens must be physically small enough so that its barrel will fit the available space inside the air bearings of the film transport, as shown in Figure 3-9; this means the barrel diameter must be physically smaller than 17 mm. Third, the lens must have a minimum working distance to the image of greater than the air bearing thickness of 0.125 inches = 3.175 mm. In addition, the focal length of the lens should be as short as possible to minimize optical path lengths in the system. If, for example, a 100x reduction of the 250 μm AOPC channel spacing were required by a specification of 2.5 μm spot center spacings, a 25 mm EFL lens would require a minimum optical path of $100 \times 25 \text{ mm} = 2.5 \text{ m}$ separation between the AOPC and the imaging lens. Finally, the lens must be capable of covering a minimum $15 \text{ spots} \times 5 \mu\text{m/spot} = 75 \mu\text{m}$ field-of-view.



Lens candidates identified for use as the reduction lens L_4 are listed in Table 3-1. All the lenses listed, except the 20X conventional microscope objective, met the required specifications. The conventional 10X microscope objective was chosen because it both met specifications and was inexpensive (the unit cost is less than \$40). Other lenses, however, were evaluated to determine whether any dramatic improvement of performance could be expected if they were used in the breadboard; the results of these evaluations are summarized in Paragraph 3.4.3. With the EDSCORP 16 mm EFL 10X microscope objective selected, the breadboard was configured to yield a 3.5 μm spot center-to-center spacing, exactly at the midpoint of the required 2-5 μm range. To meet this specification, the AOPC-to-lens working distance d is given by:

$$d = \text{EFL} \left(\frac{1}{m} + 1 \right) \quad (3.6)$$

where m is the demagnification ($3.5 \mu\text{m}/250 \mu\text{m} = 0.014$) and the EFL is the effective focal length of the lens. In this case, $d = 16 \text{ mm} (1/0.014 + 1) \cong 1.16 \text{ meters}$. The lens-to-film plane distance d' is given by:

$$d' = \text{working distance} + m \cdot \text{EFL}$$

or

$$d' = 8 \text{ mm} + 0.014 \cdot 16 \text{ mm} = 8.22 \text{ mm}$$

At this reduction ratio, the 150 μm AOPC channel width would reduce to $150 \mu\text{m} \times 0.014 = 2.1 \mu\text{m}$ if the lens were capable of resolving this aerial image. The minimum aerial image diameter is, however

$$2 w_o = 2 \lambda f^\# = 2.53 \mu\text{m}$$

in the present case.

The final important consideration is the actual spot size recorded. Since the AOPC channels are 150 μm in width on 250 μm center spacings, this indicates that

TABLE 3-1
SELECTED REDUCTION LENS CANDIDATES

Reduction Lens	$f/\#$	Potential 2 w (μm)	Working Distance (mm)	Barrel Diameter (mm)	Field of View (μm)	Focal Length (mm)	Manufacturer
Ideal Lens	1.6 to 4.0	2 to 5	>3.175	<17	>75	<25	
10x Microscope Objective	2	2.53	~8.0	16 to 18	>75	16 to 20	Various Companies
20x Microscope Objective (Conven- tional)	1.25	1.58	~2.0	16 to 18	>75	8 to 10	Various Companies
Hastings Triplet (# 01-LAT-009)	1.18	1.49	7.5	10.0	>75	10.0	Melles Griot
20x LWD (# 1-M545)	1.25	1.58	4.60	15.8	>75	11.51	Olympus
40x LWD (# 1-M555)	0.91	1.15	3.42	15.8	>75	5.45	Olympus

ELECTRO-OPTICS

HARRIS





the 150 μm AOPC channel reduces to $150 \mu\text{m} \times 0.014 = 2.1 \mu\text{m}$ if the lens were capable of resolving this aerial image. Unfortunately, the minimum aerial image diameter, as computed previously, is 2.53 μm . To achieve a recorded spot diameter smaller than this is possible, however, by taking advantage of the fact that the aerial image intensity decreases with diameter and the film has a D-log Eslope greater than unity; this is illustrated in Figure 3-13. A long exposure, E_1 , would be necessary to record the diameter $2 w_1$ shown in the figure, but a shorter exposure E_2 will result in recording the spot diameter $2 w_2$. The center spacing of the spots, 3.5 μm , will remain constant regardless of the exposure because it is only a function of the reduction ratio. The spot diameter, however, will be a function of exposure and can therefore be varied according to system requirements by exploiting the nonlinear response of the recording medium.

One final feature of the recording system is the "once-around" detector, D_1 , mounted at a distance of approximately 1.8 inches from the radius of the film transport on the back plate of the transport. This detector is actually a "document presence sensor" consisting of an infrared emitter and detector combination. In use, as a white or silver circle glued on the film surface passes over the sensor position, the leading edge of the circle is detected by this combination because of the difference in IR reflectivity of the circle and the film. This output pulse is the "once-around signal" used in the control electronic subsystems for recording and readout.

3.3.3.2 Recording Material Selection

To specify the recording material for the DIGIMEM breadboard, a few considerations are fundamental. First of all, the medium selected must be sufficiently sensitive to the 632.8 nm wavelength laser light to allow recording of the 2.53 μm spots formed by the 10X microscope objective. If the input laser power is P_i , the system optical efficiency T , the spot diameter to be recorded $2 w_o$, the number of spots to be recorded in a single data burst N , and the exposure time per data burst t_e , then the intensity available per spot at the film plane is:

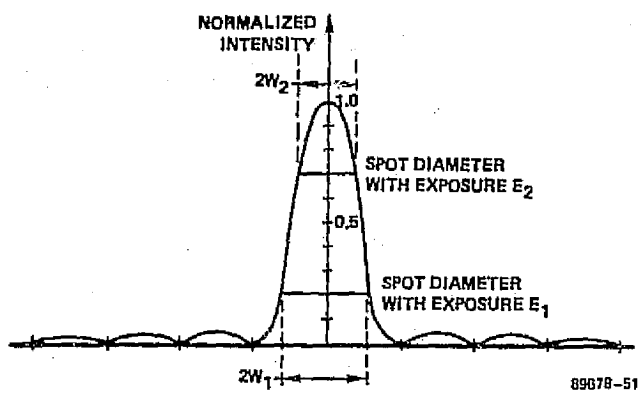


FIGURE 3-13. AERIAL SPOT INTENSITY AS A FUNCTION OF SPOT DIAMETER



$$I_f = \frac{P_i T t_e}{\pi w_o^2 N} \quad (3.7)$$

With $P_i = 50$ MW, $N = 11$ spots, $2 w_o = 2.53 \mu\text{m}$, $t_e = 25$ percent of the cycle time (or $t_e = 0.25 \times 8 \mu\text{s} = 2 \mu\text{s}$), and a worst-case optical efficiency of $T = 0.5$ percent because of the large number of uncoated optical elements in the recording path, the recording intensity per spot is:

$$I_f \approx 9000 \text{ ergs/cm}^2$$

Even allowing for reciprocity failure as a result of the relatively short exposure time, most high-resolution panchromatic photographic films easily meet this requirement. A second requirement is that the emulsion be capable of distinctly resolving the $2 \mu\text{m}$ minimum spot diameter expected to be recorded. A resolution specification of >1000 cycles/mm (equivalent to a 2X sampling of the spot diameter by the silver halide grains) is required to guarantee this. Further, the emulsion must be available on a flexible support, since photographic plates have been ruled out. In addition, a polyester (rather than triacetate) film base is desirable to obtain maximum dimensional stability. Finally, the material must be available in a 4 x 5-inch sheet format to satisfy the requirements of the floppy disc film transport.

Based on these specifications, the four photographic materials of Table 3.2 were compiled. All four film types meet all specifications except SO-285, which fails only on the base type requirement. Though the triacetate base is a present drawback for high-density optical spot recording, SO-285 is included because it is a positive working material, which is an attractive practical feature; all the other films are negative-working. A positive film gives clear logical ones and opaque logical zeroes, which is optimum in terms of maximizing signal-to-noise ratio. For negative-working emulsions, a reversal chemical process requiring a second development and fixing cycle



TABLE 3-2

SELECTED EASTMAN KODAK PHOTOGRAPHIC FILMS FOR SPOT RECORDING

Candidate Film	Exposure Required to Produce a Density of 1.0 (ergs/cm ²)*	Resolving Power (cycles/mm)**	Emulsion Thickness (μ m)	Base Type	Base Thickness (Inches)
649F Spectroscopic Film	900	>2000	6	Polyester	0.007
SO-173 Holographic Film	400	>2000	6	Polyester	0.004
SO-285 Direct Positive Laser Recording Film	30	1250	<4	Triacetate	0.005
SO-253 High-Speed Holographic Film	5-8	1250	9-11	Polyester	0.004

*All data relates to exposures from 10^{-3} seconds up to 1 second; at shorter or longer exposures, reciprocity failure may occur

**For a test object contrast of 1000:1



is necessary to accomplish this. A positive material would, therefore, be extremely desirable, despite its drawbacks in other aspects.

The results of evaluating these materials for spot recording are discussed in Paragraph 3.5 of this report.

3.3.3.3 The Readout Configuration

To read out the recorded data, the system requirements are very similar to those for recording; the recorded spots must be efficiently illuminated by a light source and these spots must be imaged with high-definition onto the photodetector array. To solve the illumination problem, the laser beam is picked off at the beam splitter (rotated to send the majority of the light down the read path) and reflected off M_{10} in Figure 3-11. Then the "beam-flip" mirror is rotated into the system optical path to reflect the reading beam down the optical axis. At this point a 50 mm EFL, 1 inch aperture cylindrical lens focuses the light in one dimension so that the image formed by the 10X, 16 mm EFL, microscope objective L_4 is a line image illuminating all 11 spots of the data bursts. (The lens spacings are set experimentally throughout the optical breadboard; in this case the spacing from C_1 and L_4 is approximately 25 mm.) The cylindrical lens C_1 and the beam-flip mirror are only used in the readout phase of system operation, and are designed for quick removal from the system during recording.

As for the imaging optics, there are several requirements. The enlargement lens L_5 must meet the same requirements as L_4 , but the readout system must in addition allow accessing of the data before it reaches the photodetector array. This is necessary both to enable visual checks on imaging and illumination quality and to readily pick off the tracking beam and the "byte sync" bit. For this reason the system of Figure 3-14 was designed for readout. The first lens, L_5 , was chosen to be a 10X, 16 mm focal length $f/2$ microscope objective identical to that used for the recording



HARRIS

ELECTRO-OPTICS

3-40

lens L_4 . The next major design requirement after this was to image the recorded spots at some point beyond M_8 in the breadboard. By using a 10X microscope eyepiece (focal length = 25 mm) as the lens L_5 , L_5 and L_6 form a projection microscope to image the spot data at the bit image plane to form an image of the bits which is approximately 0.54 inch long. At this magnification and with the 42.5 cm distance available between M_8 and the image plane, the tracking beam is picked off by mirror M_{12} and the byte sync bit is deflected by mirror M_{13} . The tracking band position detector, D_2 , and the byte sync detector, D_3 , are located alongside the main optical path. The bit image plane is maintained as a visual observation point for breadboard testing.

To provide final imaging of the spots onto the photodetector array, the first consideration is the size of the image field on that array. The RL64 array selected as the detector array has detector elements spaced on 0.002 inch centers with a spatial oversampling factor set at 4 elements per bit. For the 15-spot image field measured at the first bit image plane, this means that the size of the image field at the PDA plane must be $0.002 \text{ inch} \times 4 \times 15 = 0.12 \text{ inch}$. The required reduction ratio from the bit image plane is $0.54/0.12:1$ or approximately 4.5:1. To produce this reduction, a telescope imaging system consisting of a 9 inch EFL, $f/4$ lens L_7 and a 2 inch EFL, $f/2$ lens L_8 was selected; the resulting reduction ratio is given by the ratio of the focal lengths, or $9"/2" = 4.5$. (The lens separations recorded in Figure 3-14 for this section of the design vary slightly from the exact telescopic arrangement requiring L_7 and L_8 to be 9 inches + 2 inches = 11 inches away from each other and L_8 to be 2 inches—the focal length of L_8 —away from the PDA. This is the result of lens variations and accommodation of the exact magnification of the bit image plane formed by L_5 and L_6 .)

As a final design requirement, note that, with each bit spread over four 0.002 inch long detectors, the spot itself will spread over a 0.008 inch diameter area with conventional imaging. Since the detector area is only 0.002 inch x 0.002 inch, the detector array will detect less than 75 percent of the light in this case. As the light



HARRIS

ELECTRO-OPTICS

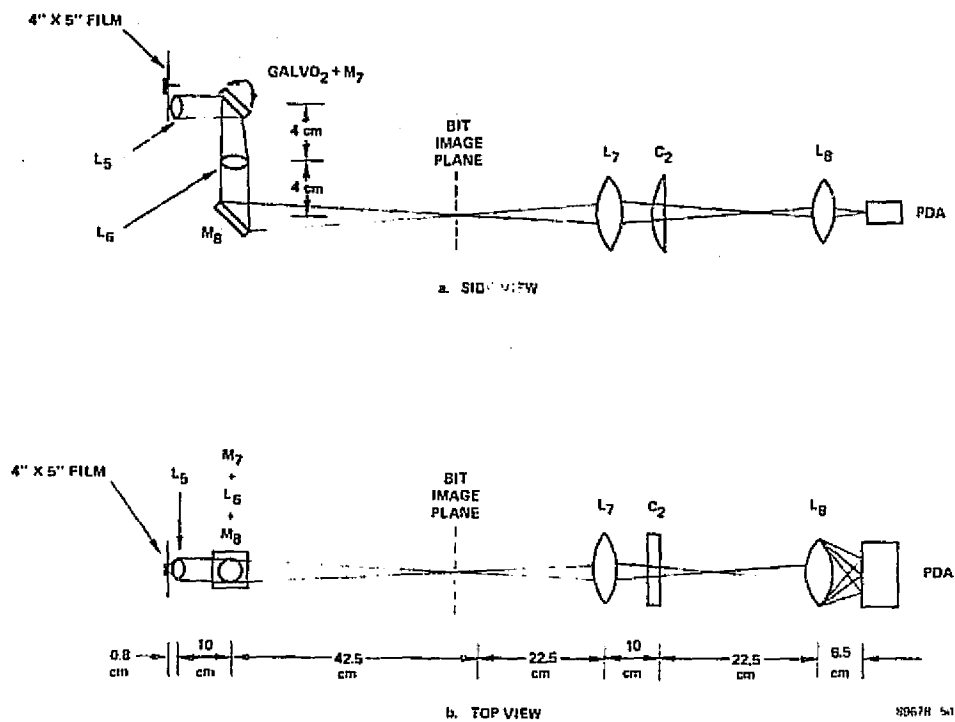


FIGURE 3-14. THE READOUT OPTICS CONFIGURATION



HARRIS

3-42

ELECTRO-OPTICS

budget discussion of Paragraph 3.3.1.2 made clear, this would eliminate too large a fraction of the output signal. For this reason, lens C_2 (a 150 mm, 2 inch aperture cylindrical lens) was placed in the readout optics to collect all available signal light from the dimension perpendicular to the linear array length onto the detector surfaces.

This then completes the readout optical configuration used in the breadboard experiments of Paragraph 3.3.3.3.

3.4 BREADBOARD EXPERIMENTS

3.4.1 The Film Transport

Based on the design requirements of Paragraph 3.3.2.1, the floppy disc transport was fabricated with the following final specifications: mechanical spacers set a gap of 0.010 inch between the two air bearings to accommodate both 4-mil and 5-mil film bases, valves were placed on the air bearing lines to maintain a constant bearing pressure of 15 pounds per square inch on each side of the film, and the required 150 rpm film speed was set by providing a motor input voltage of 4.6 volts.

To begin testing of the transport, experiments focussed on the use of the highest resolution recording material available, 50-173. Unfortunately, when this film was mounted in the transport, it was found that the recording medium always curled in the transport; further, the material always curled toward the air bearing with too high an air pressure. This often produced severe film scratching resulting from rubbing of the curled film against the air bearing. Besides the wear on the bearings, this friction would eventually reduce film speed, build up deposits on the film, and destroy recorded information through stripping of the emulsion or ferrotyping (the printout of a developed image where the unexposed emulsion had been scratched or dented on some emulsions). Further tests of the curl effect indicated that curl was observed whether the film base was coated with gelatin or not, that the direction of the curl was not affected by which side of the



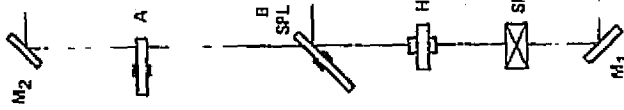
HARRIS

ELECTRO-OPTICS

3-4

base the gelatin was on, that the size of the air bearing gap is unimportant, that the larger the radius of the disc at the air bearing, the smaller the curl effect, and that the thinner the film base the more severe the effect; 4-mil bases curled almost three times as much as 7-mil bases.

To solve this problem, needle valves were installed on each of the two air bearings to precisely adjust the pressure on each side of the film. In addition, curl could be relieved either by attaching an air jet to blow across the film sheet at the top of the transport or by placing a cover plate over the front of the transport (which may trap air around the film and produce the same effect as the air jet). The reasons for the curl effect and its solution are not as easy to state, however. One hypothesis was that the air forced through the air bearings becomes water-saturated by the time it reaches the film, and that expansion of the film base in the presence of high humidity is occurring. Unfortunately, this would argue for the film curling away from the bearing with the higher air pressure, which is not the case. Another concept was the temperature drop of the air because of sudden expansion immediately after it leaves the air bearing, which would cause the side of the film base facing the bearing with the higher air pressure to contract. This suggests the need for having either a large recording radius or an air jet to allow the film to warm up again after passing through the air bearing. Initial experiments on measuring the temperature drop at the air bearing yielded a value of about 0.2°C difference relative to ambient per 5 psi of air pressure, indicating that this is probably not the only cause of curl; this is especially confusing when it is noted that it takes up to 10°C difference to produce equivalent curls outside the bearings. The cover plate and the air jet may, in fact, reduce curl by aerodynamic means - first, because it restores a symmetry to the transport and, therefore, a symmetry to the airflow, and second because it compensates for an asymmetrical airflow in the transport. Without them, air flowing across the film from the air bearings is trapped against the plate on the left and escapes on the right as shown in Figure 3-8. Because the curl



HARRIS

ELECTRO-OPTICS

3-44

can be turned toward the open side of the transport by changing the needle valves, system asymmetry is clearly not the most important effect, though a significant one. Despite the lack of any single cause to which this curl phenomenon can be attributed, eliminating the asymmetry and placing needle valves on the air bearings allowed the film to rotate without curl or scratching.

With the curl effect controlled, recordings were made on the SO-173 emulsion in the film transport and used to quantify the performance of the transport. By monitoring the system's byte sync detector output, the 150 r/min film velocity stability was verified to be between 5 percent and 10 percent, well within specifications. Further from observation of hundreds of spots recorded on the transport without changing the optical reduction ratio of the acousto-optic page composer, it is clear that spot growth as a result of axial film instability in the air bearing is being maintained to less than 20 percent; this would appear as a variation in size of a spot from one recording location to the next, and to the estimated 20 percent measurement accuracy of this spot diameter, this variation is not visible. Based on the graph of Figure 3-7 and the aerial image spot diameter of $2.5 \mu\text{m}$, this means that the air bearings are maintaining depth-of-focus of better than $\pm 3.5 \mu\text{m}$.

One last consideration in the use of the film transport is film replacement positioning repeatability, an extremely important factor if data wander is to be held to a minimum. In the present transport, when a sheet of film is remounted after development, what once was a band of data recorded on a perfect circle reads out like a circular band of data mounted off-center by up to 0.002 inch. Because the data is simply imaged onto the photodetector array, this means that a band of data $10 \text{ spots} \times 3.5 \mu\text{m} = 35 \mu\text{m}$ long wanders almost twice the height of the data band during one revolution of the film transport. Since the hole punched in the film matches the transport mounting post to $\pm 2 \times 10^{-5}$ inch, it is clearly not a positioning error on the post which is causing the problem. Instead, it appears that the film is twisted or buckled when the mounting hub is screwed



down on it; this would effectively distort the original perfectly circular ring of data. A mounting method which would eliminate this problem would be to provide a permanently bonded hub on each film disc before recording. This approach was rejected in favor of developing the data tracking subsystems, which could be required if data wander in excess of 0.001 inch were unavoidable in the system design.

3.4.2 Data Wander Correction and Tracking

The tracking subsystem described in Paragraph 3.3.2.2 was assembled in the breadboard as designed using two General Scanning G-300 PDT temperature-regulated galvanometers with a CCX-100 servo controller attached to each galvanometer. To determine the initial tracking galvanometer settings for the CCX-100, GALVO₁ was used as a data wander simulator. Using a two cycle/second sinusoidal drive signal for GALVO₁ to simulate data wander of approximately ± 3 thousandths of an inch on the readout, the reflected tracking band was detected by the position detector and this output signal was used as the input to GALVO₂'s CCX-100 servo controller. By adjusting the gain settings on the output of this controller, it was possible to compensate for the motion of GALVO₂ so that the output beam wander was approximately 5 percent of the input beam wander. The wander compensation was optimum for a gain setting of 3.28 on GALVO₂'s CCX-100.

In use in the actual system, the tracking concept requires the recording of the tracking band on film as well as the readout of that band. In recording, the optical system was configured to record a band approximately 9.6 μm wide spaced at a distance of approximately 31 μm from the "byte sync" track. The relative densities of the track and background on reversal-processed SO-173 were 1.28 and 4.40, respectively, corresponding to an approximate recorded contrast ratio of 31 dB.

In readout, the high contrast radio tracking band was illuminated by the tracking beam laser and reflected to illuminate the position detector. Despite a lateral



film position wander of greater than ± 0.002 inch, this coarse data wander correction system was found to minimize this wander to less than ± 3 bits of data movement. This made it possible for the electronically agile photodetector array to electronically compensate for the remaining data wander.

3.4.3 Key Optical Components

3.4.3.1 Microreduction and Enlargement Lenses

Since the key components in the optical system are the microreduction lens L_4 used to image the AOPC spots onto the film and the enlargement lens L_5 used to image the recorded spots onto the photodetector array, these elements were the focus of the experimental lens testing on the breadboard.

The first of the possibilities evaluated was a Hastings triplet lens manufactured by Melles Griot (Part Number 01-LAT-009). This appeared to be an excellent choice, with a potential single-Rayleigh spot resolution of $1.49 \mu\text{m}$ (as derived in Paragraph 3.3.3.1). It was mounted in a brass barrel and potted in a manner that reduced the clear aperture by about 0.03 inch and added an additional 0.06 inch to the outside diameter of the lens element. Next, it was inserted in position in the optical system of Figure 3-11 to image the page composer bits to an image plane with spots on approximately $2.2 \mu\text{m}$ center spacings; this corresponds to an AOPC-to-lens separation of about 1.1 meters. When this image was then magnified by a 10X microscope objective and the 10X eyepiece of the readout optics of Figure 3-14, the lens exhibited severe comatic and astigmatic aberrations. By tilting the lens less than a degree of arc, the aberration structure could be changed significantly: from minimal aberration and poor spot resolution to a point beyond which even the structure of the spot pattern was impossible to determine. The Hastings triplet was therefore rejected as a potential candidate for the microreduction lens.



HARRIS

ELECTRO-OPTICS

3.

The second family of lenses considered, was the LWD (long-working-distance) series, available from several manufacturers. These are microscope objectives designed for flat-field imaging in applications where high magnification of delicate specimens is required. (A typical use for such lenses would be in the examination of fragile integrated circuits before packaging.) Two such lenses considered were the Olympus 20X LWD and 40X LWD lenses as specified in Table 3-1. Because of the high cost of such lenses, running typically to between \$350 and \$500, and because it was felt that the potential 40X LWD resolution of $1.15 \mu\text{m}$ might be beyond the depth-of-focus stability of the film transport, only the 20X LWD lens was purchased for evaluation. It was tested initially by imaging high-resolution targets through a conventional microscope and found to resolve through Group 9-4 of an Itek USAF-type resolution target, for a net resolution of in excess of 724 cycles/mm. In further testing, it was found to maintain this resolution over an angular field of greater than 3.5° , and was in fact used for the microscope photographs of Figure 3-19. Though not used in the present phase of the DIGIMEM breadboard experiments, its excellent resolution and short focal length (resulting in a short object-to-image optical path, a key consideration in prototype design) make it an excellent candidate for multichannel recording.

The final set of lenses considered was the conventional line of short-working distance biological-type microscope objectives. For this investigation, the 10X and 20X Edscorp objectives were selected because of their ready availability and low cost (less than \$50 each in small quantities). In testing conditions identical to those used to evaluate the 20X LWD objective, the 10X objective demonstrated a resolution of over 512 cycles/mm over about a 7° field. The 20X quality, unfortunately, proved to be not even as good as the 10X resolution; it resolved only up to Group 8-4, or 362 cycles/mm, on the resolution target. The poor performance of this conventional 20X objective, achieved over the same 3.5° full angular field as the 20X LWD objective, may be the result of a design trade-off sacrificing maximum resolution for gaining the 20X magnifying



power at minimal cost. Accordingly, because of its high resolution, large field size and low cost, the 10X conventional microscope objective was selected as the system's micro-reduction lens L_4 and enlargement lens L_5 .

Once in the system the page composer's 15-bit image field was translated across the 10X objective entrance pupil to determine the maximum number of bits which could be simultaneously recorded in a data burst. This was accomplished by rotating the mirror on $GALVO_1$ and monitoring the output bits visually on the image plane in the readout optics. By doing this it was found that, although bit resolution was maintained for a field approximately 100 bit spacings wide (at the $3.5 \mu m$ bit-to-bit spacing on the film plane), the bit intensity began to roll off dramatically after moving more than 10 bit spacings off the optical axis. The conclusion was that the 10X objective's recording and readout field should be held to the 10 data spot field size selected as the single band size. This would allow for severe data wander and yet maintain the readout illumination required for maximum signal-to-noise ratios in readout.

3.4.3.2 Readout Illumination Devices

In the readout illumination scheme discussed in Paragraph 3.3.3.3, a laser beam illuminates the cylindrical lens C and the 10X microscope objective L_4 to form a line focus on the film. In the breadboard system design, the source for this illumination beam was to be a field component, if possible, so that there would be no need for realigning the system between recording a film disc and reading it out. To do this, two methods were tried.

The first of these was to use a pellicle at the position of the "beam-flip" mirror in Figure 3-11. This pellicle was a $7 \mu m$ thick polymer stretched over a 2 inch clear aperture elastic membrane and coated for maximum reflectance. As a mirror for the read path, the pellicle concept satisfies the requirements for a means of bypassing



the low optical efficiency AOPC path in the illumination system for readout (and thereby guaranteeing the maximum readout intensity), acts as a fixed mirror which can be in the middle of the recording optical path because it is transparent, and is thin enough that the membrane will not introduce astigmatism to the imaging path during recording, unlike a conventional glass beam splitter. During testing, however, the membrane developed a hairline scratch on the mounting surface of the pellicle despite meticulous care in handling the device. This scratch propagated to the center of the membrane and the pellicle shattered. Because of the overly fragile nature of this pellicle, the use of pellicles in future systems was rejected.

As an alternative to this approach, the "beam-flip" mirror was introduced into the system. It consists of a mirror mounted on a rotating panel which is swung out of the optical path during recording. During readout, it is flipped back into the optical path and set against an adjustable micrometer pivot. Though not a fixed mirror, it has performed well and is a reliable means of introducing the readout illumination beam with minimal adjustment.

3.5 RECORDING EXPERIMENTS

The recording experiments described subsequently categorize the performance of the DIGIMEM breadboard for high signal-to-noise, multichannel optical spot recording. All experiments were performed using the breadboard configuration described in Paragraph 3.3.3.1 of this report.

3.5.1 Film Curl

To begin the recording experiments, samples of all the potential recording material candidates identified in Paragraph 3.3.3.2 were acquired for testing. To narrow the field of candidates, the first test which all recording films had to pass was to demonstrate minimal film curl in a floppy disc film transport. The Kodak 649F and SO-173 samples passed easily, with the 0.004 inch thick SO-173 demonstrating slightly more curl than the 0.007 inch thick 649F. The Kodak SO-253 and SO-285 films, however,



showed substantial film curl and were eliminated from consideration early because of this. The SO-285 curl appears to be related to its triacetate base and curl set during storage on a 9.5 inch x 100 foot roll. The only explanation for the curl of SO-253 being greater than that of SO-173, both of which are emulsions coated on stable 0.004 inch polyester bases, appears to be that the SO-253 emulsion thickness of 11 μm is significantly greater than the SO-173 emulsion thickness of 6 μm . With as much curl as these films exhibited, it was impossible to use either SO-283 or SO-285 in a Tegrilas air bearing system.

3.5.2 Microscopic Spot Shifting

When data is recorded on the microscopic scale required by the DIGIMEM design concept, an important consideration is the degree of film emulsion and base distortion which may result from conditions of high temperature or high humidity, or even normal processing. The environmental integrity of the recording material must be preserved, since even fractional recording material distortions could result in major data wander and spot spacing problems.

To quantify the effects of environmental conditions on film, the first decision required the selection of a film for study. Since a triacetate base is considerably more unstable than a polyester base, obviously only polyester base materials need be considered. Then, since volume packing density was expected to be important in a future system design, it was decided that only the 0.004 inch polyester base materials need be candidates for this study. The thinner base, because it should be less stable than a thick base, provides a "worst-case" example for environmental testing. This narrowed the field to SO-253 and SO-173 films. Because of SO-253's film curl problems, SO-173 was ultimately selected for testing.

Next, a breadboard experiment was configured with a helium-neon laser, two beam-expanding systems (consisting of a 10X microscope objective, a pinhole spatial filter and a collimating lens), and a vacuum film holder. The two beam expanders were configured to be coincident on the film holder at an angle of $\theta = 8.7^\circ$ with respect to each other. With proper exposure and processing (developed for 5 minutes in D-19 at



room temperature, stop for 30 seconds, and fix for 5 minutes in rapid fix), this produced a sinusoidal grating on the emulsion with a grating frequency of

$$\nu = \frac{\sin \theta}{\lambda} \quad (3.8)$$

or $\nu = 240$ cycles/min for $\theta = 8.7^\circ$ and $\lambda = 632.8$ nm.

To determine the environmental sensitivity of the recordings, a grating subjected to some environmental distortion was overlayed on an undistorted reference grating. If the distorted grating had changed its dimensions, had a new grating frequency ν_2 , and the original reference grating had a frequency ν_1 , then when the two gratings are overlayed they produce a beat frequency $\Delta\nu$ equal to:

$$\Delta\nu = \left| \nu_1 - \nu_2 \right| \quad (3.9)$$

By measuring the beat frequency, the percent distortion can be calculated as

$$\text{Percent distortion} = \frac{\Delta\nu}{\nu_1} \quad (3.10)$$

The summary of these recording experiments appears in Table 3-3. The results indicate, first of all, that SO-173 is dimensionally stable under even severe environmental conditions to better than 0.30 percent. Secondly, while processing alone produces dimensional variations of up to 0.10 percent, there is evidently a shrinkage of 0.20 percent relative to the 0.040 inch thick 649F emulsion glass plate sample. Also, reversal processing of the SO-173 film with process 2460 (described in Paragraph 3.5.4) does not produce distortions greater than 0.14 percent, which is fortunate if reversal-processing is required. In the present breadboard, even the maximum 0.28 percent distortion will only amount to a $0.1 \mu\text{m}$ band spacing increase over a ten spot field of spots on $3.5 \mu\text{m}$ centers. On a larger image field, however, these distortions could become significant.



TABLE 3-3

PERCENT DISTORTION OF SO-173 EMULSION AND FILM BASE FOR VARIOUS DEVELOPMENT AND ENVIRONMENTAL CONDITIONS

<u>Experimental Condition</u>	<u>Percent Distortion</u>
Distortion as a result of normal processing*	0.10
649F emulsion on 0.040 inch glass plate sample	0.20
Reversal-processed film (process 2460)	0.14
After incubation at 40° F for 4 hours	0.10
After incubation at 95° F for 1 hour	0.14
After incubation at 170° F and 92 percent relative humidity for 1 hour	0.28
Film processed in D-19 for 5 minutes at 95° F	0.17

NOTE: All samples were processed identically to the reference and free-air dried for 24 hours before subjected to the conditions noted. The percent distortions were measured 24 hours after the tests were completed.

*To establish a reference for measuring distortion, samples of SO-173 film were exposed and processed (for 5 minutes in D-19 developer at 68° F, for 30 seconds in stop bath, and for 5 minutes in rapid fix) at the beginning of the experiment. By comparing these samples against one another, a mean distortion of 0.10 percent was determined to be the result of normal processing variations.



3.5.3 Bleaching of the Sensitizing Dye in SO-173 Film

An inconvenient feature of the SO-173 film type is the green sensitizing dye used to increase the film's sensitivity. Though especially apparent in that it becomes virtually opaque during simulated machine processing in D-19 at temperatures above 90° F, the dye still causes a base density of more than 0.10 D after processing at 68° F in D-19. One possibility for eliminating this residual dye density was to bleach the emulsion with a relatively weak oxidizing agent to clear the dye without damaging the recorded information.

As a preparation for this experiment, an incandescent white light source was used to contact copy an Itek USAF-type resolution target on eight samples of SO-173 film. The transferred resolution was visually measured to be that of group 8-5, or approximately 362 cycles/mm. These samples were then bleached in various concentrations of the commercial bleach Clorox (5 percent sodium hypochlorite). To determine the effect of the bleach, the resolution targets were reevaluated for changes in image resolution. In addition, microdensitometer traces were recorded on four areas of the film: the large unexposed areas, the large exposed areas, the microscopic areas of the resolution target where the film was unexposed, and the microscopic exposed areas of the target. Processing was for 5 minutes in D-19 at 68° F.

The results of the experiment were mixed. The 3 percent solution of Clorox recommended by Kodak removed most of the dye within 15 seconds, but also strongly attacked the emulsion. A weaker 0.5 percent solution performed its task more slowly, as shown in Figure 3-15, but it too produced evidence of emulsion damage. In less than 15 minutes of soaking, for example, the image density decrease by from 0.1 D to 0.03 D and some emulsion mottling was visible. Milder soaking solutions have less disastrous effects on the emulsion, but they also produced minimal changes in the dye density. Because of the relatively minor advantage of using Clorox or similar bleaching agents to oxidize the SO-173 sensitizing dyes and the great disadvantage of reducing the emulsion resolution and spot signal-to-noise ratio, it was decided to use SO-173 without bleaching out the dye.

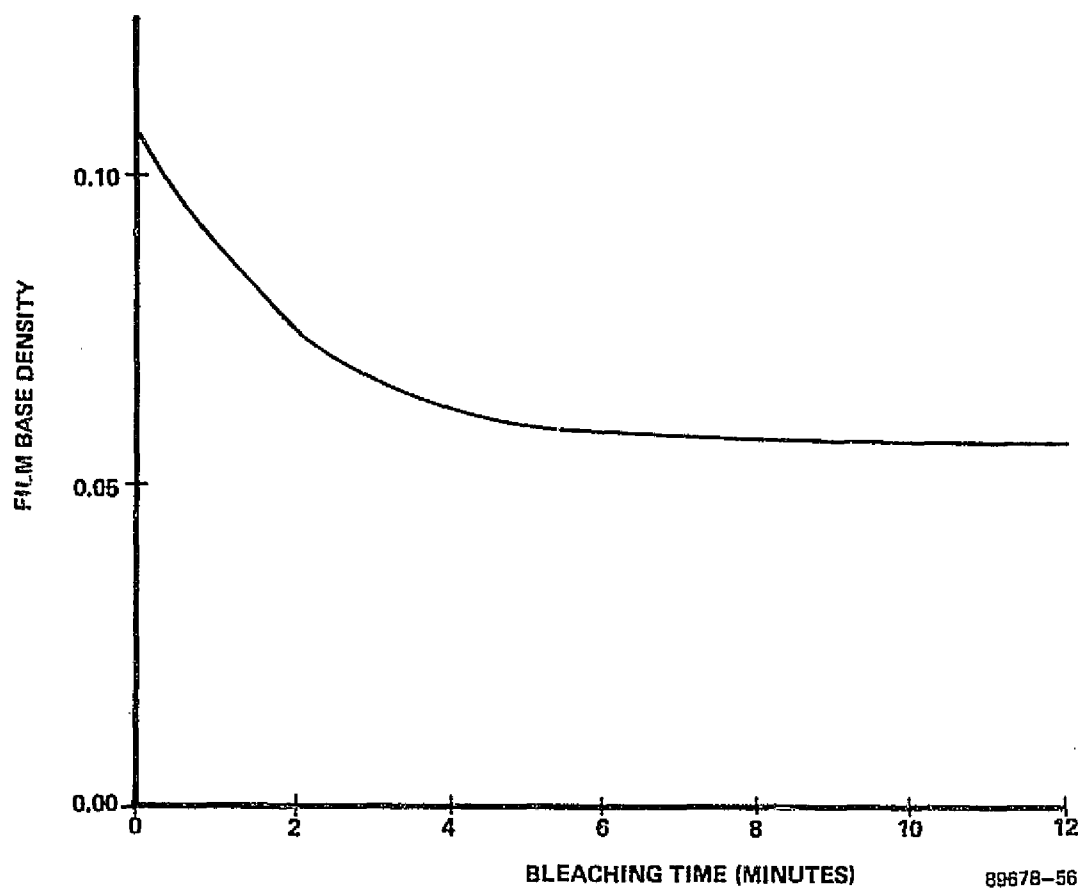


FIGURE 3-15. SO-173 BASE SENSITIZING DYE DENSITY AS A FUNCTION OF SOAKING TIME IN 0.5 PERCENT CLOROX SOLUTION



HARRIS

ELECTRO-OPTICS

3.5.4 Spot Recording

To begin the spot recording experiments, it was first necessary to determine whether the mountings on the recording end of the optical breadboard were sufficiently stable to maintain the optical depth-of-focus for the minimum spot size to be recorded. To test this in a manner that would eliminate any depth-of-focus problems on the film transport, the first recording experiments were conducted using an X-Y microfiche film transport at the film plane instead of the floppy disc. A vacuum platen was used as the film holding mechanism, and 649F 4 x 5 inch, 7-mil polyester film was used for recordings. Using a 10X microscope objective as the imaging lens, the breadboard was configured so that spots would be recorded at approximately a 100:1 reduction ratio. Since at this early stage the control electronics for recording had not been fabricated, these initial tests were made using an integrated circuit "clock" and pulse generator to produce recordings on the film at a total data rate of 10^5 bits/sec. The results of this experiment, shown in Figure 3-16 indicate that the 8-bit data bursts maintain proper focus during the recording and demonstrate that the mountings for the optical components in the breadboard were sufficiently stable.

In the second phase of experiments, the breadboard was configured as described in Paragraph 3.3.3.1 with the recording data burst rate set at 125 kHz (for a net user recording rate of $8 \text{ bits} \times 125 \text{ kHz} = 1 \text{ MHz}$). Data was loaded into the PROM's, used as the recording system memory banks, in the form of human-readable alphabetic characters; this was done to make any recording errors readily recognizable to the eye under microscopic examination. The data burst recording time, the exposure time for each of the spots, was set at $2 \mu\text{s}$. This meant that, although a perfectly circular spot was recorded, it would acquire an elliptical shape because of film movement during that $2 \mu\text{s}$ exposure. Since the data burst recording rate is 125 kHz, the spot-to-spot cycle time is $8 \mu\text{s}$, and the eccentricity of the elliptical blur is 25 percent. All the remaining recordings during this investigation were recorded with the settings just described, a recorded spot center spacing of $3.5 \mu\text{m}$, and 4 x 5 inch SO-173 film on a 4-mil polyester base as the recording medium.



HARRIS

ELECTRO-OPTICS

ORIGINAL PAGE IS
OF POOR QUALITY

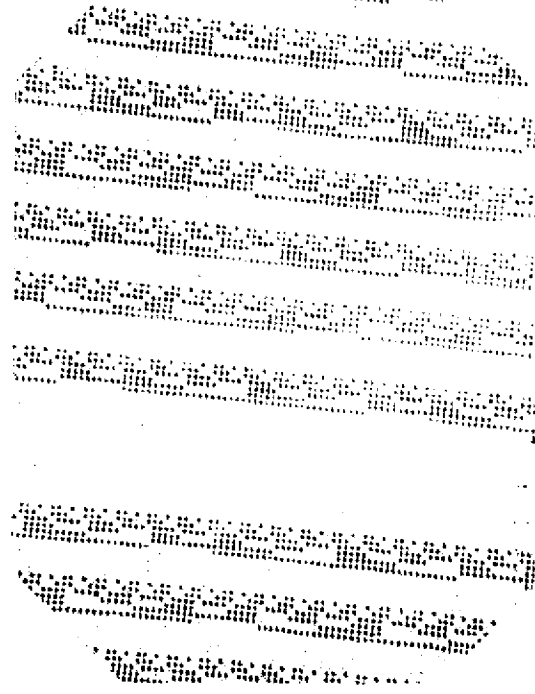


FIGURE 3-16. KODAK 649F MICROFICHE-TRANSPORT SPOT RECORDINGS
(2.0 μm SPOT CENTERS)



In initial experiments, the SO-173 film was processed conventionally in D-19 developer for 5 minutes, in the stop bath for 30 seconds and in rapid fix for 5 minutes; a typical result is shown in Figure 3-17. (The irregular letter shapes recorded on the film were the result of programming errors in the first set of PROM's implemented in the DIGIMEM breadboard, and not because of any electronic or optical problems.)

At these data rates and with this emulsion type, an initial result of this study was that there is some reciprocity failure on SO-173 film. For a $2\text{ }\mu\text{s}$ exposure, for example, each recorded spot required 1.52 pJ of 632.8 nm laser light per spot, for a net exposure of more than 3000 ergs/cm^2 based on an aerial spot size of $2.53\text{ }\mu\text{m}$. The exact amount of reciprocity failure is difficult to determine because of the relative inaccuracy of microdensitometry for the spot sizes under discussion. In addition, some recording spot size effects are undoubtedly present here, in that as the recorded spot grows smaller and closer to the photographic grain size the recording material sensitivity will undoubtedly change from what it was for large-area exposures. Accordingly, the most accurate interpretation of results would be to present a plot of the recorded spot size as a function of the 632.8 nm exposure calculated using the aerial spot size diameter of $2.53\text{ }\mu\text{m}$. These data are presented in Figure 3-18. These results remained accurate for up to 3 hours between the original recording time and the processing time, indicating that there is minimal latent image decay for this type of emulsion and recorded image.

An additional observation of the conventionally-processed SO-173 experiments was that the spots were resolved and well shaped, but had low contrast (a consequence of the Eberhard effect). For this reason, reversal-processing of the film using Process 2460 was adopted for the remaining recording experiments. Process 2460 involves bleaching out the developed silver particles of the image, followed by exposure and redevelopment of the background. The result is that the spots appear as clear information on an opaque background. The steps of Process 2460 are summarized in Table 3-4.

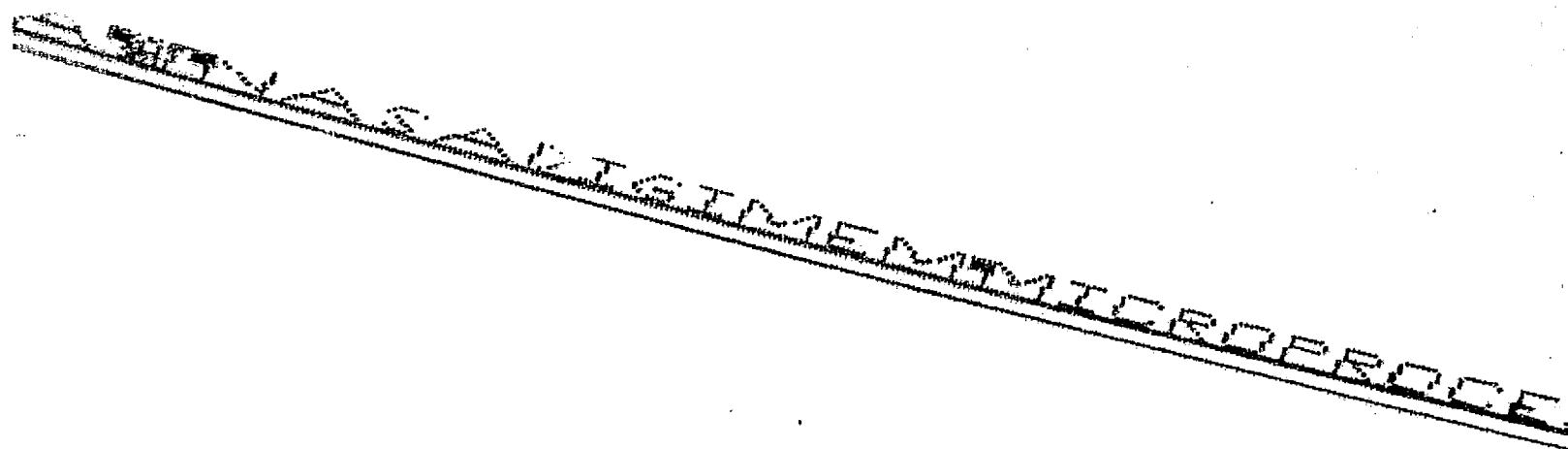
Using this chemical development process, a $2\text{ }\mu\text{s}$ exposure time, and newly-programmed PROM's as the data source, spots were recorded on $3.5\text{ }\mu\text{m}$ centers with a net exposure of 22.3 pJ per spot instead of the 15.2 pJ per spot for negative-processed



HARRIS

ORIGINAL PAGE IS
OF POOR QUALITY

ELECTRO-OPTICS



89678-48

FIGURE 3-17. CONVENTIONALLY PROCESSED SPOT RECORDINGS ON
SO-173 FILM (3.5 μ m SPOT CENTERS)



HARRIS

ELECTRO-OPTICS

3-59

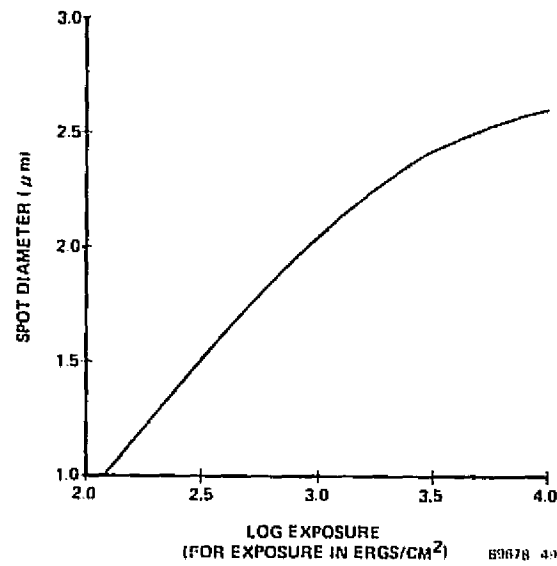


FIGURE 3-18. SPOT SIZE AS A FUNCTION OF EXPOSURE ON SO-173 FILM
(FOR 2 μ s EXPOSURES AND AN AERIAL SPOT DIAMETER OF 3.5 μ m)



HARRIS

ELECTRO-OPTICS

3-60

TABLE 3-4

REVERSAL PROCESS 2460

1.	Pre Wet*		90 Seconds	70° F
2.	Drain		1 Minute	
3.	Develop	D-19	7 Minutes	70° F
4.	Rinse		30 Seconds	70° F
5.	Bleach**		45 Seconds	70° F
6.	Rinse		1 Minute	70° F
7.	Turn on Room Lights			
8.	Clearing Bath†		30 Seconds	70° F
9.	Rinse		30 Seconds	70° F
10.	Reexposure		15 Seconds	100 Watt Bulb
11.	Redevelop	D-19	3 Minutes	70° F
12.	Fix		3 Minutes	Kodak Rapid Fix
13.	Wash		10 Minutes	70° F

Agitate once every 10 seconds for the first minute, then every 30 seconds thereafter.

*Pre Wet

Kodak Photo Flo 200 dil 100:1
Two drops Kodak Anti Foam

**Bleach R-9

Distilled Water 1.0 liter
Potassium dichromate 9.5 g
Sulfuric Acid (concentrated) 12.0 mil

†Clearing Bath R-21

Water 1.0 liter
Sodium Sulphite (Anhyd) 50G
Sodium Hydroxide 35G

Allow a few seconds drain between each step.



HARRIS

ELECTRO-OPTICS

3-61

recordings. The results of this experiment are shown in Figure 3-19. The recording format has the galvanometer tracking band at the bottom, the "byte sync" track directly above it, the two data location bit tracks above that, and above all of these the actual user data. As the pictures show, the reversal-processed approach yielded a dramatic increase in information signal-to-noise ratio. With a background density of approximately 4.4 D, the recordings were measured from relative density differences to have a spot signal-to-noise ratio of 15 to 20 dB across track (within a data burst) and 20 to 30 dB along track (from one data burst to the next).

Several other observations can be made about these photographs. First of all, spots recorded in isolation in a data burst (as in the center of the "M" and in the top and middle arms of the "E") appear larger than those recorded adjacent to other spots in a data burst. This marginal decrease in spot size for adjacent spots, a photographic anomaly, known as the Kostinsky effect, is not enough to cause concern in readout (where a smaller spot might mean a lower transmitted signal on the photodetector array). In addition, there appears to be a duty cycle effect in that, when there are fewer spots in the user data section of the data burst, the remaining spots grow larger. This is especially evident on the "byte sync" spot, which was deliberately made dimmer to increase the modulation of the "byte sync" signal. This "loading" effect is probably an electrical loading as a result of driving multiple channels with a single page composer driver card; when one channel is switched off, the remaining channels are driven harder. This is clearly not a problem in a prototype design where each individual AOPC channel will be driven by a separate driver electronics package.

3.6 READOUT EXPERIMENTS

For the readout experiments, all the components were fabricated and arranged as described in Paragraph 3.3.3.3 of this report. Reversal-processed SO-173 film recordings were placed in the transport, the film was rotated at the required angular velocity and the tracking subsystem put into operation. The "byte sync" signal was connected to the read electronics and spots were imaged on the electronically-agile

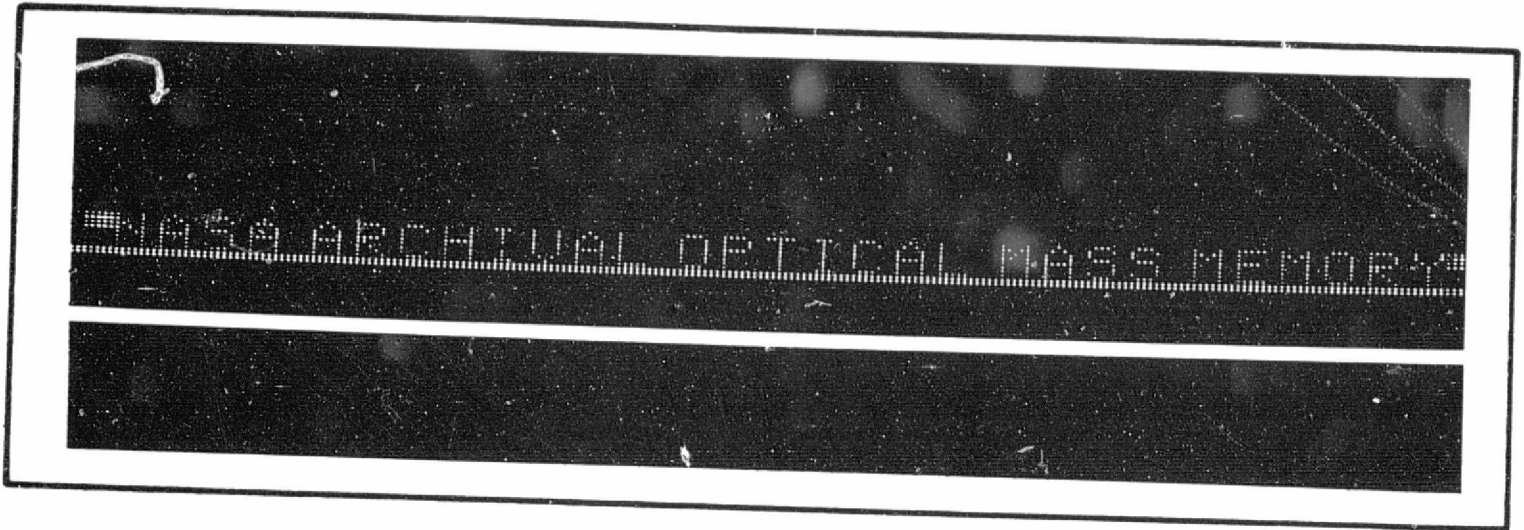


HARRIS

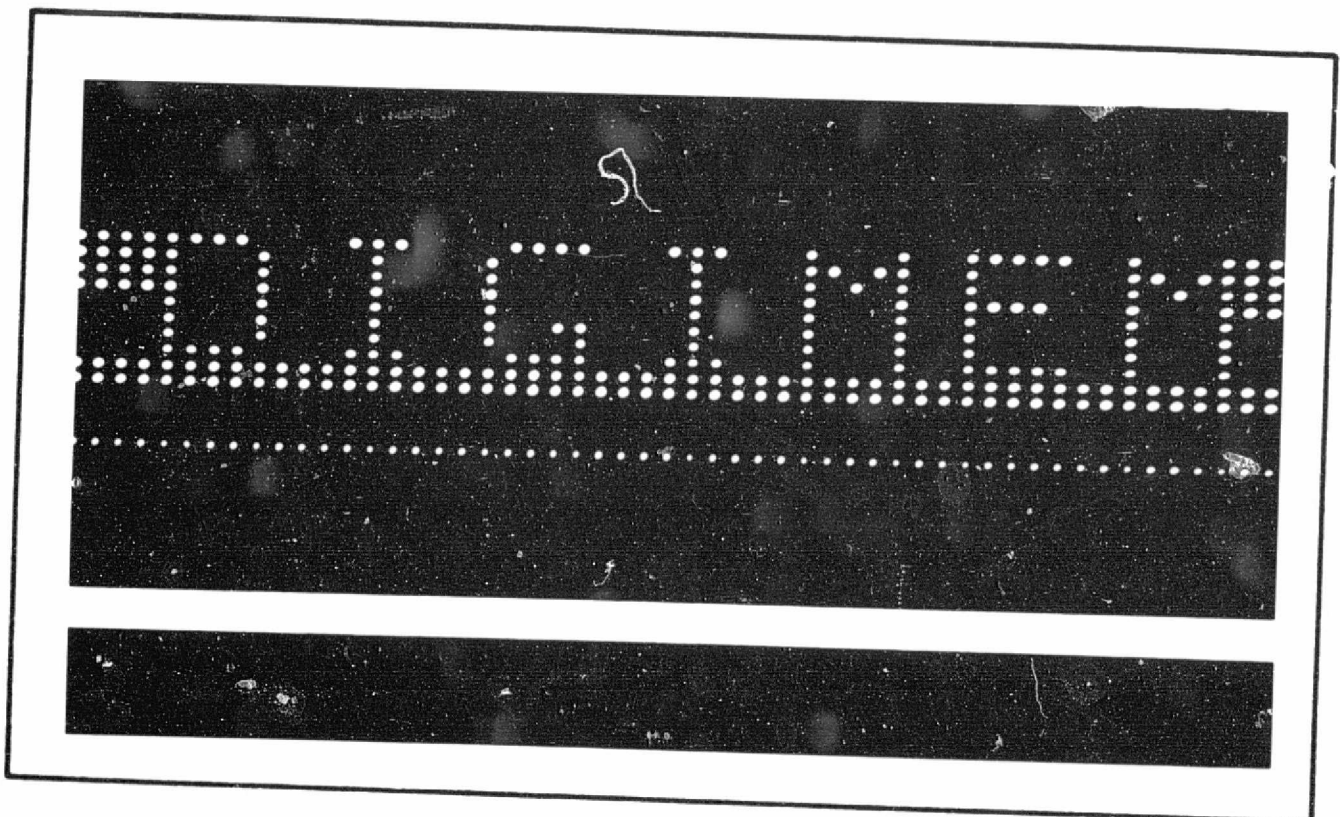
ELECTRO-OPTICS

3-62

ORIGINAL PAGE IS
OF POOR QUALITY



a. 240X MICROSCOPIC MAGNIFICATION OF
RECORDED DIGIMEM SPOTS



b. 860X MICROSCOPIC MAGNIFICATION OF
RECORDED DIGIMEM SPOTS

89678-45

FIGURE 3-19. REVERSAL-PROCESSED SPOT RECORDINGS ON
SO-173 FILM (3.5 μ m SPOT CENTERS)



HARRIS

ELECTRO-OPTICS

3-63

photodetector array shown in Figure 3-20 with spots on four detector spacings, or 4×0.002 inch/detector = 0.008 inch spacings.

The raw optical data signals detected by the photodetector array had an average 5 dB signal-to-noise ratio, down considerably from the recorded 15 to 20 dB signal-to-noise ratio across track; this SNR varied up to $\pm 15\%$ around the disc. The decrease in output signal-to-noise relative to recorded SNR is primarily because of the large number of lenses and mirrors between the film plane and the photodetector array image plane. Since most of these lenses would be unnecessary in the one-step imaging system of a prototype (as compared to the complicated breadboard configuration requiring a visual image plane in the readout plane), this is not considered to be a major drawback to the design of an engineering model. Other factors which contribute to low SNR are illumination rolloff at the film plane and the fact that the PDA is reading out at near the peak of its capabilities, 8×10^6 detector elements/sec or 10^6 data bits/sec.

With the detector array threshold set to detect an optical signal as a logical "one" bit if three out of the four detectors assigned to that bit produce a voltage above the threshold, the photodetector array converted the optical signals to bits and successfully recognized the data wander location bits. The resulting stable user data readout was displayed on an oscilloscope, as shown in Figure 3-21. This readout was achieved at the required 10^6 user data bits/sec required readout rate, and was displayed so that the oscilloscope would present the data exactly as it appeared when viewed under a microscope.

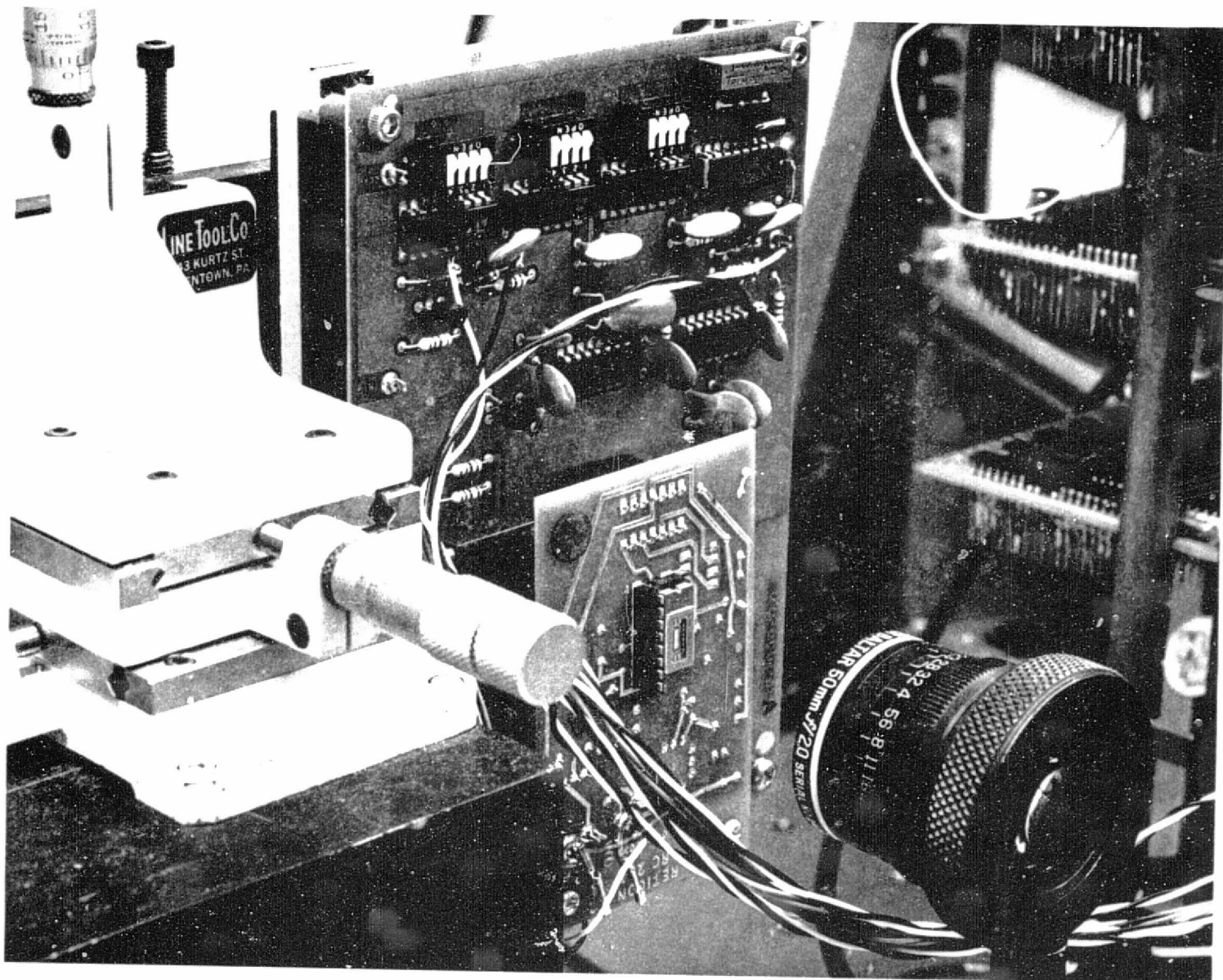
As for reliability and repeatability, the readout system worked consistently and continuously once it was properly adjusted. Besides requiring no adjustment between turning it on and looking at the display to guarantee an accurate display, the readout configuration demonstrated continuous maintenance-free operation of greater than 72 hours in one experiment. This last experiment could have run longer, but as the breadboard performed so flawlessly, it was felt that further testing was unnecessary.

A photograph of the complete breadboard system appears in Figure 3-22.



HARRIS

ELECTRO-OPTICS

ORIGINAL PAGE IS
OF POOR QUALITY

77-0870

FIGURE 3-20. THE ELECTRONICALLY AGILE PHOTODETECTOR ARRAY

ORIGINAL PAGE IS
OF POOR QUALITY

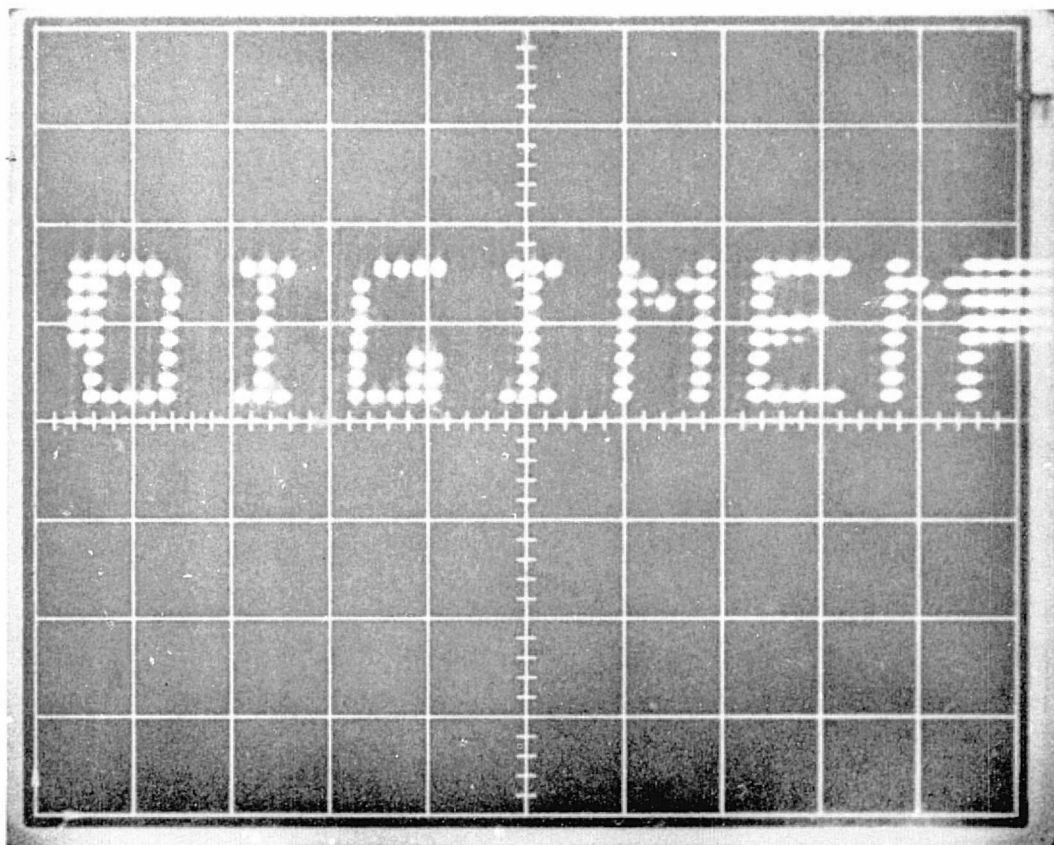


HARRIS

ELECTRO-OPTICS

3-65

ORIGINAL PAGE IS
OF POOR QUALITY



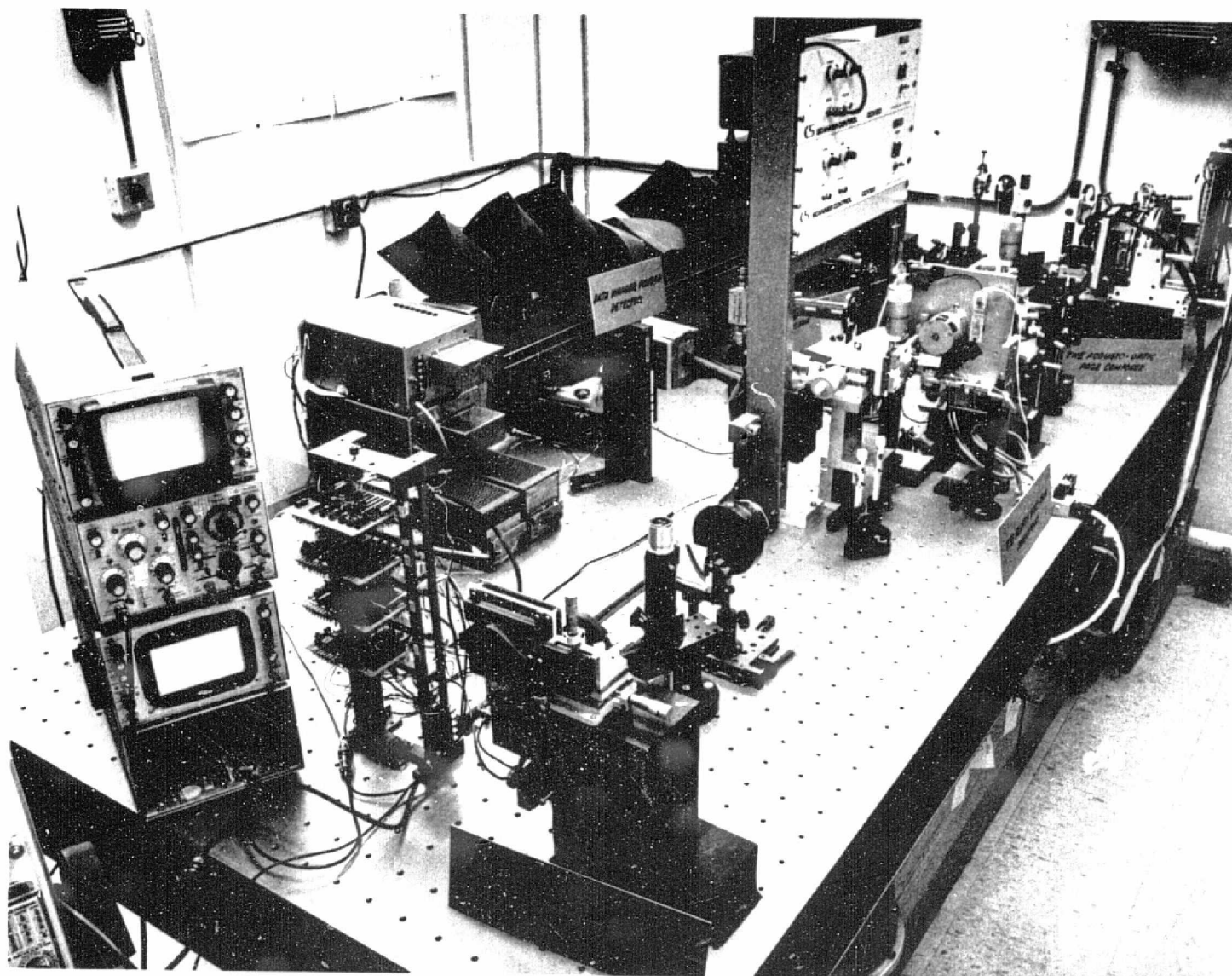
89678-46

FIGURE 3-21. OSCILLOSCOPE READOUT OF RECORDED DIGIMEM SPOTS
FROM THE ELECTRONICALLY AGILE PHOTODETECTOR ARRAY



HARRIS

ELECTRO-OPTICS



77-0997

FIGURE 3-22. THE DIGIMEM BREADBOARD SYSTEM

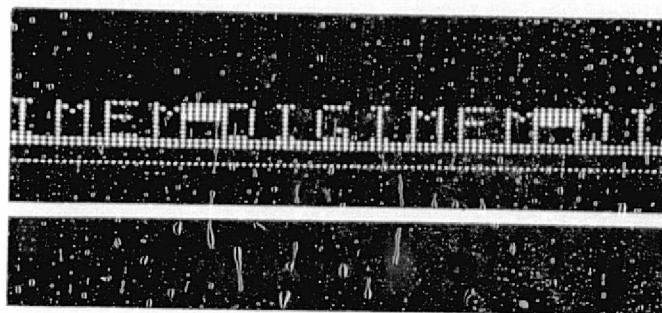


3.7 REPLICATION EXPERIMENTS

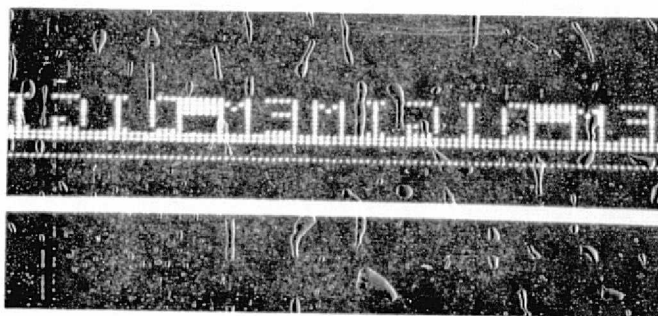
The successful implementation of DIGIMEM depends in part on a capability to quickly and accurately replicate master optical spot recordings for remote user readout stations. As a preliminary study of this problem, an experiment designed to permit contact printing of high quality SO-173 4- x 5-inch recordings on Xidex diazo microfiche types P5-213 and P7-216. The light source used for exposing the diazo in all cases was a Spectraline B-100 mercury vapor lamp positioned to produce an irradiance of $314 \mu\text{W}/\text{cm}^2$ (uniform to $\pm 2.5\%$) over the copying surface. A 0.25-inch thick microflat glass plate covered the SO-173 master and the diazo material. Further, all diazo samples were processed in a GAF 240 diazo processor twice at the slowest speed and highest ammonia concentration settings.

The results of this investigation were mixed. Though both the 5-mil thick P5-213 and 7-mil P7-216 copies faithfully reproduced the original information, the spots tended to blur in the copies, as shown in Figure 3-23. More important, however, was the relatively low background density of the copies compared to the original. While the P5-213 and P7-216 copies never achieved a background density over 2.0 D, the SO-173 original was measured to have a background of over 3.8 D. As a result, the spot contrast on the copies was insufficient to allow readout of the recorded data in the breadboard recorder/reproducer. We note that this is a limitation of the PDA, not the basic concept.

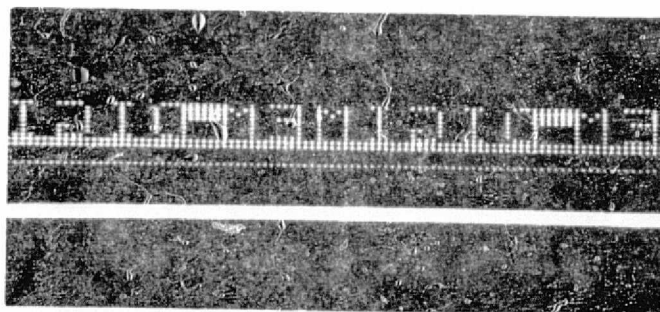
In the process of producing the above results, several other problems were observed, as are shown in Figure 3-24. In the P5-213 copies of Figures 3-24(a) and 3-24(b), the effects of dirt on recording quality are obvious. For a clump of dirt particles, the result is large burst errors on the copy. In the case of a dirt smudge on the platen, the glass transmission and the resulting recorded spot contrast ratio are reduced. If an air pocket occurs between the master and the copy (or between the master and the glass), the effect is similar to that of a dirt smudge, and is demonstrated in the P7-216 recording of Figure 3-24 (c). Great care must therefore be used in replicating high resolution recordings.



a. MASTER ON KODAK SO-173 HOLOGRAPHIC FILM



b. XIDEX P5-213 DIAZO COPY OF MASTER (10 MINUTE EXPOSURE)



c. XIDEX P7-216 DIAZO COPY OF MASTER (10 MINUTE EXPOSURE)

89678-76

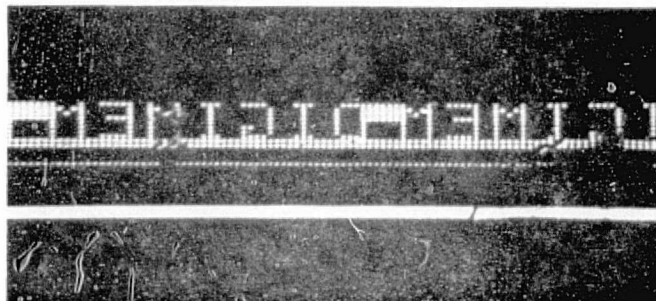
FIGURE 3-23. MASTER AND REPLICATED COPIES OF DIGIMEM RECORDINGS



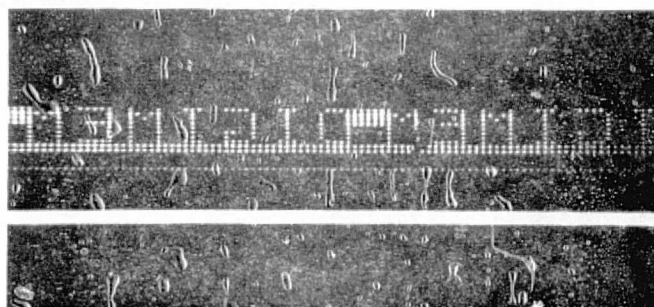
HARRIS

ELECTRO-OPTICS

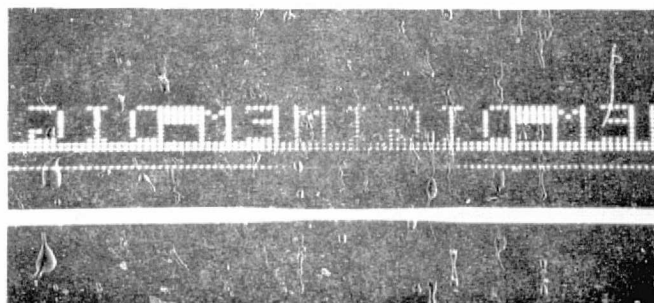
3-69



a. DIRT PARTICLES IN COPY PLATEN



b. DIRT SMUDGE IN COPY PLATEN



c. AIR POCKET IN COPY PLATEN

89678-75

FIGURE 3-24. THE EFFECTS OF DIRT AND AIR POCKETS ON REPLICATED DIGIMEM RECORDINGS

[Handwritten signature]



The conclusion of these preliminary studies is that further investigation of the replication problem is necessary before full implementation of a DIGIMEM system is possible. The emphasis of such an investigation must include an analysis of the requirements for this process, a detailed materials evaluation program, and subsequent system testing to compare copy and master performances. When such a study is completed, it will be possible for a master library of DIGIMEM data to be replicated for distribution to remote users.

3.8 COMPARISON OF BREADBOARD RESULTS TO DESIGN GOALS

The DIGIMEM breadboard was designed, first of all, to demonstrate both the advantages and the disadvantages of multichannel optical spot recording and readout. One disadvantage discovered was that data wander in excess of ± 0.002 inch could be expected in an operational model. However, a system based on a tracking mirror and feedback unit together with an electronically-agile photodetector array fully compensated for the data wander. Another disadvantage is the tight depth-of-focus requirements necessary for high information storage densities. This problem was minimized through scratch-free film handling in air bearings. The high-resolution requirements of spot imaging were found to be tractable with relatively inexpensive microscope objectives. By way of advantages, 2- μ m diameter spots were recorded on film consistently and repeatably without any system maintenance. Since this is very close to the theoretical limit for any system in resolution, this uniform performance represents a significant experimental result. Readout was also achieved consistently and repeatably throughout the experimental investigations, again a significant milestone.

The baseline system goals and the breadboard results are summarized in Table 3-5. As the figures show and the experimental results prove, the DIGIMEM breadboard successfully met or exceeded all the design goals set for this program. In addition, the breadboard achieved this result with a system concept that can be easily extended to higher data transfer rates or other film formats. We conclude, therefore, that the feasibility of multichannel optical digital recording has been fully demonstrated during the present experimental investigation.



HARRIS

ELECTRO-OPTICS

3-71

TABLE 3-5

SUMMARY OF DIGIMEM BREADBOARD RESULTS

<u>System Goal</u>	<u>Units</u>	<u>Required</u>	<u>Achieved</u>
I. Recording			
Number of channels recorded in parallel	—	2 or more	11 (8 user)
Information Storage Density	bits/cm	4×10^6	8×10^6
Data Transfer Rate (User)	bits/sec	10^6	10^6
II. Readout			
Number of channels readout in parallel	—	2 or more	11 (8 user)
Data Transfer Rate (User)	bits/sec	10^6	10^6



HARRIS

3-72

ELECTRO-OPTICS

3.9

REFERENCES

1. Wideband Holographic Recording and Reproduction, Final Technical Report, by the Electro-Optics Department, Harris Electronic Systems Division, for Contract No. F30602-73-C-0155, November 1976.
2. Reticon Array Evaluation, by the Electro-Optics Operation, Radiation, Incorporated, for Contract No. DAAB03-74-A-0013, December 1973.
3. Product Literature, Reticon Corporation, 1976.
4. Kogelnik, H. and T. Li, "Laser Beams and Resonators," Proc. IEEE, 54, pp. 1312-1329.
5. Optics Guide, Product Literature, Melles Griot, 1975.
6. Product Literature, Olympus Corporation, 1976.



HARRIS

ELECTRO-OPTICS

4-1

SECTION IV

TRANSPARENT ELECTROPHOTOGRAPHIC FILM STUDY



SECTION IV

TRANSPARENT ELECTROPHOTOGRAPHIC FILM STUDY

To support the overall DIGIMEM concept development we performed an experimental study of several transparent electrophotographic (TEP) films. The objective of our investigation was to determine the suitability of TEP films for optical data storage applications, especially those using direct digital optical spot recording. The characteristics of TEP films that motivated the evaluation are good sensitometric and data recording properties, relatively high resolution, and a number of attractive applications characteristics, e.g., long shelf life, good environmental integrity and exceptional image permanence. In addition, TEP films have an add-on capability. A general description of TEP films is given and experimental data are summarized in this section.

4.1 INTRODUCTION

Light-sensitive materials play a central role in the development and ultimate performance of direct digital optical and other optical information handling systems. Baseline recording media specifications for high-density storage and retrieval applications¹⁻⁹ often include a writing exposure sensitivity of less than 1 mJ/cm^2 , a spectral response closely matched to the output of a proven commercial laser (particularly helium-neon at 632.8 nm), resolving power greater than 1,000 cycles/mm, a low noise figure (as measured relative to either rms granularity or Wiener spectrum) and a high storage capacity. Other characteristics such as shelf life, processing, dimensional stability, environmental integrity, image permanence, and archival lifetime must also satisfy relatively stringent criteria if the recording medium is to be considered qualified for systems applications. These specifications are often generated independently of the storage technique, e.g., direct digital, holographic, or conventional microreduction.

A survey¹⁰ of conventional and unconventional recording media showed that there is only a small set of films that are qualified for high-density data storage when evaluated in terms of the baseline criteria. Included in this group are silver halide,



diazo, photoresist, free radical, and photopolymer films. Each of these materials has particular advantages, e.g., high storage capacity, low cost, on-line processing, and so forth. None of these films, however, completely satisfy what have been identified as key requirements of both the system designer and the end user.

Transparent electrophotographic (TEP) films¹¹⁻¹⁷ may be an exception to this general conclusion. These films have several attractive advantages when compared to more conventional recording materials; for example, a room temperature shelf life of at least 4 years, on-line processing, an add-on capability, a low sensitivity to environmental conditions (temperature and relative humidity), and a long archival lifetime. Simultaneously, TEP films can have peak spectral response at important laser wavelengths such as 488 nm (argon) and 632.8 nm (helium-neon), writing speeds comparable to Lippmann emulsions (sensitivity of about 10 to 100 $\mu\text{J}/\text{cm}^2$), a resolving power approaching 1000 cycles/mm, and a (binary) storage capacity approaching 10^8 bits/ cm^2 .

These potential advantages (together with no major disadvantages), relatively low cost, and commercial availability motivated a general study of TEP films and a specific evaluation of several Scott Graphics TEP films. The objective of the investigation was the characterization of TEP films as optical storage media. In the following paragraphs, we report the results of our investigation. Since electrophotographic media with a high-density optical data storage capability are relatively new, we begin with a general outline of the method of use and characteristics of TEP films, and subsequently report the experimental evaluation.

4.2 GENERAL DESCRIPTION AND CONSTRUCTION

TEP films are imaging materials that consist of a polyester base, a transparent electrically conductive layer, and an organic photoconductive topcoating. To store information, the TEP film is charged and then exposed to light. This creates an electrostatic latent image that can be developed with either a dry or liquid electro-developer (toner). The visible image (or hologram) produced by the development



step is made permanent by fixing with heat. Updating, or add-on, is accomplished by repeating the recording process.

Sensitometric properties of TEP films are process dependent. D-log E curves ranging from those obtained with very high contrast litho films to those of medium-contrast fine-grain microfilm can be obtained with a suitable combination of electro-developer and processing electrodes. TEP films yield, when properly processed, high resolution continuous tone imagery in either a positive or negative imaging mode. Imagery on a fully processed TEP film is durable, heat and light stable, and neutral black in color on a clear background.

Typical construction of a TEP film is shown in Figure 4-1. Its components are a polyester substrate, a transparent conductive layer (TCL) and a photoconductive coating. The conductive layer, which may be either an ionic or electronic conductor, is about 300 Å thick, and serves as an internal ground plane. The photoconductive coating is a polymeric matrix about 8µm thick that contains a derivative of m-phenylene diamine as the organic photoconductor (OPC) in combination with a dye sensitization system. Other photoconductors, both organic and inorganic, can be used to vary the properties of TEP films.

4.3 INFORMATION STORAGE MECHANISM AND PROCESSING

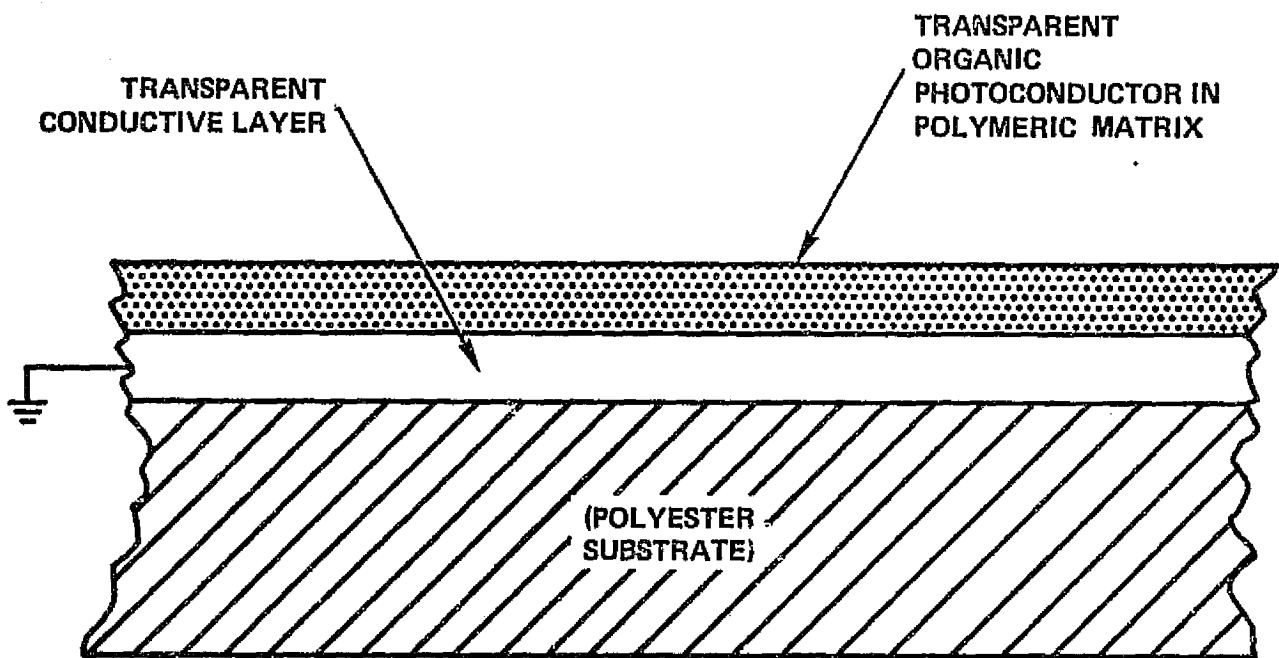
Information storage in TEP films is accomplished through the basic steps typical of electrophotography; i.e., charging, exposure, development (often called toning), drying (in the case of an liquid electrodeveloper), and fixing (heat fusing).¹⁸ Charging makes the TEP film light sensitive. Lack of sensitivity in the uncharged state provides an effective gating mechanism and, provided other components are stable, the shelf life of TEP films is many years. A corona discharge in air is commonly used for charging. Because the film is electrically bipolar, positive or negative corona can be used for charging. Corona charging (in the dark) generates an electric field of about 10^6 V/cm between the upper surface of the photoconductor and the transparent ground plane; apparent surface voltage (ASV) is in the range of 800-1200 volts. Exposure to light in



HARRIS

ELECTRO-OPTICS

4-5



89678-104

FIGURE 4-1. CONSTRUCTION OF A TRANSPARENT ELECTROPHOTOGRAPHIC (TEP) FILM



the spectral response region of the TEP film causes a signal-dependent discharge of the photoconductive layer. In unexposed areas the initial charge distribution is essentially unchanged because the high dark resistance of the photoconductive matrix permits only negligible conduction. Hence, an electrostatic latent image is formed as a function of the incident light distribution. Development converts the electrostatic latent image into a visible image (or hologram) by creating a signal-related optical density variation. A liquid electrodeveloper containing charged toner microparticles is generally used for development to obtain maximum resolution. A dry electrodeveloper is used for lower resolution applications. The toner microparticles can have a charge of the same or opposite polarity relative to the charge initially applied to the TEP film by the corona. Drying is needed only in the case of liquid electrodevelopers. Flowing air is generally used for this step to encourage rapid evaporation of the liquid phases of the electrodeveloper. Fixing provides image permanence. It causes the toner microparticles deposited by the electrodeveloper to fuse to themselves and to the surface of the organic photoconductor layer. The basic steps required for information storage by direct digital optical recording (or holography) are summarized in Figure 4-2 in terms of exposure to a square wave irradiance distribution $I(x)$.

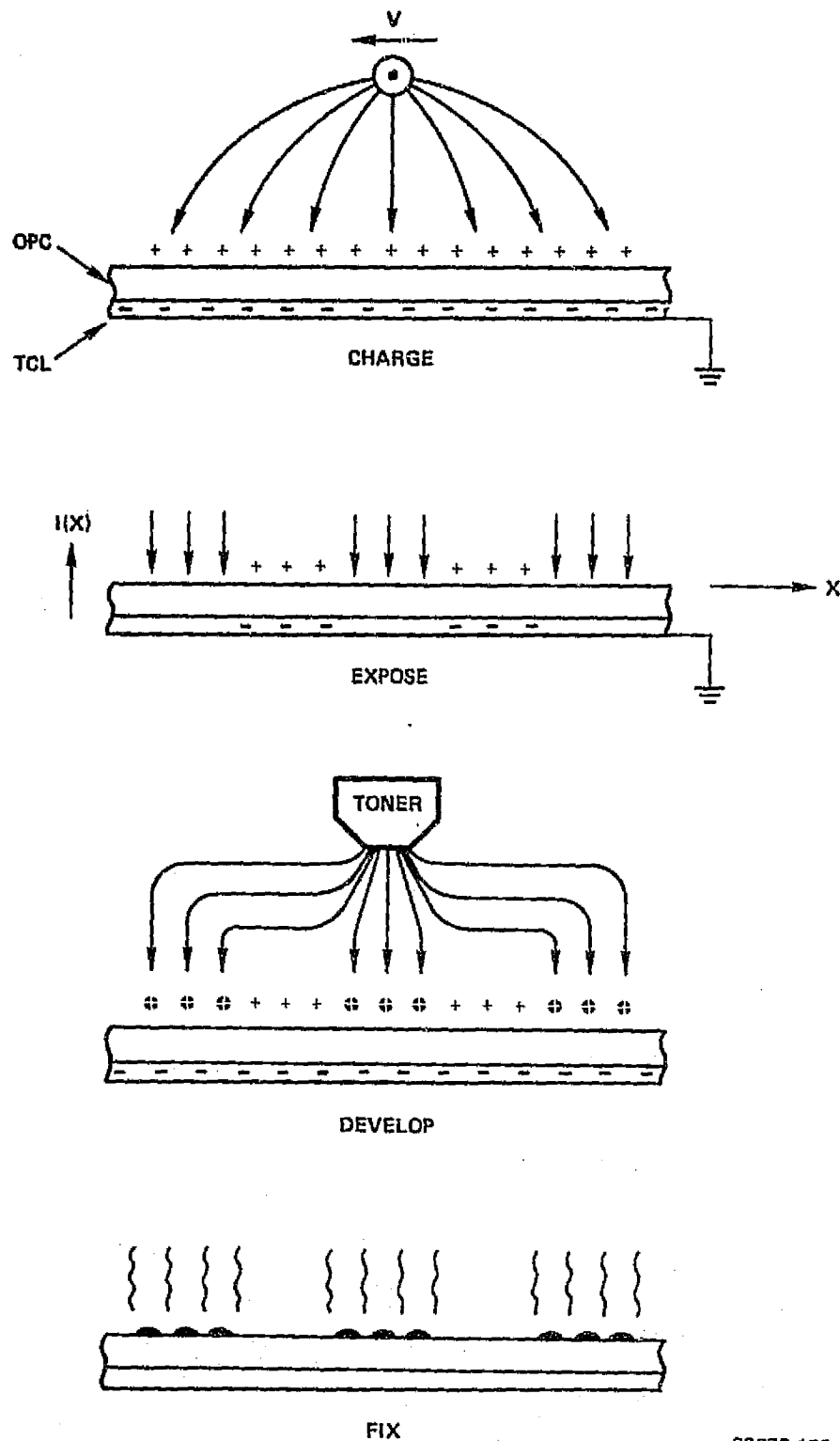
The exposure and development processes can be analyzed in greater depth. During exposure absorbed photons create electron-hole pairs in the photoconductive matrix. Electrons migrate toward the positive interface of the photoconductive layer; holes move in the opposite direction and partially discharge the film. Since charges of opposite polarity attract, the use of a positively charged electrodeveloper, combined with a negative ASV, provides a positive imaging mode; i.e., one having the same tonal values as the incident irradiance pattern. With the same positive electrodeveloper, a positive ASV yields a negative imaging mode, or opposite tonal values. A negative electrodeveloper gives a negative imaging mode in the first case and a positive imaging mode in the second case. Figure 4-2 shows the negative imaging mode for a positively charged film and electrodeveloper.



HARRIS

ELECTRO-OPTICS

4-7



89678-103

FIGURE 4-2. THE BASIC STEPS OF IMAGE FORMATION ON A NEGATIVE-WORKING TEP FILM



As in the case of silver halide materials, electrophotographic films have a gain or amplification mechanism.¹⁹ The amplification for TEP films systems, defined as the ratio of deposited carbon atoms to the number of absorbed photons, is greater than 10^5 . While this is less than that obtained for the faster silver halide films, which have amplification factors of up to 10^9 , it is significantly greater than that obtained by diazo, free radical, vesicular and most photopolymer systems.

Electrophotographic sensitometry requires several general comments to aid the interpretation of subsequent experimental data. In electrophotographic imaging systems there is an electrical as well as a sensitometric means of determining the response of the system to light.^{20,21} The electrical sensitometry of a TEP film is unique, since it can be fully determined independent of other image processing variables such as electrodeveloper characteristics and fixing. Electrical sensitometric measurements are analogs to latent image measurements in an exposed silver halide film.

Unlike the silver halide process, the density-producing elements of the electrophotographic image are wholly external to the film, as they are obtained from the electrodeveloper. Since the development process is electrophysical, factors that affect the electrical or physical properties of the electrodeveloper system also strongly affect the sensitometry and, consequently, the information capacity of the toned TEP film. Changes in either the properties of the electrodeveloper, or its application method and parameters, alter the resultant sensitometry. Thus, the transformation of the electrical charge pattern formed by exposure (electrostatic latent image) into an information-bearing optical density pattern depends on a series of interacting factors. We add that it is always necessary to define the TEP film processing system in order to relate optical sensitometric and electrophotographic responses.

Sensitometric curves for electrophotographic films are dependent on the electrodeveloper, the type of processor and the recording application. In some systems, the exposure pattern may affect the electrical and physical performance of the development unit, and an image-dependent sensitometry results. This is of particular concern for high-density digital optical recording applications.



The electrodeveloper has a fundamental impact on the electrophotographic process, and thus merits further discussion. An electrodeveloper is a mixture of opaque toner microparticles, such as carbon black, a toner polymer and either a solid or liquid dielectric carrier. In general, the toner microparticles range in size from $0.1\mu\text{m}$ to $1\mu\text{m}$ in diameter. As a specific example, in one investigation with hologram gratings that had a frequency of 166 cycles/mm, we found that on the average there were about five toner microparticles of uniform size per dark fringe. Since this spatial frequency yields a dark fringe width of about $3\mu\text{m}$, the toner microparticles appear to have an average diameter of approximately $0.6\mu\text{m}$. From these data, we infer a resolving power of 833 cycles/mm. The Scott Graphics TEP films appear to obtain this limit.

As mentioned previously, a TEP film obtains image permanence by fixing with heat. Heat causes the toner microparticles to be fused to each other and onto the OPC layer. The fusion of the toner microparticles is due to flow of the toner polymer and softening of the thermoplastic components of the OPC. The final composition of a TEP film image is suspension of fine carbon particles in an inert polymer matrix coated on a polyester film base. These characteristics are responsible for the exceptional image permanence and a long archival life of TEP films.

As unexpected discovery of a previous experimental investigation that relates to information storage is the existence of significant surface relief. We hypothesize that the observed surface relief is due to 1) the physical deposition of the toner polymer by the electrodeveloper in exposed areas (negative-working mode) or in unexposed areas (positive-working mode) and 2) surface deformation of the thermoplastic components of the OPC during fixing. For conventional imaging applications this effect can be ignored. However, for high-density optical spot recording this could lead to adjacency effects and possibly beam spreading.

There also appears to be a relationship between surface relieving effects and resolution. The flow of toner polymer during heat fixing tends to obscure fine detail owing to random toner microparticle transport; this ultimately leads to a loss of resolution. This effect can be minimized in some cases by exposing the surface of the TEP film to methylene



chloride vapors before heat fixing. The methylene chloride vapors cause the toner microparticles to coalesce, thus preventing lateral diffusion.

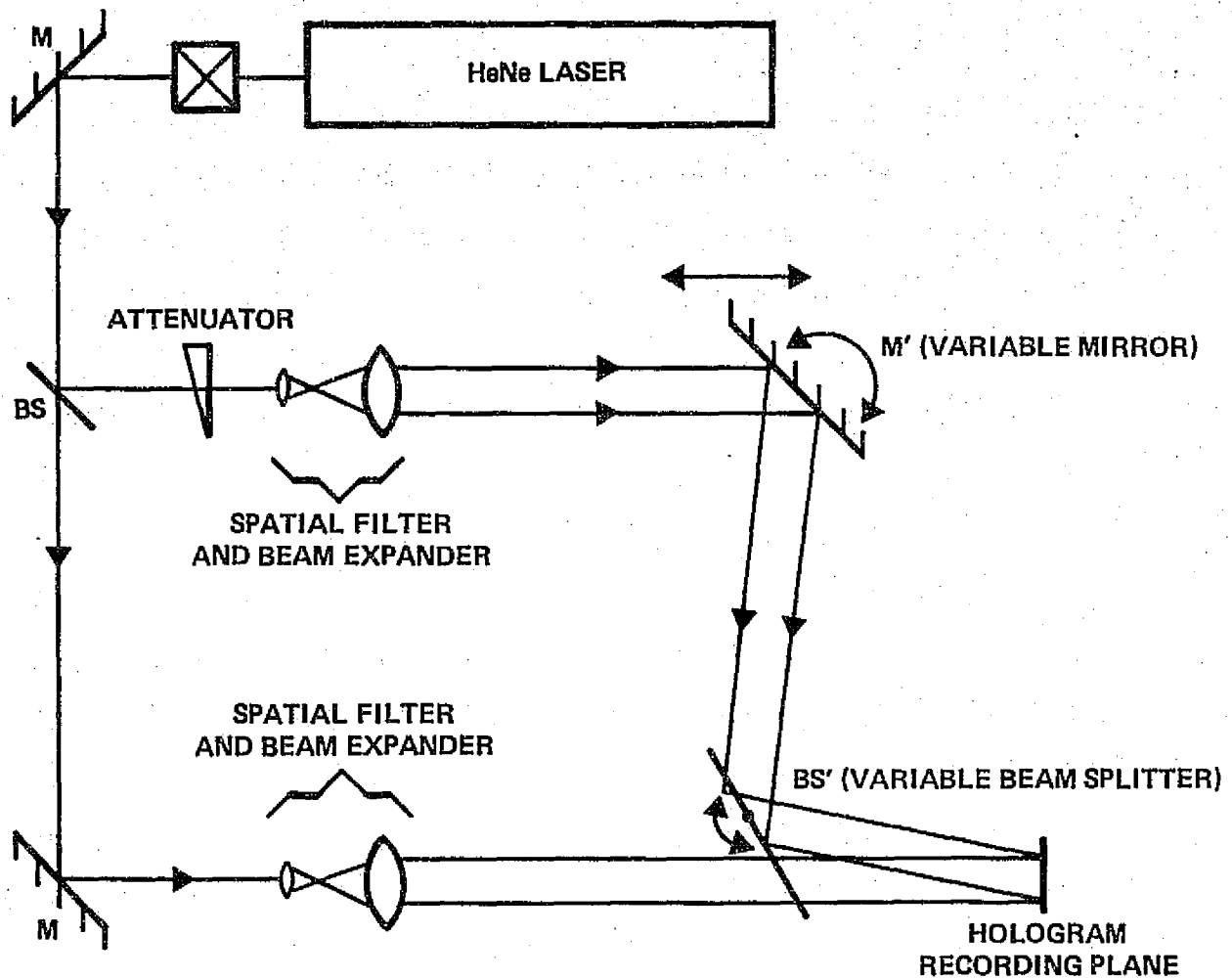
4.4 EXPERIMENTAL EVALUATION

The objective of the experimental evaluation was the measurement of data storage performance of several Scott Graphics TEP films. After preliminary test and evaluation, we chose a specific electrodeveloper and TEP P5-003 and P4-005 films for a more complete characterization. TEP P5-003 is a commercial product used in the A.B. Dick/Scott Updatable Microfiche System. It is sensitive to orange-red light and has a peak sensitivity at 590 nm. TEP P4-005 is special helium-neon laser recording film that has peak sensitivity at 633 nm. Experimental activities included the generation of characteristic, frequency response and information storage capacity curves.

Although we were mainly concerned with optical spot recording, holographic testing methods were employed where suitable. Holographic measurement techniques are the best quantitative method for determining the storage performance of high-resolution recording materials. Frequency response and information storage capacity can be inferred from the diffraction efficiency (DE) of hologram gratings and the signal-to-noise ratio (SNR) of data masks reconstructed from Fresnel holograms, respectively.

4.4.1 Experimental Apparatus

A schematic diagram of the experimental setup is shown in Figure 4-3. It is a modified form of the Mach-Zehnder interferometer. A helium-neon laser ($\lambda = 632.8$ nm) was the coherent light source for both recording and readout. Exposure time was controlled with an electromechanical shutter. The mirror M^1 and the combining beam splitter BS^1 were fully adjustable. This permitted fairly accurate path length equalization (as implied by fringe contrast) and the generation of spatial frequencies ν in the 0 to 800 cycle/mm range (where ν is given by $\sin \theta / \lambda$). The TEP film was held in position with a vacuum platen mounted on an X-Y translation stage.



89678-77

FIGURE 4-3. MACH-ZEHNDER INTERFEROMETER USED FOR RECORDING HOLOGRAMS ON TEP FILM

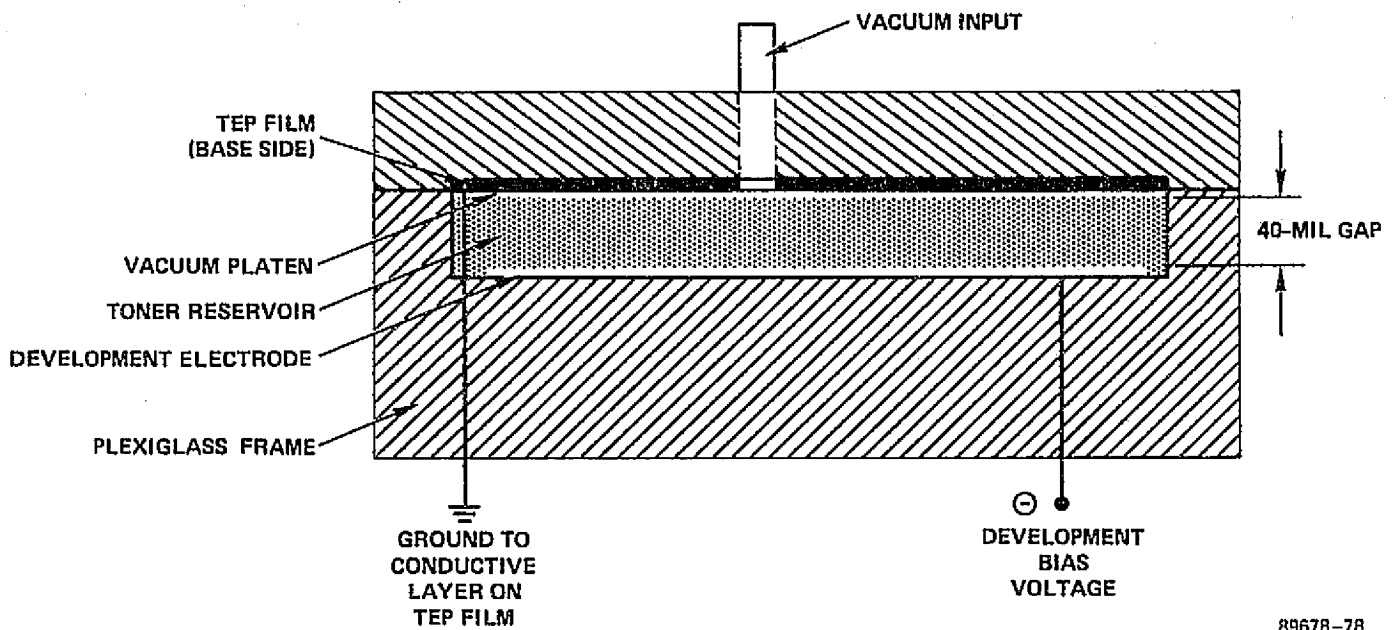


4.4.2 Experimental Procedure

The TEP film was found relatively easy to use, a definite plus for systems applications. Sensitization was obtained by charging. First, the transparent conductive layer was grounded, and then the film was subjected to a high voltage (7 kV) corona discharge. The corona was produced by a Scorotron unit. Three fine parallel wires are positioned above the film and held at high voltage to produce the corona. The control grid is eleven parallel wires positioned a few millimeters above the film plane. The combination is mounted on a carriage that travels at 3.8 cm/s. Negative charging was used throughout at the recommendation of Scott Graphics. They have found empirically that negative charging provides the highest resolving power. After exposure, the TEP film was developed, rinsed, and dried in still air. All samples were evaluated one or more times before fixing.

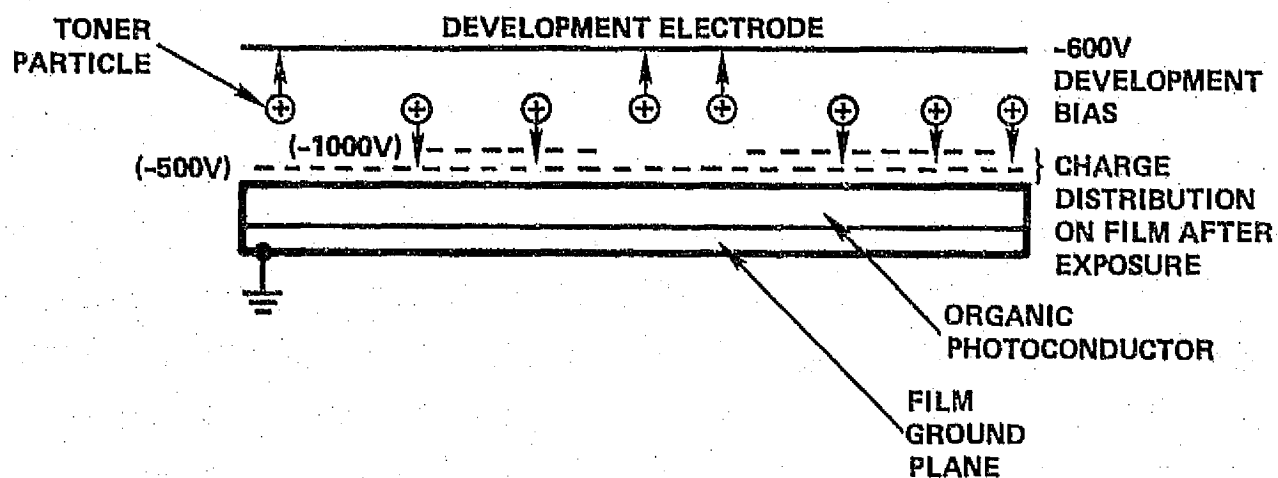
Development was with a liquid electrodeveloper, since it is again empirically known to provide the highest resolving power. Figure 4-4 shows the liquid parallel plate processing (LP³) cell used. The parallel plate, 40 mils away from the film surface can be held at any desired potential. Figure 4-5(a) shows conditions for the development of a positive image. The film was initially charged to -1000 V; where exposed, the apparent surface voltage (ASV) dropped to -500 V. If the development bias is less than -500 V, the positive toner particles will be drawn to the photoconductor resulting in an entirely black image. By biasing the electrode to -600 V, toner particles will be attracted to the development plate in exposed areas and to the photoconductor in unexposed areas. This type of biasing is complicated because optimum biasing depends on the exposure level. The corresponding case for a negative image is shown in Figure 4-5(b). Charging and exposure remain the same, but the toner microparticles are negatively charged. The optimum bias level is just below the maximum voltage. Thus, it is dependent on the initial charge, but not on the exposure.

The liquid electrodeveloper used was T4-18 (Type 4 at 18 percent transmittance), which was specially formulated by Dr. Johan Dirks of Scott Graphics. This electrodeveloper

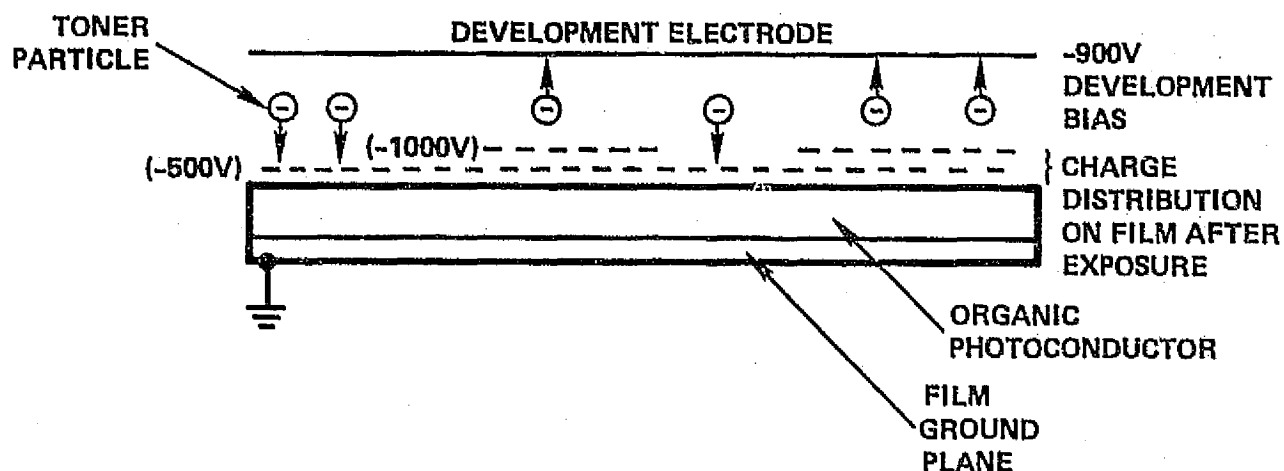


89678-78

FIGURE 4-4. LIQUID PARALLEL-PLATE PROCESSING CELL
USED FOR ELECTRODEVELOPMENT OF TEP FILMS



a. POSITIVE IMAGE



b. NEGATIVE IMAGE

89678-79

FIGURE 4-5. SCHEMATIC REPRESENTATION OF TEP DEVELOPMENT
FOR POSITIVE AND NEGATIVE IMAGING MODES
(SQUARE-WAVE EXPOSURE ASSUMED)



was chosen to optimize data storage parameters of the TEP film. We found the shelf life of T4-18 was approximately 7 days after mixing. This was inferred from densitometric and holographic data, whose magnitude decreased monotonically as a function of the electrodeveloper age. The reason for this behavior is charge bleed-off; the toner microparticles must be charged to remain suspend in the liquid carrier, and thus to be stable.

4.4.3 Sensitometry

The sensitometric characteristics of the TEP films are summarized in Figures 4-6 through 4-9. Figures 4-6 and 4-7 are plots of T_A (amplitude transmittance) as a function of exposure E for the P5-003 and P4-005 films, respectively. Data for both unfixed and fixed exposure samples are shown. For P5-003 the exposure required to achieve $T_A = 0.5$ is $190 \mu\text{J}/\text{cm}^2$ unfixed, and $240 \mu\text{J}/\text{cm}^2$ fixed. For P4-005, the corresponding exposures are $60 \mu\text{J}/\text{cm}^2$ unfixed and $70 \mu\text{J}/\text{cm}^2$ fixed. The difference between the data for fixed and unfixed TEP films is minimal. Not surprisingly, the P4-005 He-Ne laser recording TEP film is about four times faster than TEP P5-003. Figures 4-8 and 4-9 are plots of D (optical density) as a function of $\text{Log } E$ (exposure) for P5-003 and P4-005, respectively. Data are again plotted for unfixed and fixed samples. Maximum density is greater for P5-003, with a maximum density of about 1.5; P4-005 reaches a maximum density of about 1.3 for unfixed samples. The fixing process tends to spread the microparticles resulting in a lower density. The contrast is about 1:1 for P5-003 and close to 1:1 for P4-005. Overall, the sensitometric properties of these TEP films is analogous to a high resolution photographic film such as Kodak 649 F developed in a low contrast developer. At 632.8 nm, exposure to obtain a net $D = 1$ for fixed samples is on the order of $100 \mu\text{J}/\text{cm}^2$ for P4-005 and $400 \mu\text{J}/\text{cm}^2$ for P5-003.

4.4.4 Diffraction Efficiency

Diffraction efficiency is defined as the ratio of laser power diffracted into the first order reconstruction to the laser power incident on the hologram, less reflection and irrelevant absorption losses (in this case owing to the residual photosensitizing dye which

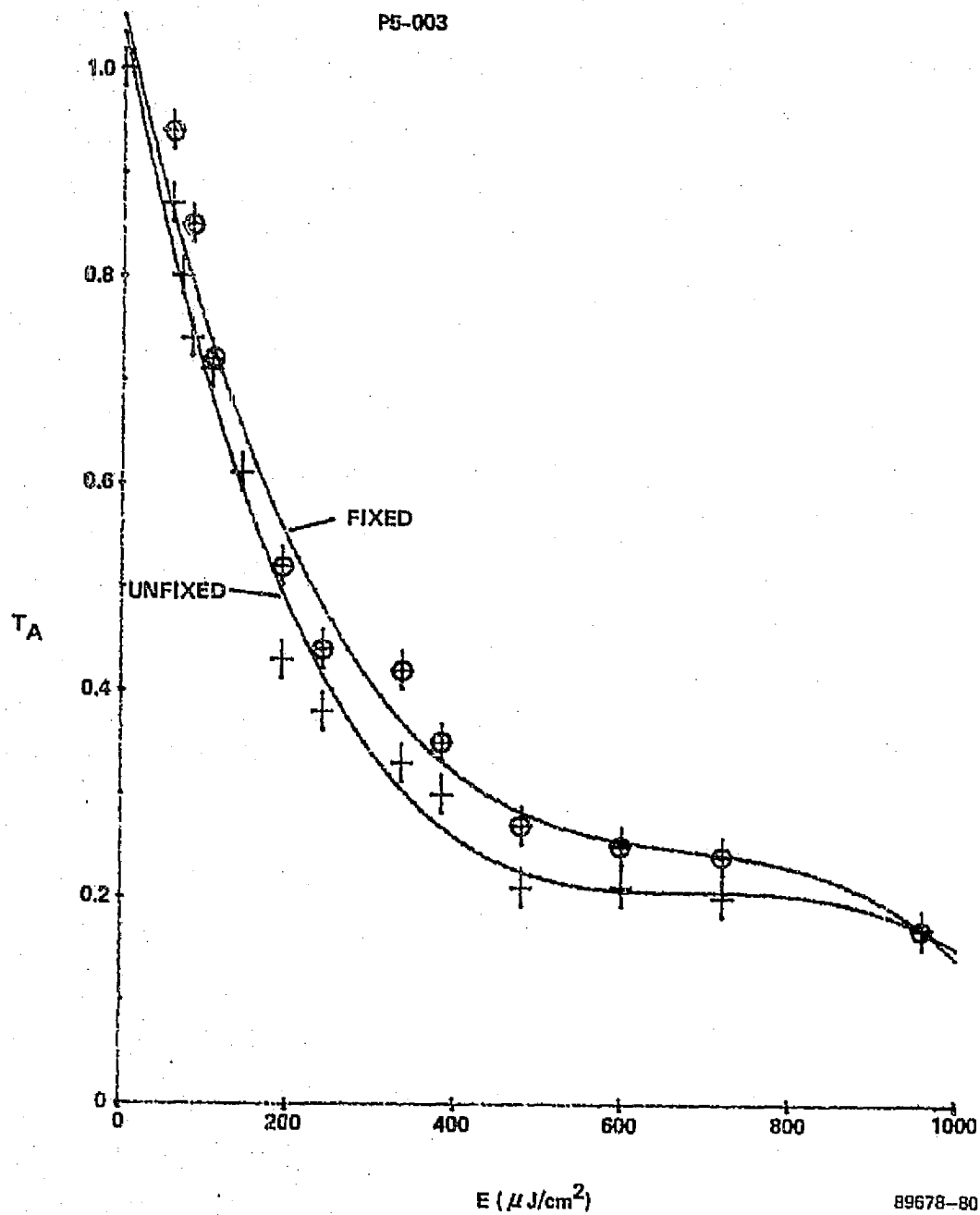


FIGURE 4-6. AMPLITUDE TRANSMITTANCE T_A AS A FUNCTION OF EXPOSURE E FOR TEP P5-003

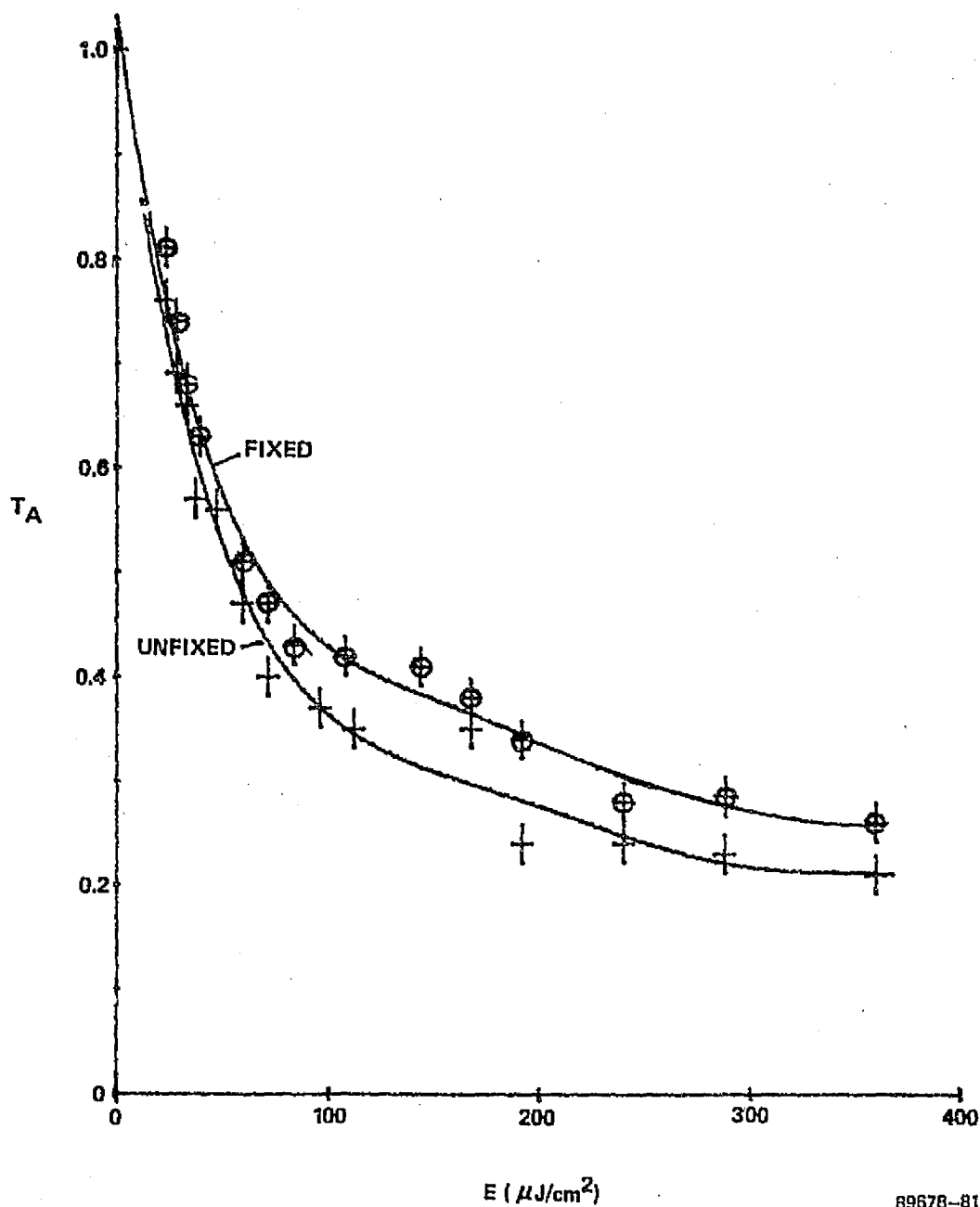


HARRIS

ELECTRO-OPTICS

4-17

P4-005

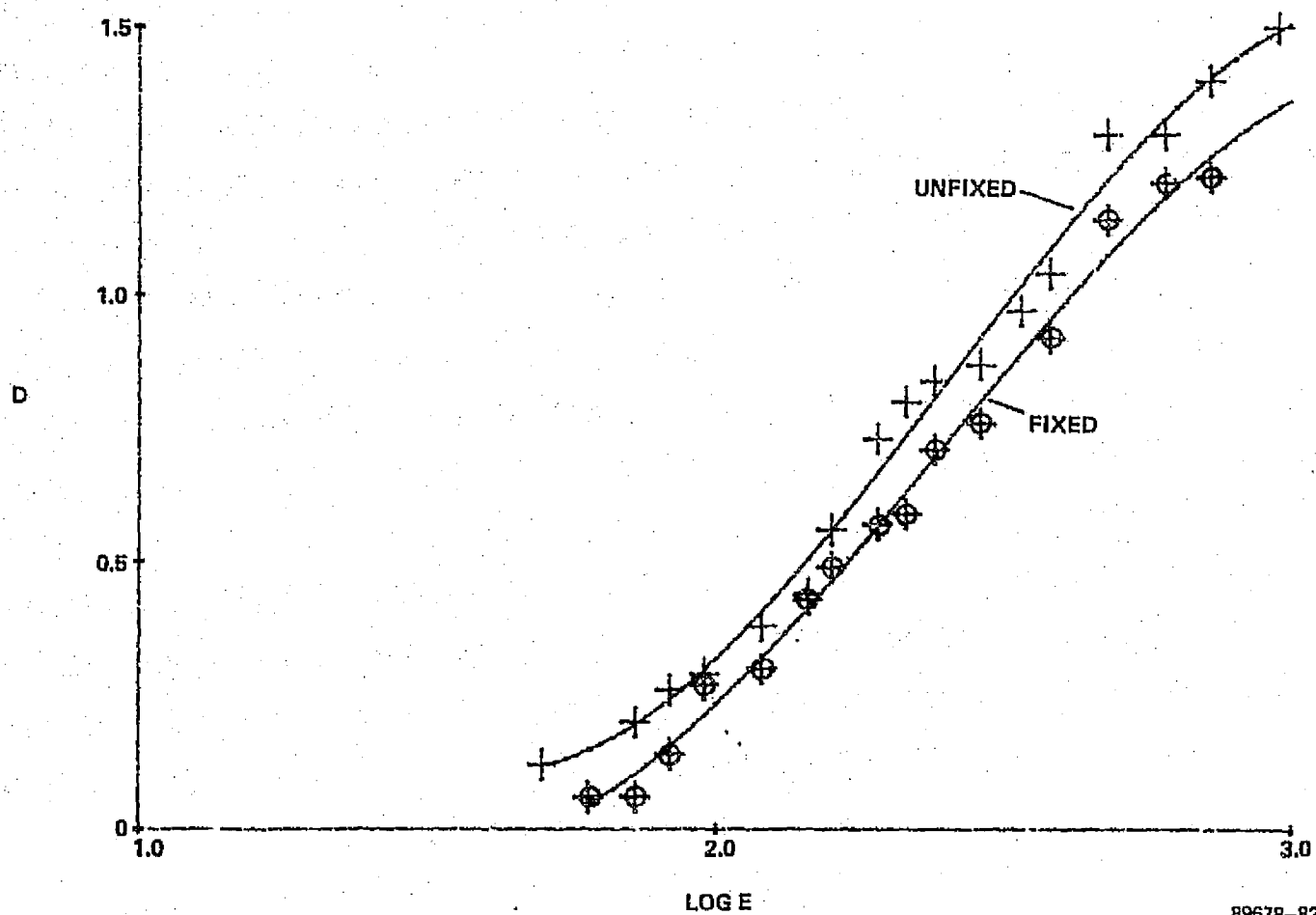


89678-81

FIGURE 4-7. AMPLITUDE TRANSMITTANCE T_A AS A FUNCTION OF EXPOSURE E FOR TEP P4-005



P5-003



89678-82

FIGURE 4-8. DENSITY D AS A FUNCTION OF EXPOSURE E
FOR TEP P5-003 (D-LOG E CURVE)

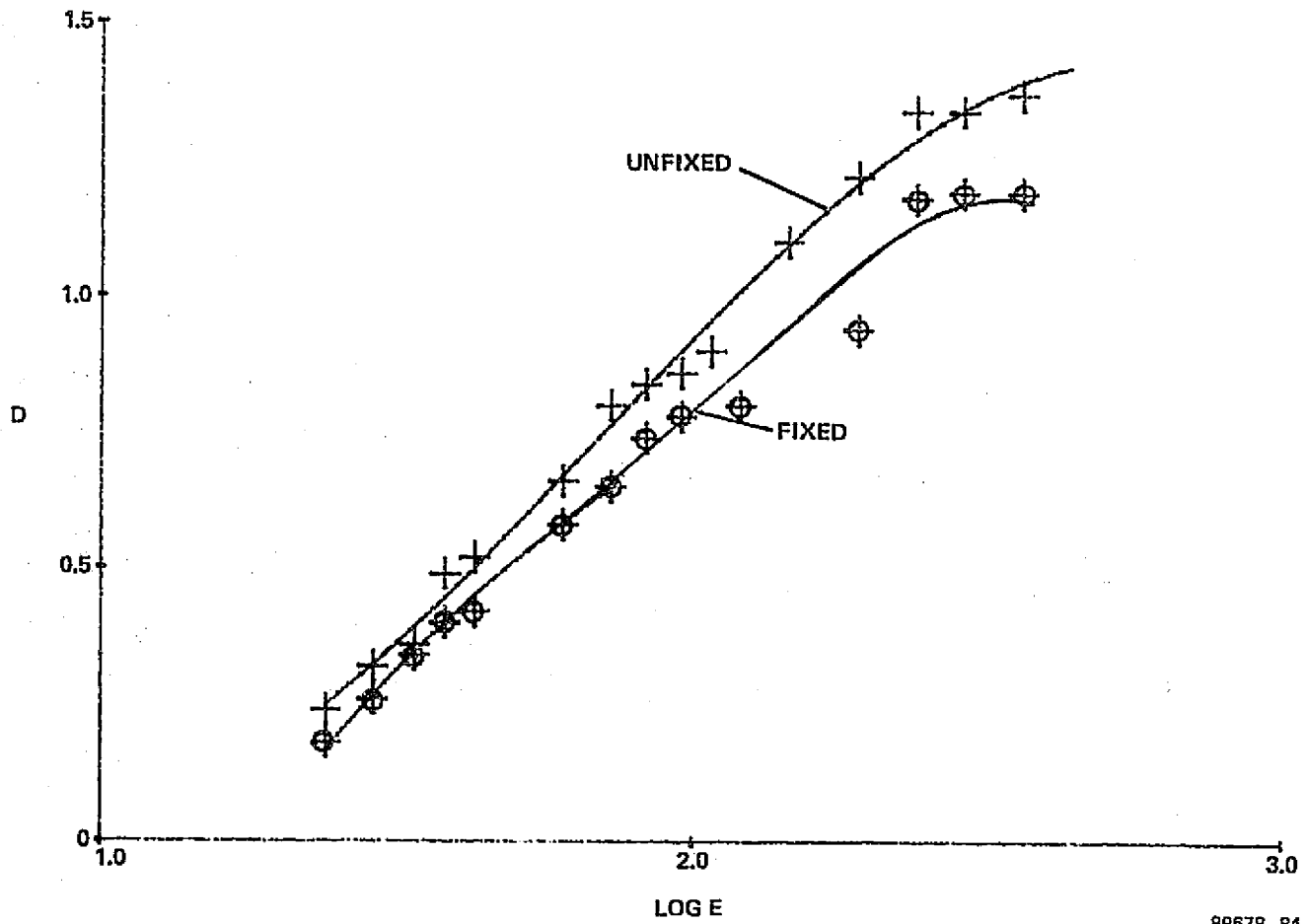


HARRIS

ELECTRO-OPTICS

4-19

P4-005



89678-84

FIGURE 4-9. DENSITY D AS A FUNCTION OF EXPOSURE E
FOR TEP P4-005 (D-LOG E CURVE)



is not photobleachable; this stability is required for updating). This definition is used to permit an explicit comparison between experimental and theoretical values of diffraction efficiency. A complete specification of DE requires a statement of the overall insertion loss. In the present experimental work, the insertion loss was typically 3.5 dB (45 percent transmission) for P5-003 and 5.5 dB (28 percent transmission) for P4-005 at 633 nm.

We evaluated diffraction efficiency performance by recording plane wave gratings over a range of exposure values. In Figures 4-10 and 4-11, diffraction efficiency is plotted as a function of exposure E for samples that were unfixed, fixed, and fixed and index-matched in a liquid gate. The recording parameters were a beam ratio $K = 1$ and a spatial frequency $\nu = 100$ cycles/mm. As the curve in Figure 4-10 for P5-003 shows, a maximum DE of 4.6 percent is reached, before fixing, for an exposure of about $240 \mu\text{J}/\text{cm}^2$. After fixing, the peak DE drops to about 3 percent. There is virtually no difference between fixed and fixed and index-matched holograms. The exposure for peak DE remains about the same, $240 \mu\text{J}/\text{cm}^2$. For P4-005, maximum DE is 5.8 percent for an exposure of $70 \mu\text{J}/\text{cm}^2$ before fixing. After fixing, the peak DE dropped to 4 percent and when indexed to 3.5 percent. Figures 4-12 and 4-13 are plots of DE as a function of E for $K = 10$. Maximum DE is about 2 percent for P5-003 and 2.5 percent for P4-005, respectively. Again maximum DE decreased by about 50 percent after fixation. Index matching caused no further decrease in diffraction efficiency. In comparing the two films, P4-005 had higher diffraction efficiency and required 70 percent less exposure than P5-003.

The diffraction efficiency of plane wave grating holograms was used as the control variable to examine performance consistency of the TEP films. We recorded ten gratings with $K = 1$ and $\nu = 150$ cycles/mm at exposure levels of $60 \mu\text{J}/\text{cm}^2$ for P4-005 and $225 \mu\text{J}/\text{cm}^2$ for P5-003. The first exposure was made 30 seconds after charging; subsequent exposures were made every 20 seconds thereafter. Table 4-1 summarizes the experimental data for unfixed and fixed holograms. The DE data are not uniform, but there is no tendency to decrease with time between charging and exposure. This indicates little or no surface charge decay. P5-003 film showed less variation than P4-005.

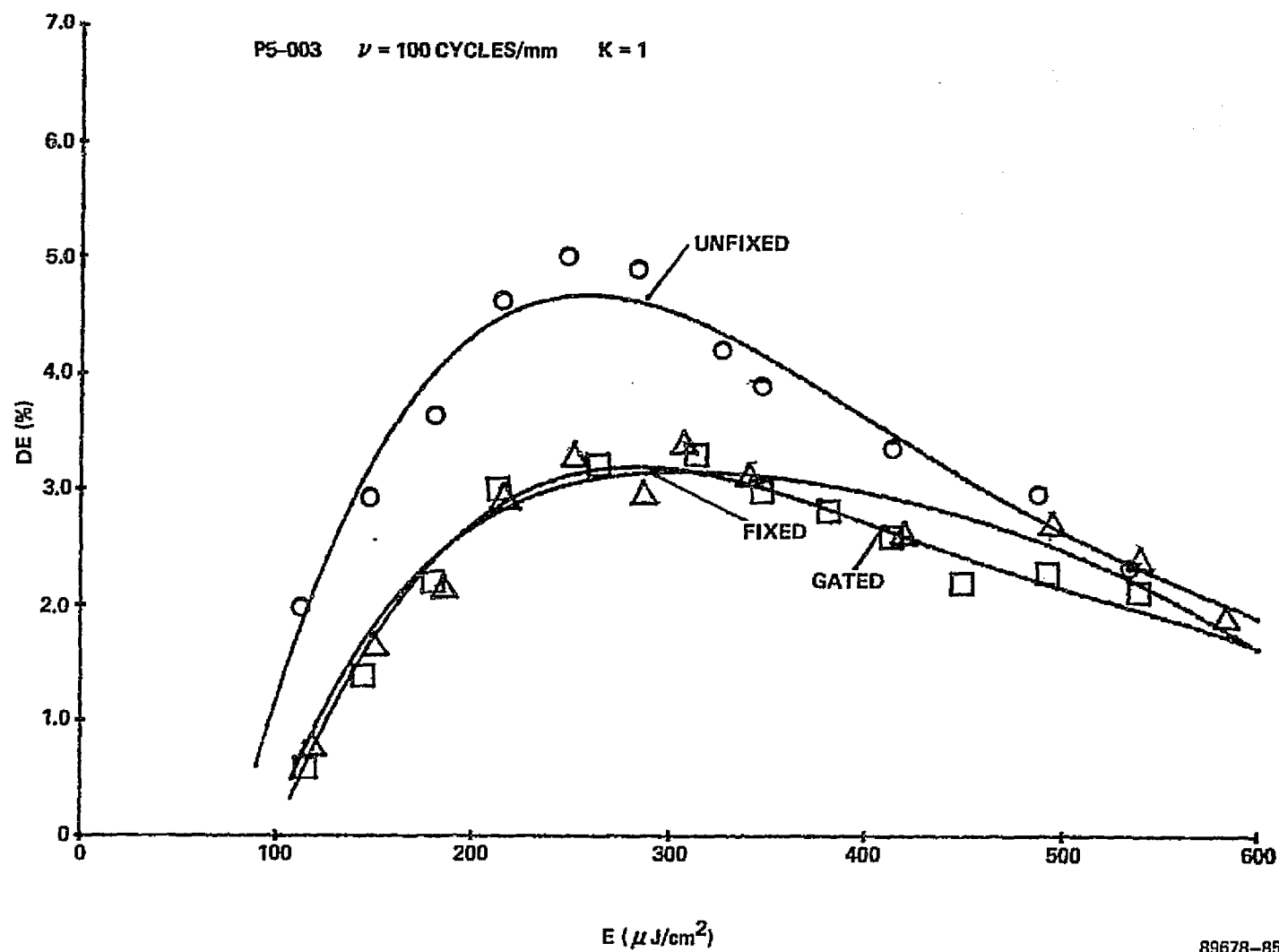


FIGURE 4-10. DIFFRACTION EFFICIENCY DE AS A FUNCTION OF EXPOSURE E FOR TEP P5-003





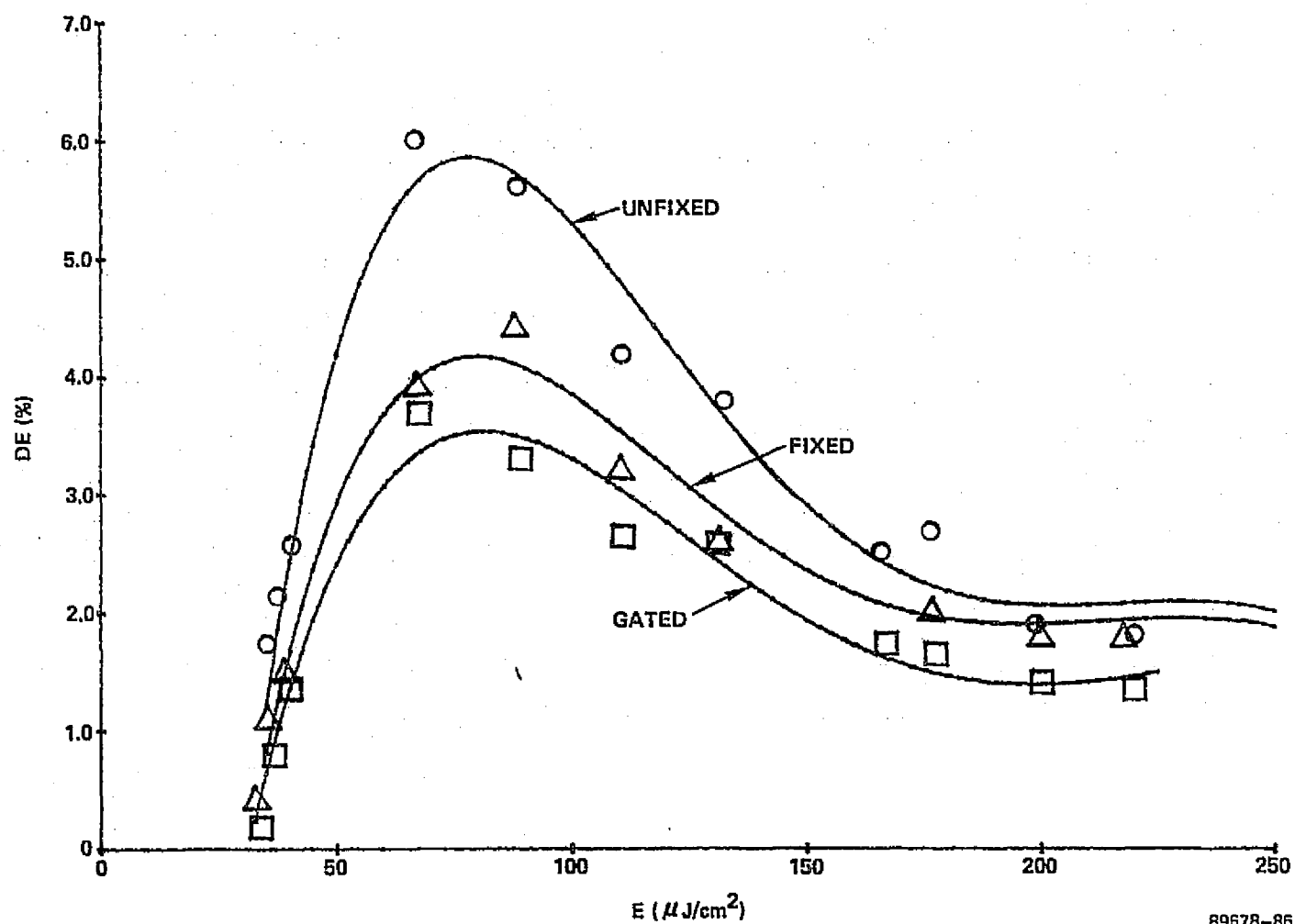
HARRIS

ELECTRO-OPTICS

P4-005

 $\nu = 100$ CYCLES/mm

K = 1



89678-86

FIGURE 4-11. DIFFRACTION EFFICIENCY DE AS A FUNCTION OF EXPOSURE E FOR P4-005

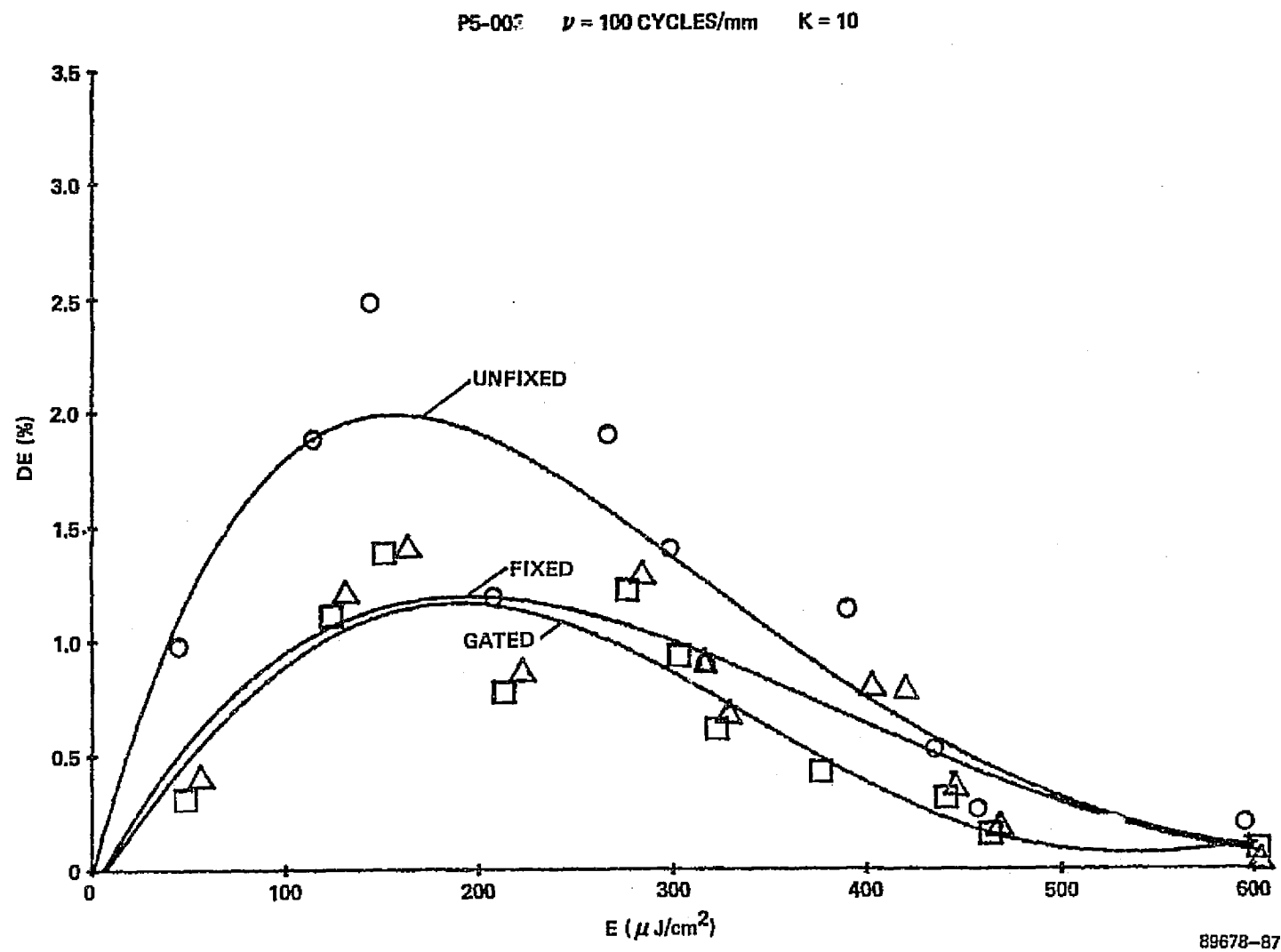


FIGURE 4-12. DIFFRACTION EFFICIENCY DE AS A FUNCTION OF EXPOSURE E FOR TEP P5-003



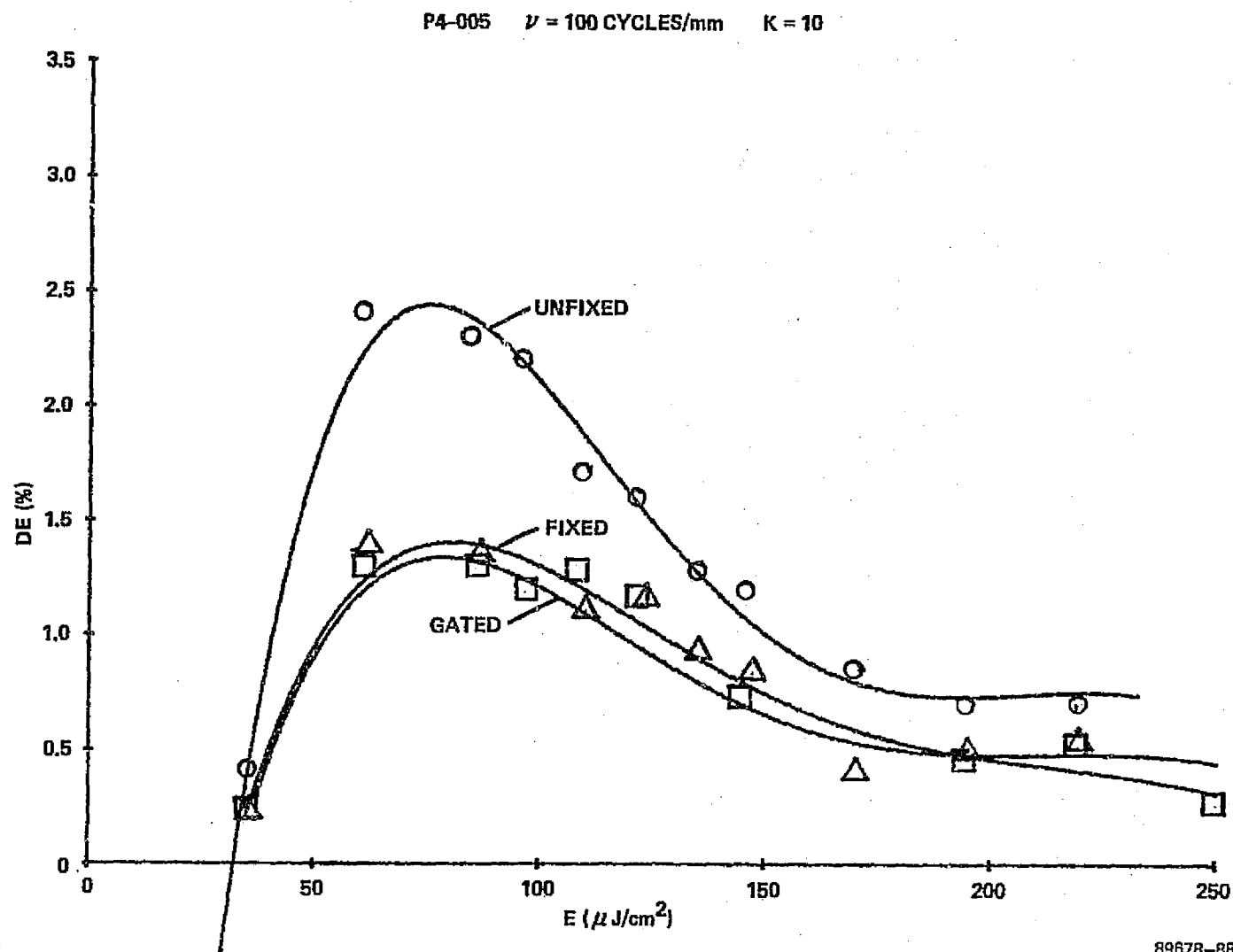


FIGURE 4-13. DIFFRACTION EFFICIENCY DE AS A FUNCTION OF EXPOSURE E FOR TE P4-005



TABLE 4-1

PERFORMANCE CONSISTENCY DATA FOR SCOTT GRAPHICS TEP FILMS

<u>EXPOSURE NUMBER</u>	<u>DE (UNFIXED)</u>	<u>DE (FIXED)</u>
I. <u>P4-005</u>		
1	2.13	1.08
2	1.31	0.67
3	1.06	0.56
4	1.67	1.1
5	1.89	1.12
6	1.14	0.70
7	1.14	0.81
8	1.49	1.09
9	1.52	1.09
10	1.39	0.85
II. <u>P5-003</u>		
1	1.0	0.45
2	1.0	0.50
3	1.03	0.60
4	0.87	0.49
5	0.87	0.47
6	1.09	0.63
7	1.03	0.60
8	0.88	0.43
9	0.80	0.56
10	0.83	0.53



4.4.5 Frequency Response

Frequency response is a measure of modulation transfer as a function of spatial frequency. It was determined indirectly by measuring the diffraction efficiency of plane wave grating holograms recorded over a range of spatial frequencies. The determination of frequency response for the TEP films required careful measurement and interpretation of the experimental data. Two factors complicated the situation. First, surface relief resulted in a diffracted wave being generated by a planar phase hologram, in addition, to the one formed by the toner microparticles (amplitude hologram). We compensated for this effect by index matching in triethanolamine ($n = 1.4852$). (Typical index matching fluids used for photographic emulsions, such as Xylene, strip the data from the TEP film, although without apparent damage to the organic photoconductor.) Second, fixation was known to have an adverse and uncompensatable effect on frequency response.

Figures 4-14 and 4-15 show maximum DE as a function of spatial frequency for P5-003 and P4-005, respectively. The drop in efficiency with spatial frequency is much more rapid for P5-003 than for P4-005. In both cases, fixation caused a loss in diffraction efficiency, and hence, a decrease in frequency response. It is possible to infer from these data that, in terms of a classical MTF curve, both P5-003 and P4-005 have 50 percent response at 400 cycles/mm. We note that neither processing nor our technique were necessarily optimum. Under more ideal conditions, there is the prospect of obtaining 50 percent response at spatial frequencies as high as 1000 cycles/mm. This hypothesis is supported by SEM data for electrostatic latent images from which 2000 cycles/mm resolution was measured and by (unfixed) 1000 cycle/mm resolution targets successfully contact copied onto Coulter Information Systems' KC film. The keys to very high resolution are the fixing step and the electrodeveloper composition.

4.4.6 Storage Density

Data storage performance was evaluated by recording Fresnel holograms of a ground glass diffuser with an opaque central region. The transmitting region of the input

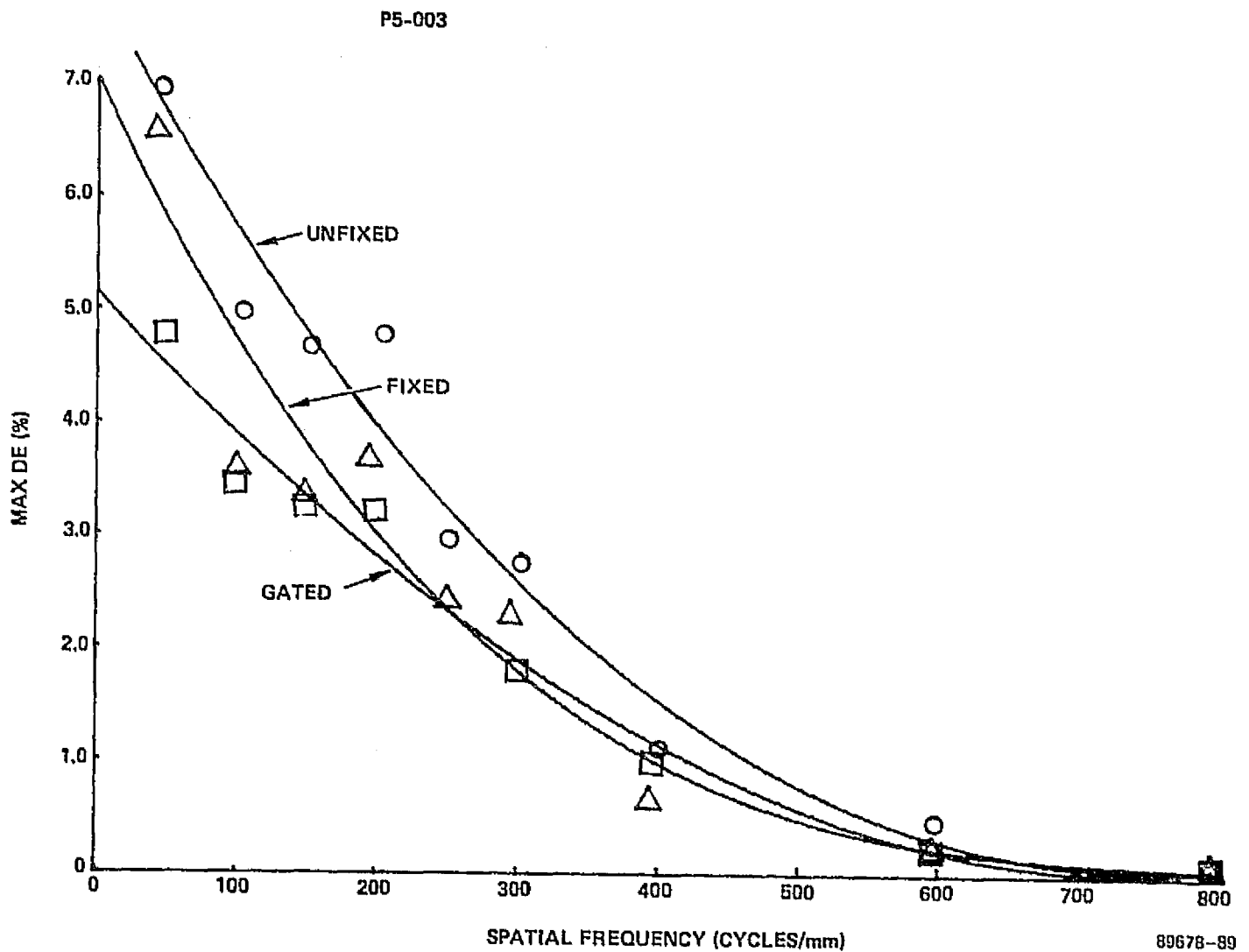


FIGURE 4-14. MAXIMUM DIFFRACTION EFFICIENCY AS A FUNCTION OF SPATIAL FREQUENCY FOR TEP P5-003

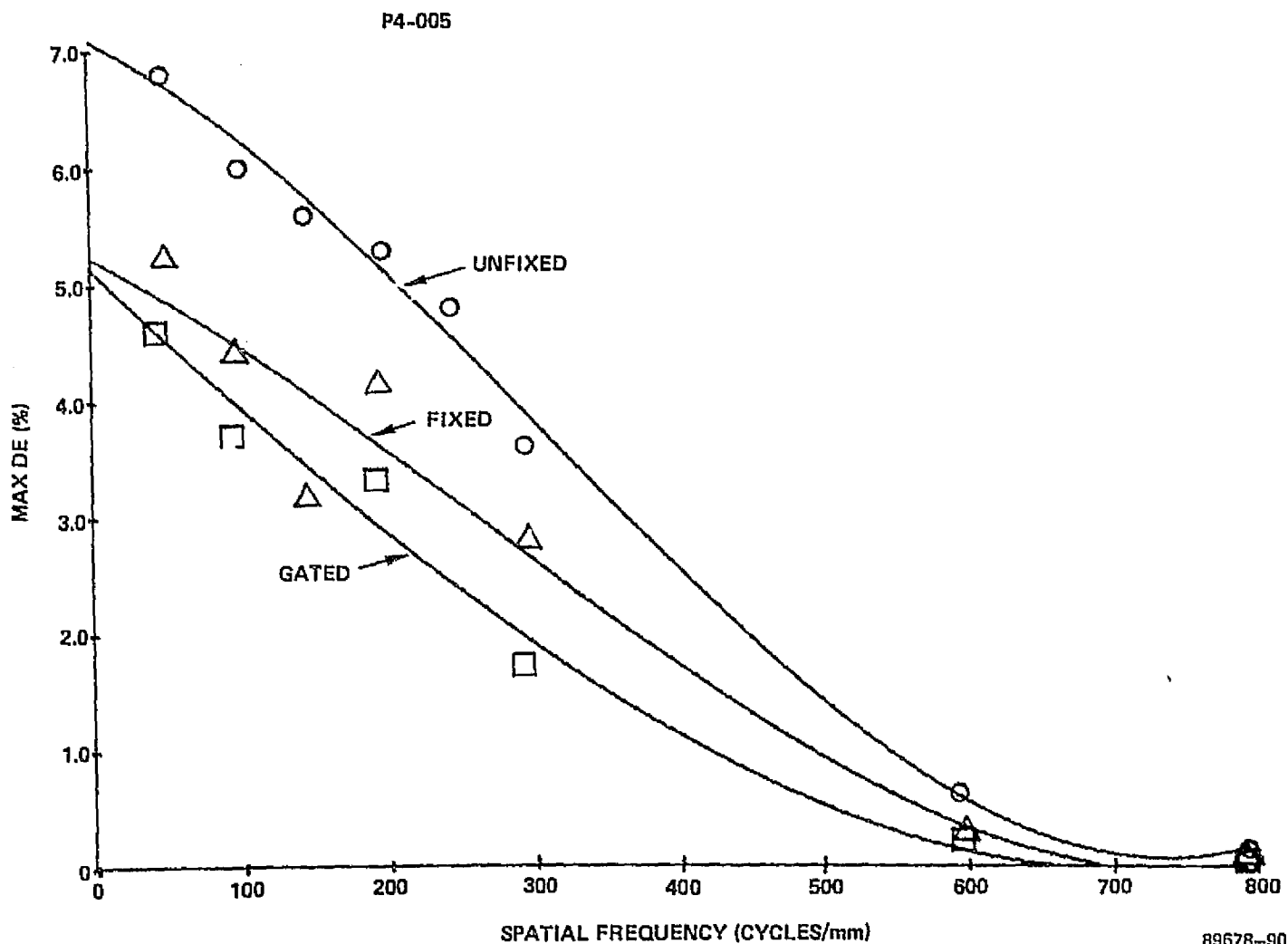


FIGURE 4-15. MAXIMUM DIFFRACTION EFFICIENCY AS A FUNCTION OF SPATIAL FREQUENCY FOR TEP P4-005



signal is equivalent to a wideband stochastic (white noise) source; the opaque region provides an absolute reference for noise measurement. The signal had a clear area of 300 mm^2 , and was positioned 200 mm from the hologram recording plane. Each hologram were 8 mm in diameter. If we assume linearity and spatial invariance, then this geometry is equivalent to a diffraction-limited information packing density of about $2 \times 10^6 \text{ bits/cm}^2$.

The experimental procedure was as follows. First, we set the carrier frequency at ν_c at 160 cycles/mm. This was held constant. Then a series of holograms was recorded over a range of average exposures E and processed as described previously. Finally, we reconstructed the real image of each hologram, and measured diffraction efficiency and signal-to-noise ratio. The procedure was repeated for K -values of 2, 10, 25, and 100. For practical reasons we did not employ index matching.

The average signal power and average noise power (light scattered and diffracted into the opaque region of the signal) were measured for the real image of each hologram by means of a scanning photomultiplier. From these data we computed an average signal power to average noise power ratio. We note that the noise power is comprised of both scatter and signal-dependent nonlinear noise.

Figures 4-16, 4-17, and 4-18 show DE and SNR as functions of E for P5-003 with $\nu_c = 160 \text{ cycles/mm}$, $\rho = 1 \times 10^5 \text{ bits/cm}^2$ and $K = 2, 10, \text{ and } 25$. Because of frequency response rolloff, we have plotted the SNR values for two spatial frequencies within the signal bandwidth that nominally correspond to 100 and 180 cycles/mm, respectively. We note that the fairly rapid decrease of frequency response over the signal bandwidth caused the illuminated area of the signal to be nonuniformly reconstructed. The image intensity rolloff provided a verification of the holographic frequency response data. Figures 4-19, 4-20 and 4-21 show the same data for P4-005.

A study of the graphical data reveals that DE varies with exposure as expected (curve shape is correct), but that peak DE is obtained for progressively lower values of E as K increases. Peak DE decreases monotonically with K . For P5-003, the maximum DE value, obtained with $K = 2$, is about 2.6 percent for an exposure of $220 \mu\text{J/cm}^2$.

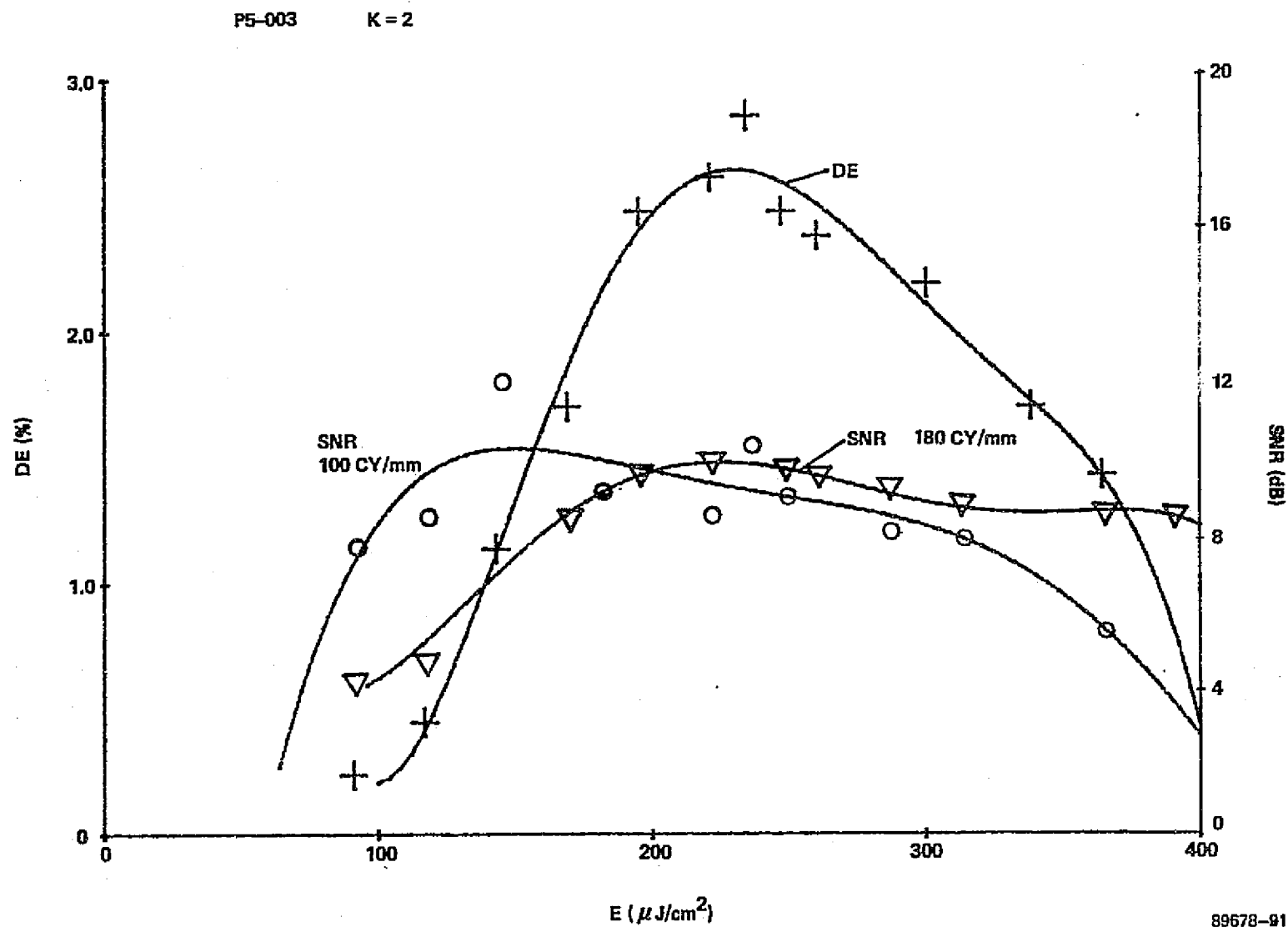


FIGURE 4-16. DIFFRACTION EFFICIENCY DE AND SIGNAL-TO-NOISE RATIO SNR AS FUNCTIONS OF EXPOSURE E FOR UNFIXED TEP P5-003 WITH K=2

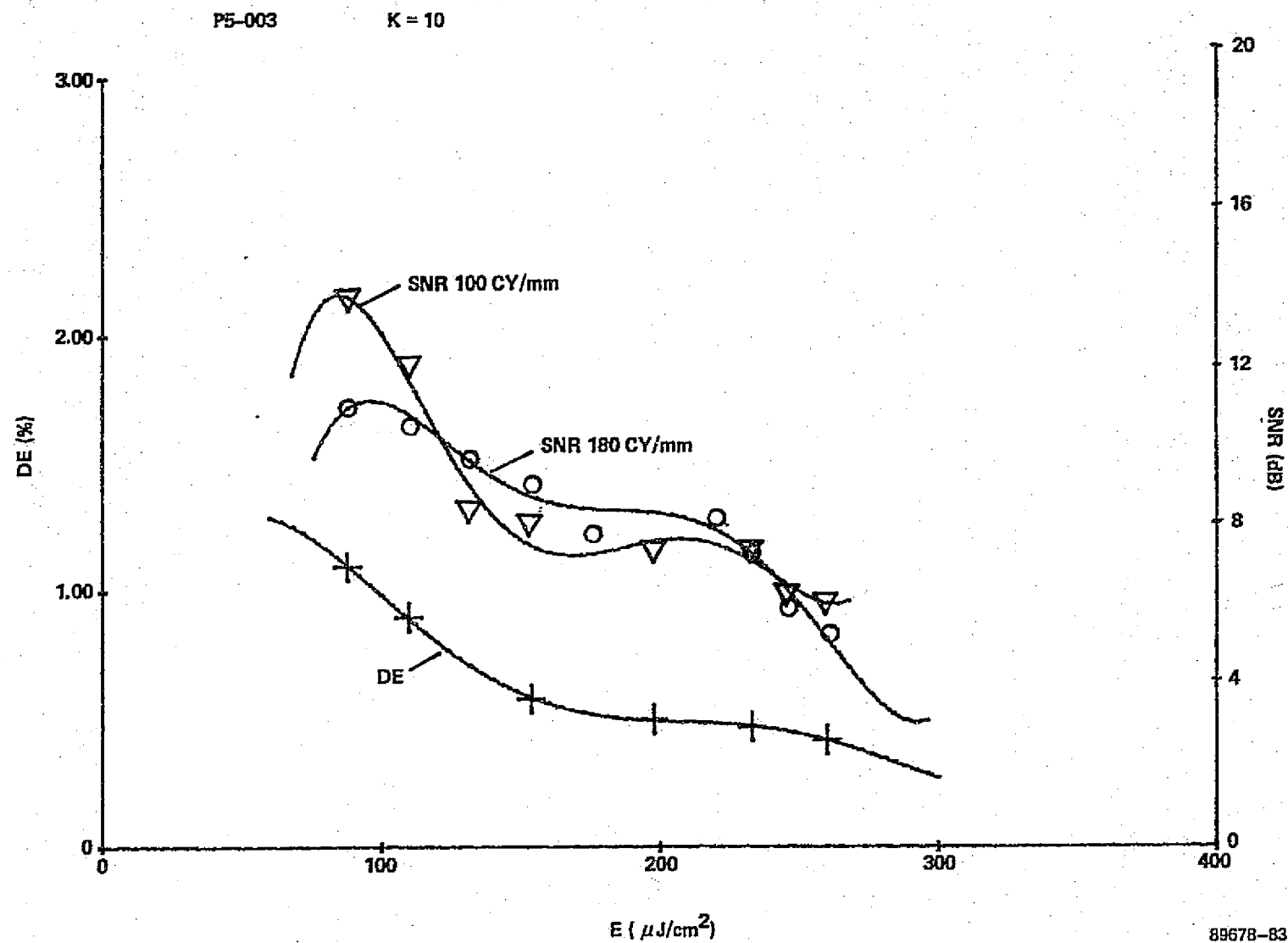


FIGURE 4-17. DIFFRACTION EFFICIENCY DE AND SIGNAL-TO-NOISE RATIO SNR AS FUNCTIONS OF EXPOSURE E FOR UNFIXED TEP P5-003 WITH $K=10$



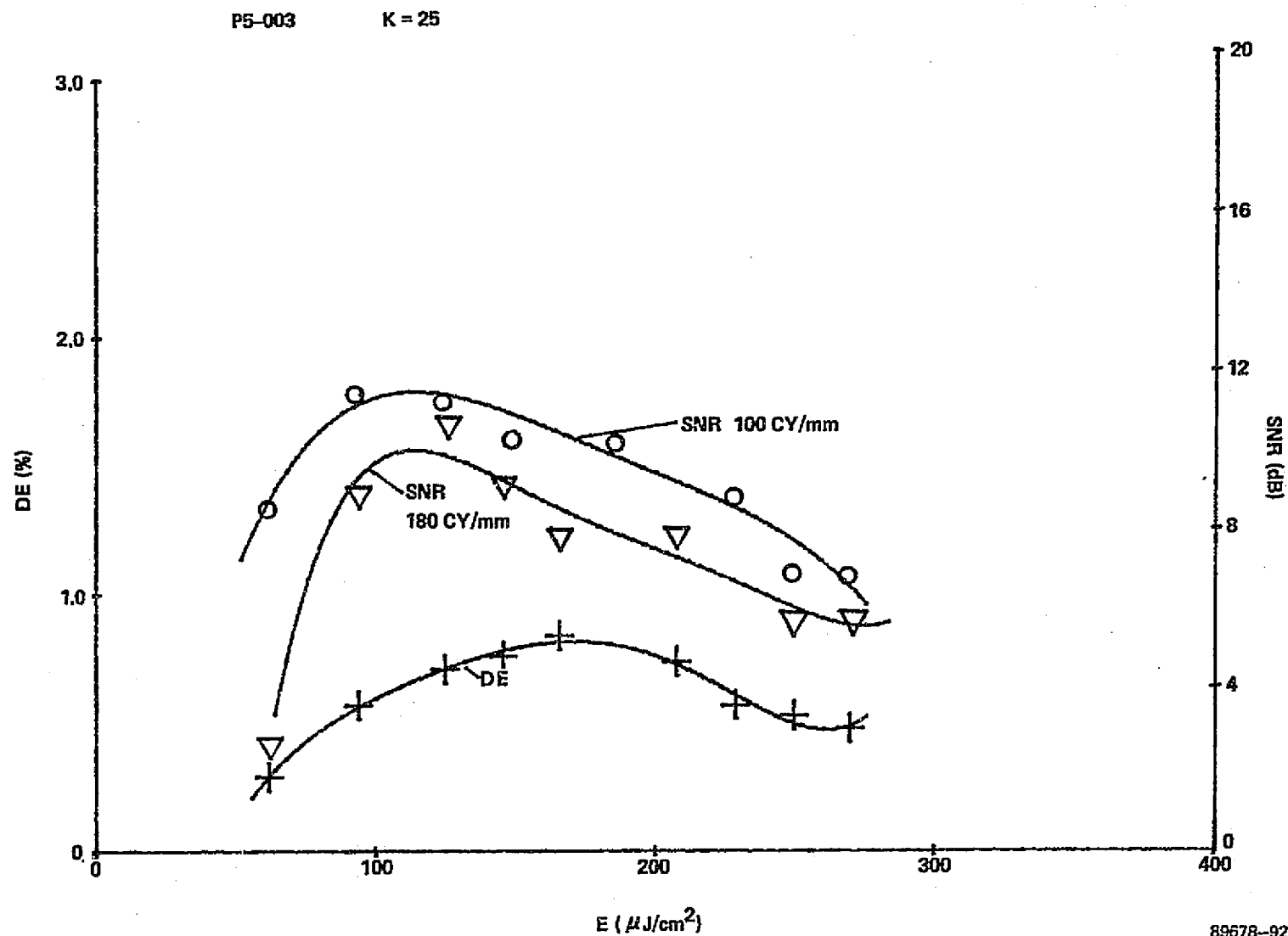


FIGURE 4-18. DIFFRACTION EFFICIENCY DE AND SIGNAL-TO-NOISE RATIO SNR AS FUNCTIONS OF EXPOSURE E FOR UNFIXED TEP P5-003 WITH $K=25$

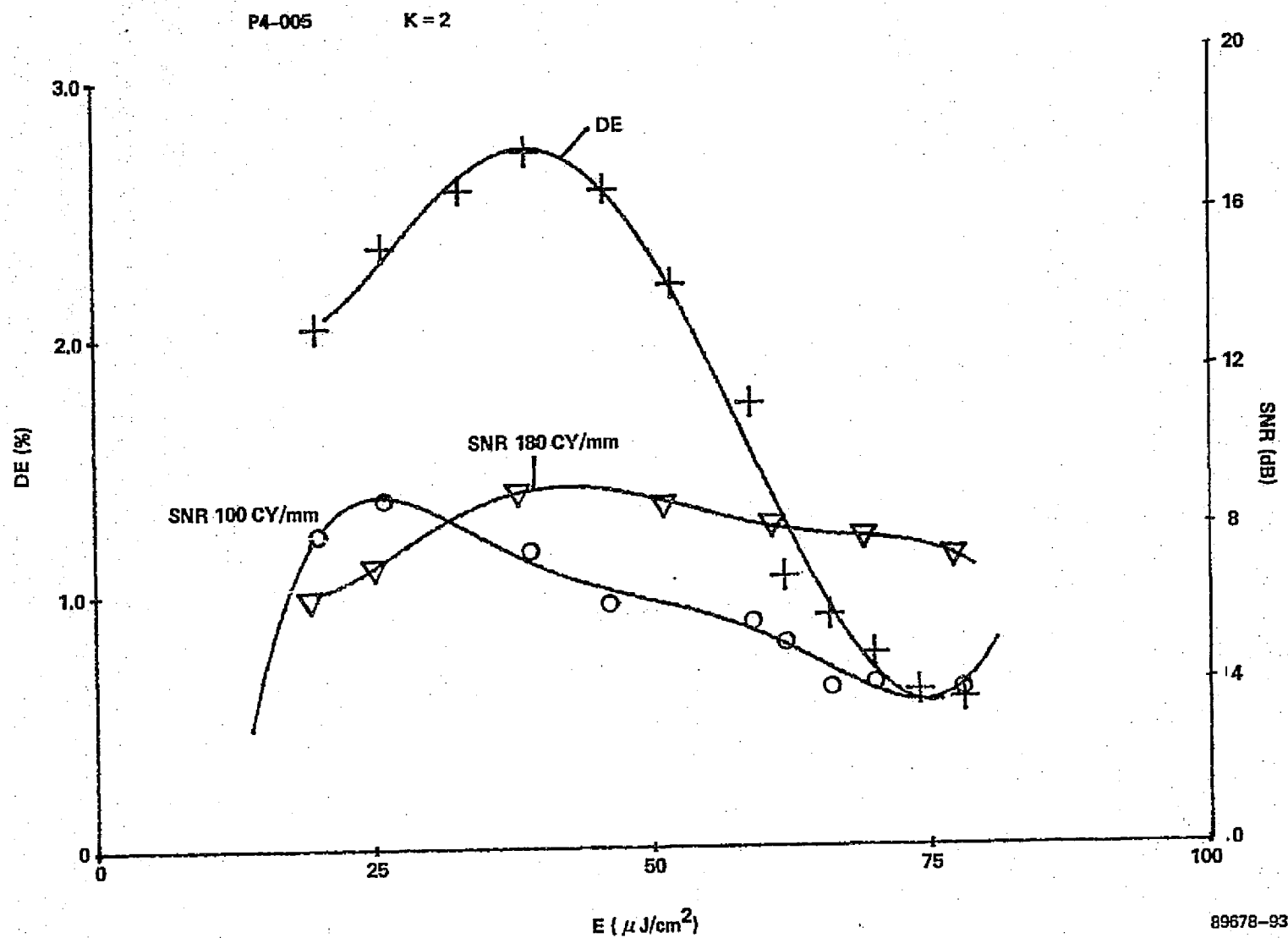


FIGURE 4-19. DIFFRACTION EFFICIENCY DE AND SIGNAL-TO-NOISE RATIO SNR AS FUNCTION OF EXPOSURE E FOR UNFIXED TEP P4-005 WITH K=2



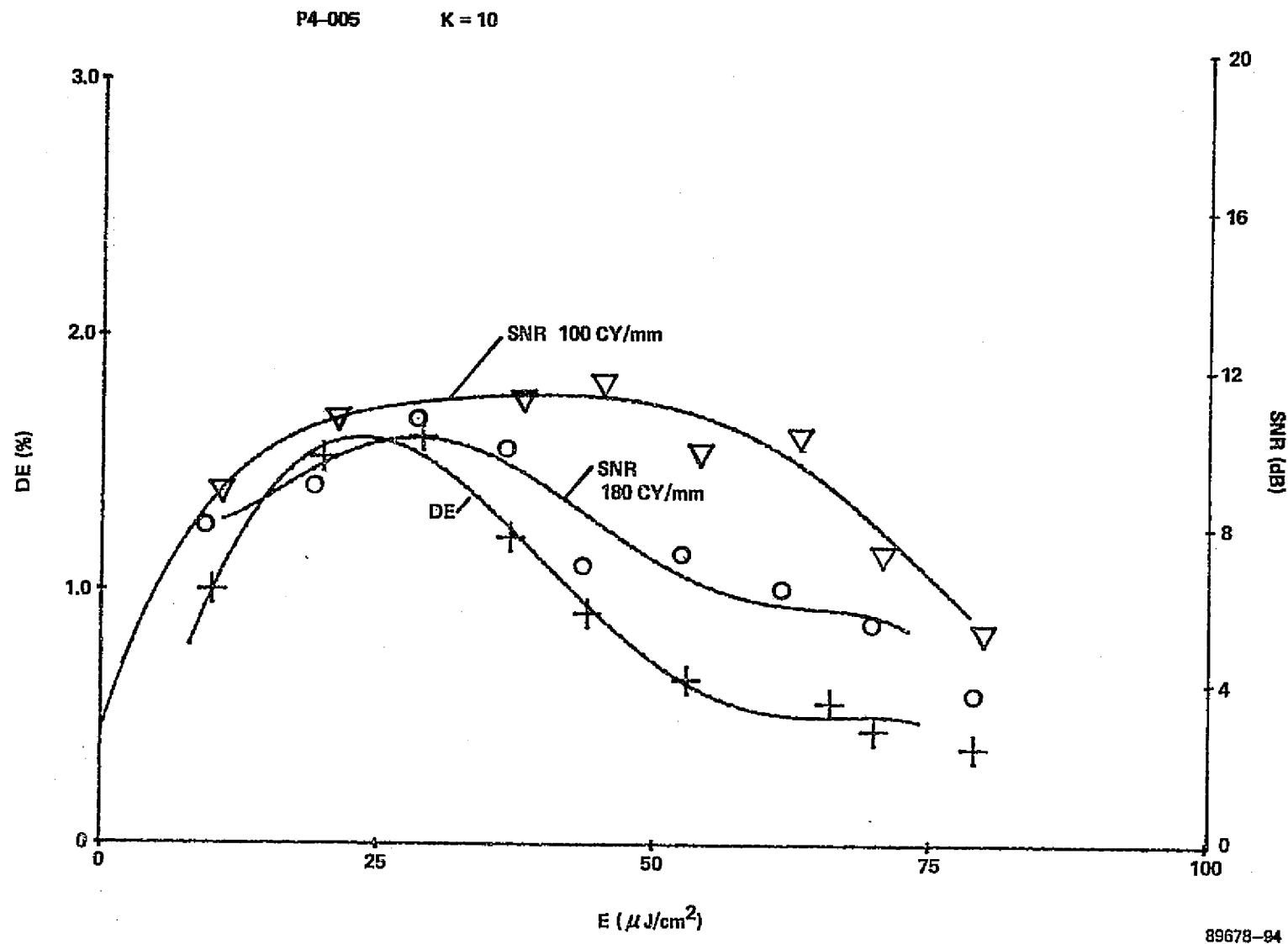


FIGURE 4-20. DIFFRACTION EFFICIENCY DE AND SIGNAL-TO-NOISE RATIO SNR AS FUNCTIONS OF EXPOSURE E FOR UNFIXED TEP P4-005 WITH $K=10$

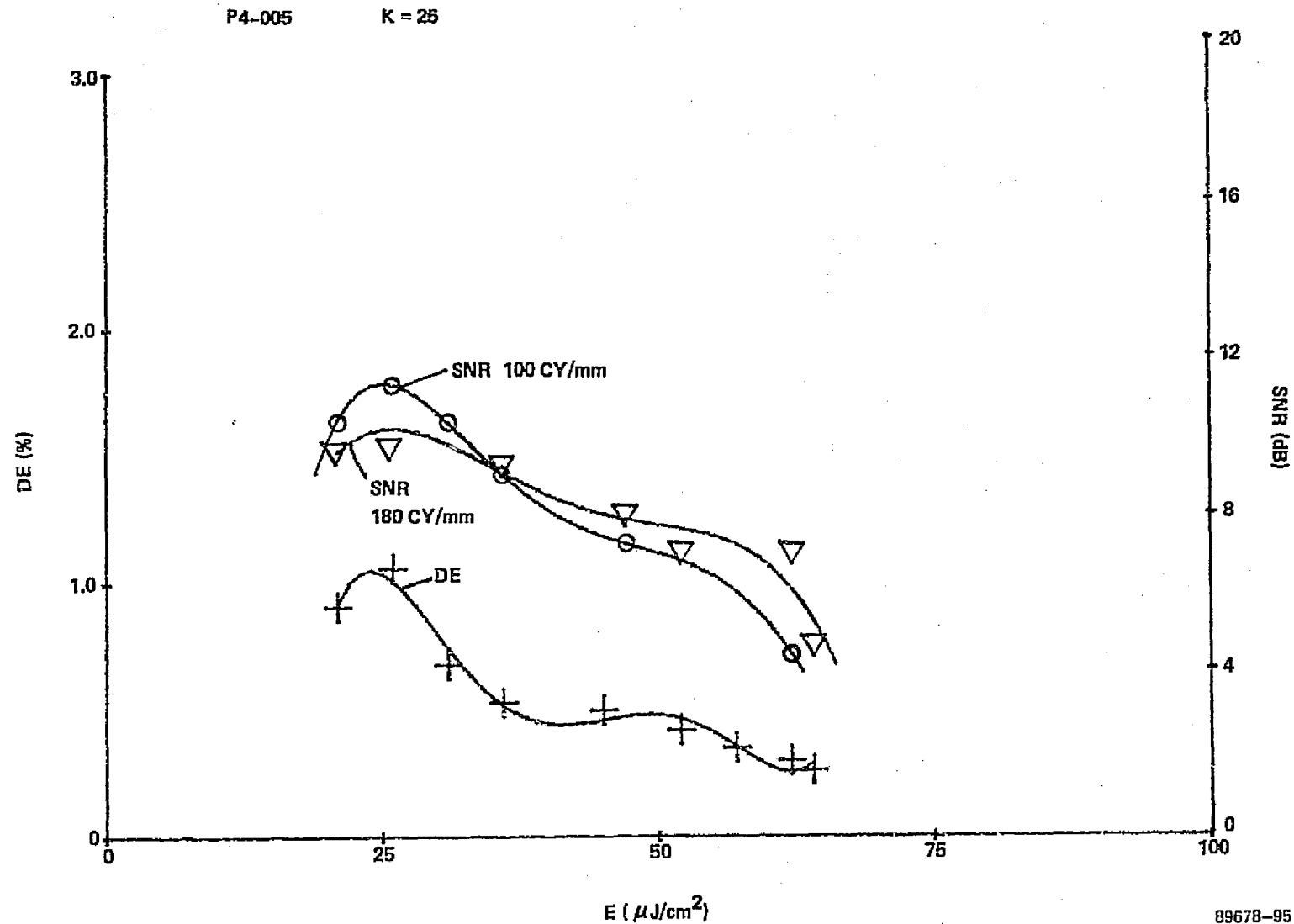


FIGURE 4-21. DIFFRACTION EFFICIENCY DE AND SIGNAL-TO-NOISE RATIO SNR AS FUNCTIONS OF EXPOSURE E FOR UNFIXED TEP P4-005 WITH K=25





Maximum SNR is 12 dB obtained for $K = 10$. For P4-005, the maximum DE is about 2.8 percent for an exposure of $40 \mu\text{J}/\text{cm}^2$. Maximum SNR is about 12 dB for $K = 10$. The difference in SNR data for $\nu = 100$ and $\nu = 180 \text{ l}/\text{mm}$ is small, and is less than expected. Higher SNR values are obtainable, as shown in the next experiment.

Figures 4-22 and 4-23 are plots of SNR as a function of exposure for P4-005 with $K = 10$. Figure 4-22 shows DE and SNR data after fixation. Figure 4-23 shows the same data after index matching the holograms. Comparing these results with Figure 4-20 (the unfixed data), we see that fixation has caused a decrease in diffraction efficiency of about 30 percent. Index matching results in a further DE loss. Peak SNR is 16 dB for $\nu = 100$ cycles/mm and there is now a distinct difference between the SNR values at $\nu = 100$ cycles/mm and $\nu = 180$ cycles/mm. However, index matching does not greatly affect SNR. Less than optimum storage performance for the TEP films can be attributed to excessive scatter noise and decreasing frequency response over the signal bandwidth. Obviously, the impact of the fixation step is very great on the storage capacity potential of TEP films.

4.4.7 Contact Printing

Some preliminary efforts were made to contact print a 1951 USAF Resolution Target onto the TEP films. The process we employed takes advantage of the persistent conductivity of the photoconductor. If the OPC is greatly overexposed, it remains partially conductive after the exposure has ended.

The procedure followed was to contact print the resolution target with an exposure of about $12 \text{ J}/\text{cm}^2$. After exposure, the film was charged and immediately developed. The proper development bias for this experiment was difficult to determine, since the charging is dependent on pre-exposure and on the time between exposure and development. Using this procedure, we were able to resolve Group 7-5 (204 cycles/mm). This is not an absolute limitation on the film, but rather on the technique. Higher resolution is achieved using the standard charge, expose, and develop approach.

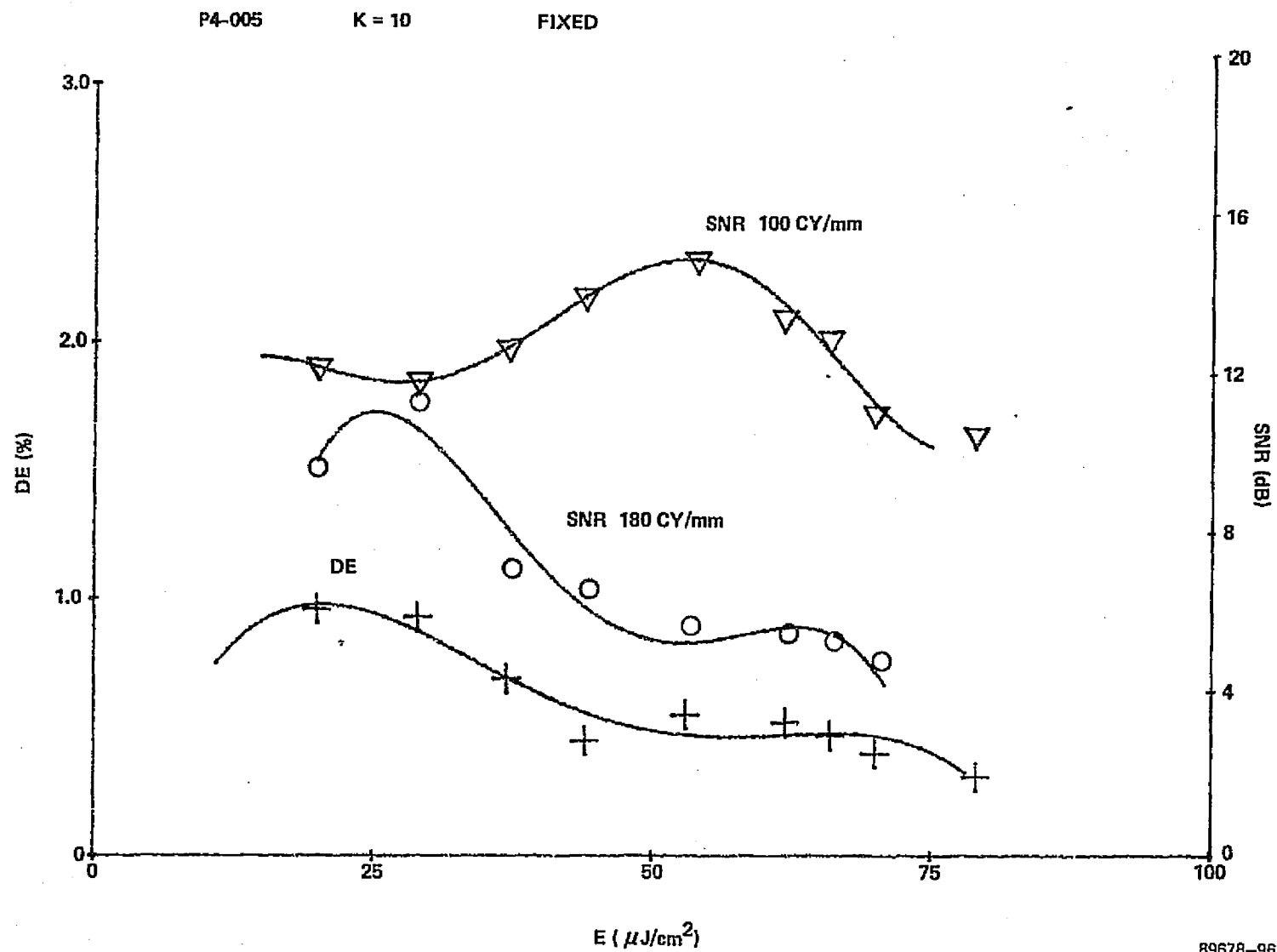


FIGURE 4-22. DIFFRACTION EFFICIENCY DE AND SIGNAL-TO-NOISE SNR AS FUNCTIONS OF EXPOSURE E FOR TEP P4-005 AFTER FIXATION WITH K=10



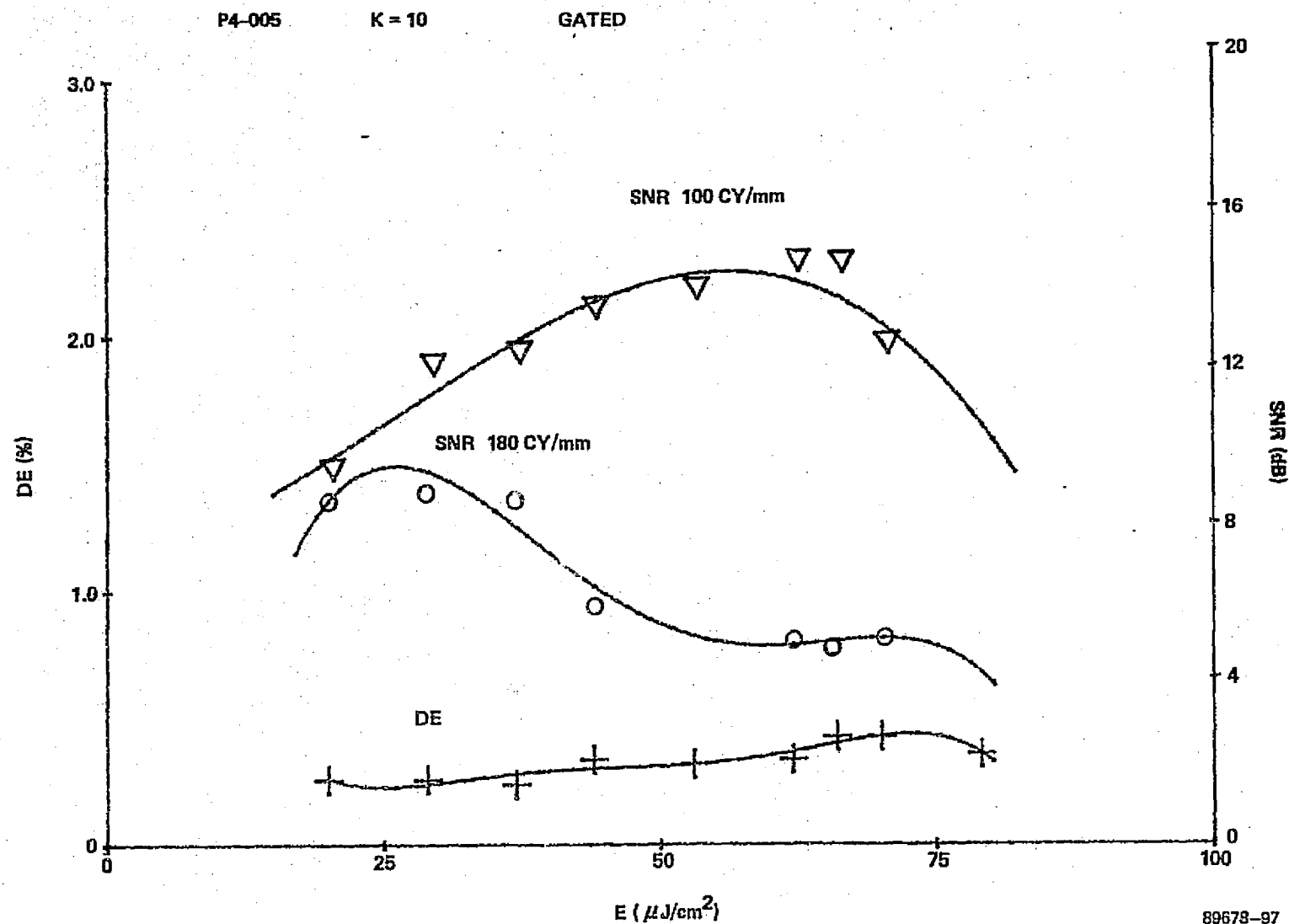


FIGURE 4-23. DIFFRACTION EFFICIENCY DE AND SIGNAL-TO-NOISE SNR AS FUNCTIONS OF EXPOSURE FOR TEP P4-005 WITH INDEX MATCHING WITH K=10



4.5 DISCUSSION, COMMENTS, AND CONCLUSIONS

Our experimental investigation shows that the Scott Graphics TEP films have the qualifications required for direct digital optical recording and other optical data storage applications. In summary, for TEP P5-003 film we measured for helium-neon laser light ($\lambda = 633 \text{ nm}$) an exposure sensitivity of $240 \mu\text{J}/\text{cm}^2$, a 50 percent spatial frequency response of 400 cycles/mm and peak SNR of 12 dB. The corresponding data for TEP P4-005 film are $70 \mu\text{J}/\text{cm}^2$, 400 cycles/mm and 16 dB. In both cases, we state data for fixed film samples. Overall, the P4-005 film is rated best for laser recording applications. The performance data suggest that both TEP films are also suitable for high-reduction micrography (e.g., COM and ultrafiche) and facsimile applications.

In regard to high-density direct digital optical storage we conclude, that under optimum condition, spots separated by $1.25 \mu\text{m}$ with a contrast ratio C of 3 can be recorded on P4-005. This corresponds to an information storage density of $64 \times 10^6 \text{ bits}/\text{cm}^2$. Signal-to-noise ratio, however, would be close to unity. These numbers are obtained by applying the sampling theorem, assuming white noise, and using best-case experimental data for 50 percent frequency response and signal-to-noise ratio. The error rate for $C = 3$ and $\text{SNR} = 1$ is, of course, very high and, hence, this example is of no practical merit.

A factor not accounted for in the previous discussion is the impulse response of the recording medium. The recorded spot size can be no smaller than the impulse response spot size. If we attempt to record smaller spots, we obtain a recorded spot size equal in diameter to the impulse response plus the input spot size. There is a decrease in net optical density and contrast (analogous to the Eberhard effect). For the Scott Graphics TEP films this effect was very dramatic for spot recording on centers of less than $5 \mu\text{m}$. At a $5 \mu\text{m}$ center spacing we appeared to reach a threshold. Larger spots could easily be recorded at near maximum density and contrast.

If we consider an example based on $5 \mu\text{m}$ spots, the data storage potential of TEP films is much higher. Now the information packing density has decreased to



4×10^6 bits/cm², but the contrast ratio has increased to 10 and signal-to-noise ratio to 6.5 dB. This yields an (uncorrected) statistical error rate of less than 10^{-6} . Performance at this level is better in terms of storage density and archivality than that obtained with most advanced magnetic technology, e.g. Ampex TBM[®].

As the construction, method of use, and processing (especially the composition and application of the electrodeveloper and fixing) are not optimized, it is reasonable to hypothesize that significant improvements in the data storage performance of TEP films are possible. In our judgment, improved TEP films can be competitive with Lippmann photographic emulsions in terms of information storage density and cost for spots as small as 2 μ m. The TEP films will also provide environmental integrity, image permanence and archivality superior to photographic emulsions. Of equal or greater importance, TEP films can be processed in-line (no wet chemicals) and have an add-on capability, an important systems and operational consideration. Continued research and development to improve the performance of all TEP films is highly recommended.



4.6 REFERENCES

1. Damon, R. W. and D. H. McMahon, *Electro-Opt. Sys. Des.* 2, 68 (1970).
2. Rajchman, J. A., *J. Appl. Phys.* 41, 1376 (1970).
3. Stepke, E. T., *Electro-Opt. Sys. Des.* 4, 12 (1972).
4. Tufte, O. N. and D. Chen, *IEEE Spectrum* 10, 26 (1973).
5. Gaylord, T. K., *Opt. Spec.* 8, 29 (1974).
6. Bardos, A., *Appl. Opt.* 13, 832 (1974).
7. Roberts, H. N., J. W. Watkins, and R. H. Johnson, *Appl. Opt.* 13, 841 (1974).
8. Eward, R. S., *Opt. Spec.* 9, 25 (1975).
9. Chen, D. and J. D. Zook, *Proc. IEEE* 63, 1207 (1975).
10. Zech, R. G., L. M. Ralston, and M. W. Shareck, "Holographic Recording Materials," (Final Technical Report, Contract No. F30602-74-C-0030, Rome Air Development Center), July 1974.
11. Dailey, F. E., Jr., "Films Using Organic Photoconductors," 21st Annual NMA Meeting, New York, NY, May (1972).
12. Dailey, F. E., Jr., and E. Bennett, "Some Considerations for a New Photorecording Technology," SPSE Winter Symposium on Micrographics Science, New Orleans, LA, February (1973).
13. Habib, D. P. and J. D. Plumadore, "A Microelectrophotographic System," 26th Annual SPSE Conference, Rochester, NY, May (1973).
14. Dirks, J. F., "Photorecording and Organic Photoconductors," SPSE Electro-Optical Systems Design Conference, New York, NY, September (1973).
15. Dailey, F. E., and J. D. Plumadore, *J. Appl. Phot., Eng.* 1, 31 (1976).
16. Schaffert, R. M., *Electrophotography*, 2nd Ed., John Wiley and Sons, New York (1975), pp. 630-631.
17. Zech, R. G., "Applications of Electrophotography to Optical Data Storage," IEEE/IAS Conference Record 31A, 301 (1975).



HARRIS

18. Comizzoli, R. B., G. S. Lozier, and D. A. Ross, RCA Rev. 33, 406 (1972).
19. Bird, G. R., R. Clark Jones, and A. E. Ames, Appl. Opt. 8, 2389 (1969).
20. Plumadore, J. D., and N. A. Nielson, TAPPI 55, 1345 (1972).
21. Fritz, F. G., D. C. Hoesterey, and L. E. Brady, Appl. Phy. Lett. 18, 277 (1971).
22. Schaffert, R. M., Electrophotography, 2nd Ed., John Wiley and Sons, New York (1975), pp. 242-245.
23. Zech, R. G., Ph.D. Thesis, University of Michigan (1974), pp. 194-217.
24. Kelley, D. H., J. Opt. Soc. Am. 51, 319 (1961).
25. Kozma, A. and J. S. Zelenka, J. Opt. Soc. Am. 60, 34 (1970).
26. Biedermann, K., and S. Johansson, J. Opt. Soc. Am. 64, 862 (1974).
27. Lee, W. H. and M. O. Greer, J. Opt. Soc. Am. 61, 401 (1971).



HARRIS

ELECTRO-OPTICS

5-1

SECTION V

DATA BASE MANAGEMENT CONSIDERATIONS



SECTION V

DATA BASE MANAGEMENT CONSIDERATIONS

Data base management becomes increasingly important as greater volumes of data are acquired at higher data rates by a wide variety of data acquisition systems. Although much of our discussion has general validity, we focus our attention on those requirements relating to imagery forming systems. It is not important to distinguish between data collected by satellite, airborne or shipborne sensors or by the particular wavelength used to form the image. We shall assume that after detection the data are digitized and transmitted for subsequent processing.

5.1 GENERAL CONSIDERATIONS

The first step in the set of ground processing operations is to record the data. Some data may also be processed in real time, but recording all the incoming data must, in general, be accomplished. This data store is already large and based on the projected growth in the number and quality of new sensor systems such as LANDSAT D, will grow more rapidly than it has in the past. An important need, therefore, is to provide more cost-effective data storage systems.

Data processing is an important element of data base management since it provides methods for extracting the desired information from the data. Clearly, many processing operations may be performed on the same data to provide information to many different investigations. The computer compatible (magnetic) tapes, or CCT's, of LANDSAT 1 and 2 data generated by Goddard Space Flight Center are an example. In the early stages of developing the required software, interactive displays as well as hard copy displays help the investigator to more rapidly reduce the data to a useful form. Subsequently, displays are fundamental to data analysis and further data exploitations. Thus, another important requirement is to provide higher resolution displays that do not require the use of the computer processing facility.



To reduce the load on the computational facility and the size of the data store, effective methods of preprocessing or screening are required. Some data are useless for their intended purpose because of extensive cloud cover, sensor malfunction, data transmission quality and so forth. If the quality of the incoming data could be determined in real time, the useless or marginal data could be discarded before they are processed or stored. Eventually some of these techniques may be implemented at the sensor and thereby reduce the required data transmission rate as well. A goal of achieving a data transmission reduction factor from 100 :1 to 1000 :1 without loss of useful data content, is reasonable.

Some recommendations for improving data storage, data display and data preprocessing techniques follow:

5.1.1 Data Storage

A data processing station consists of one or more computers having a hierarchy of memories, one of which may be an archival optical mass store. The size and access times of these memories are generally determined by the incoming data rate and the complexity of the software programs that are executed. Parallel processors are also frequently used to reduce computational time and cost. The mainframe processors are not normally used to archivally store the data, and must therefore be reusable.

Data that are stored archivally should be recorded on a medium that is permanent, has a low cost per bit, can be recalled many times without reducing data quality, requires minimum maintenance and can be duplicated easily. Magnetic tape has been used almost exclusively to date for the archival storage of data. Yet it has few of the desired characteristics. Data stored on magnetic tape are not permanent; to store data reliably for several years requires periodic respooling to avoid data degradation and careful control of the storage environment. Frequent recall of data stored on magnetic



tape results in a deterioration of the data quality and mass duplication, if desired, requires multiple machines. Head wear, maintenance and alignment procedures contribute to the annual cost of archival storage. All of these problems become worse if the information storage density increases.

A more logical choice of media for storing data archivally is photographic film or its equivalent. Optical techniques for recording digital data on photographic film and other light and heat sensitive media have advanced significantly in the past decade owing to the development of reliable and low-cost devices such as lasers, light modulators, beam deflection devices and photodetector arrays. In the future, optical techniques may also compete with magnetic techniques in those areas where the storage media must be reusable. At present, optical technology should be applied to the development of archival data storage systems. These same techniques should prove to be of general usefulness when an acceptable read/write optical recording media is developed. The principal advantages of storing data optically are very high information density, the low media costs (on a per bit basis) and the almost negligible maintenance costs.

5.1.2 Data Displays and Recorders

To properly use data acquired from image forming sensors, a broad spectrum of image display and recording devices is needed. A recording device is generally used to create an image that is preserved for a significant period of time (sometimes archivally). Displays are used to create images or portions of images for temporary usage. Although there are several significant advances in electro-optics technology that will lead to important advances in recorders (e.g., laser beam recording at very high resolution and image fidelity, direct platemaking for mass production of prints and remote photographic quality facsimile transmission of images), we focus here on the need for higher quality displays which have characteristics similar to CRT displays.



CRT displays have limited resolution and grey scale (or color) capability. A need exists for displaying images from future sensor systems that have 5,000 to 10,000 resolution elements along each scan line and an equivalent number of scan lines (in a framing mode). Some systems operate in a mode in which a strip of terrain is scanned continuously as the sensor moves. Such systems should ideally use a "falling raster" display. CRT's do not efficiently handle the latter mode of operation because they need an associated refresh memory that becomes increasingly complicated and expensive as the image quality increases.

Laser beam recorders using dry silver or electrophotographic films or a reusable media such as photoplastic recording film offer an attractive solution to this problem. The incoming data is recorded in a line scan format while the film moves in the cross-scan direction. After a short time delay for processing (approximately 1 second in some cases), the image can be viewed directly or projected onto a rear projection screen. The screen would have all the appearances of a very high resolution CRT display and can be operated in either a "frame" or a "falling raster" mode. Color displays are possible by using coding techniques.

A secondary benefit of developing such displays is that the images could be integrated with the digital data base to provide for subsequent browsing. An investigation could browse through the imagery file to select potentially useful data and then request the digital data for detailed processing. The digital transfer of data to existing CRT displays is therefore not needed, saving both time and cost.

5.1.3 Data Processing

Another technique for saving costs is to eliminate or greatly reduce the amount of data subjected to detailed processing or storage. Image quality assessment (e.g., to detect excessive line jitter or loss of sync) immediately after reception would



eliminate those data from which no useful information can be easily extracted. After appropriate algorithms have been more fully developed, data processing for feature extraction or classification could be more fully automated. Optical techniques should prove particularly useful because they inherently allow two-dimensional parallel processing. In principal, these and related techniques could be used for on board processing to reduce the data rate required of the downlink.

5.2 PRELIMINARY DATA BASE MANAGEMENT/END-USER SURVEY

Early in the DIGIMEM phase of the Optical Mass Memory Investigations Program it was decided to examine at a low level the data base management requirements of potential end-users of DIGIMEM technology. There was general agreement that the development of DIGIMEM technology should proceed in parallel with the identification of end-users and their data handling problems. To that end, several NASA facilities (Johnson Space Center, Goddard Space Flight Center and Marshall Space Flight Center) together with the Department of the Interior's EROS Data Center were selected as baseline data sources.

5.2.1 Summary of Survey Data

The top level data obtained from our survey activities are summarized in Table 5-1. In Table 5-1 are listed the facility surveyed and its applicable primary mission, function and requirements. We emphasize that the entries in Table 5-1 are narrow in the sense that they apply only to our specific interests. Obviously, with the possible exception of the EROS Data Center, the mission of these facilities covers a much broader spectrum of activities.

TABLE 5-1. SUMMARY OF DATA BASE MANAGEMENT/END-USER SURVEY ACTIVITY

Facility	Applicable Mission	Function(s)	Applicable Need(s)	Comments
I. Johnson Space Center (Houston, Texas)	<ul style="list-style-type: none"> Space Shuttle 	<ul style="list-style-type: none"> Mission support/ Space Shuttle Data Management 	<ul style="list-style-type: none"> Read/write instrumentation recorder Rapid-access, very low error rate, on-line recorder/reproducer Read-only archival mass storage system 	<ul style="list-style-type: none"> Space Shuttle data management system planned and funded Complete upgrade to Central Data Facility planned by 1981 Archival storage of 70 billion bytes and on-line disc storage of 2 billion bytes planned Key needs are reduction of search time in archival store and access time to/volume of fast on-line store
II. Goddard Space Flight Center (Greenbelt, Maryland)	<ul style="list-style-type: none"> LANDSAT image processing 	<ul style="list-style-type: none"> Processing of raw LANDSAT data to effect geometric and radiometric corrections to multispectral scanning imagery Generation of CCT and photographic MSS data Archiving of MSS data 	<ul style="list-style-type: none"> High-speed, high-resolution laser recorder High-density archival mass storage system High-rate parallel image processor 	<ul style="list-style-type: none"> GSFC converts downlink LANDSAT MSS data into high-density digital tapes (14-track; 20,000 bpi) Supplies CCT to EROS Data Center Supplies photographic data to various Government users (Department of Agriculture, JSC, NOAA, etc.)
III. Marshall Space Flight Center (Huntsville, Alabama)	<ul style="list-style-type: none"> Charter responsibility for data base management 	<ul style="list-style-type: none"> Managing survey of existing state-of-the-art and projected future data handling hardware and software 	<ul style="list-style-type: none"> Awareness of current trends in mainframe and peripheral computer technology Technology developments in support of very high capacity archival stores Data base management techniques for high-rate parallel processing using very large on-line data stores 	<ul style="list-style-type: none"> MSFC administers the "Optical Mass Memory Investigations" program
IV. EROS Data Center (Sioux Falls, South Dakota)	<ul style="list-style-type: none"> Repository for unclassified remote sensing data 	<ul style="list-style-type: none"> Storage and dissemination of remote sensing data Training of users of remote sensing data 	<ul style="list-style-type: none"> Archival Mass Storage System High-speed, high-resolution Laser Image Recorder High-resolution Facsimile System Expansion/Improvement of Data Base Management 	<ul style="list-style-type: none"> Stores remote sensing data in photographic form and on CCT's Present facility nearing capacity for both CCT's and film Significant improvements in cost-effectiveness and turn-around time a major goal

ORIGINAL
PAGE IS
OF POOR
QUALITY

ELECTRO-OPTICS

HARRIS





After a brief study of Table 5-1 it becomes clear that, although each facility has a different mission, there is a thread of commonality. The development and implementation of advanced data base management systems to process and store massive amounts of hard data is a common need. We learned that at present there is far more data being generated by an ever growing number of sources than can be organized and accessed. As a result, much potentially valuable information lies stored in various warehouses so unorganized that few users attempt access. Moreover, the computer tape and photographic modes of storage currently used are not proving to be archival; hence, there is considerable permanent data loss. Another key need identified is for a cost-effective, archival mass storage system to which the user has reasonable access time. A common opinion was that conventional magnetic technology could be adapted for mass stores as large as 10^{14} bits. For larger stores, however, newer and more efficient technologies were required. The potential of a DIGIMEM approach with on-line storage was well-received. Finally, a need for high-speed, high-resolution laser image recorders to produce hardcopy of remote sensing data was noted. Timely data dissemination could be improved by the development and use of wideband imagery transmission systems, e.g., laser facsimile.

5.2.2 Specific Example: Goddard Space Flight Center

Goddard Space Flight Center plays a key role in the processing dissemination, and archiving of LANDSAT data. Although the mission of Goddard SFC is expected to change in the near future, the following data is currently applicable:

- 1) Data Source: LANDSAT remote sensing data satellites (multispectral scanner and return-beam vidicon). The data from each LANDSAT is telemetered down in 10 minute bursts hourly. This data is processed and recorded on a high-density digital tape format at the present time.



The processing involves only restoration of the radiometric and geometric fidelity of the received data, plus the annotation of timing and geographic identification codes. The data may be stored in either fully processed, partially processed or raw formats, depending on the nature and objective of the mission, in some cases there is a need for multiple parallel recording.

2) Data Recorders:

a) Now

- i. High-density Digital Tape: the present system is a 10-track, 20,000 bpi recorder operating with 9600 foot reels of tape. It is considered an inefficient, state of the art recorder. This system is used to record LANDSAT information directly.
- ii. Photo-Recorder: A He-Ne laser recorder developed by RCA that uses wet processed film and electro-optic modulators and that has a 1000 lines/inch resolution capability on a 9 inch B&W format. This system's intended use is for converting the high-density digital tape data into photographic form for dissemination. (At the present time, film hardcopy is generated by an electron beam recorder.)
- iii. Color Photo-Recorder: An EPSCO Laboratory laser recorder system that uses argon- and krypton-ion lasers for three-color recording. The system produces color prints without the registration problems of printing three different B&W negatives.

b) Future

- i. High-Density Digital Tape: Goddard SFC has recently entered into a contract with Martin Marietta to produce an improved version



of the 10-track, 20,000 bpi recorder. The new recorder is a 40-track system with everything else the same. This system is not expected to solve a projected need for a much higher information storage density.

- ii. New Photo-Recorders: Goddard SFC recently purchased a Harris LASERFAX transceiver.
 - iii. Additional High-Density Digital Recorders: There is considerable interest in exploring the possibilities of other mass memory systems for archival storage of LANDSAT data.
- 3) Goddard SFC's Role Relative to NASA's Mass Storage Requirements
- a) As an ARCHIVER

The LANDSAT data originals are all kept at Goddard SFC; thus Goddard SFC has the need to store the data in an archival format. This applies only to the original raw data in magnetic tape, however, and not to the photographic materials.

- b) As a DATA SOURCE

Mainly by default, Goddard SFC functions as a data source and distributor to other remote distribution centers throughout the country. The reason is that, of the major users of LANDSAT data, only the Department of the Interior's EROS Data Center has the facilities to read the high-density digital tape Goddard SFC provides. As a result, Goddard SFC has the responsibility for converting its digital data into photographic form for others. Among the users of this photographic information are the



Agriculture Centers, NOAA, and Johnson Space Center's LACIE (Large Area Crop Inventory Experiments) program. The EROS Data Center receives second generation data on computer compatible tape, rather than the original information.

4) Data Base Definition:

Data are requested by three primary means:

1. Latitude/Longitude
2. Image ID (time)
3. World Reference System (WRS) number

The WRS number is a six-digit number, with each digit having a specific meaning. A WRS key is available to the public. This is a verification of a definite keying hierarchy for file organization and access, which is important for analysis of data base management requirements.

5) Near-term Mass Storage Requirements: See Table 5-2

5.2.3 Conclusions

The technology development of DIGIMEM for an archival mass storage system can be justified in terms of NASA facility mass storage requirements. Very large capacity stores with short access times are a well-defined need. However, the data base management required to control and use these large memories is of equal importance. We recommend that a continuous and detailed interaction be maintained between technology developer and technology user and that emphasis be placed on the overall architecture and management of the mass store.



TABLE 5-2

NASA GODDARD SFC NEAR-TERM
MASS STORAGE SYSTEM REQUIREMENTS

Data Source:	LANDSAT Satellites
Largest data block:	1 scene = up to 10×10^8 bits
Access time to largest data block:	Not critical
Data Recording Rate:	1 scene every 30 seconds, or approximately 30 Mb/s
Largest continuous stream of data:	1 satellite pass = 10 minutes of data, or 20 scenes = 2×10^{10} bits
Time between adjacent satellite passes:	60 minutes
Amount of data recorded per day:	From 50 to 200 scenes per day for LANDSAT D, or up to 2×10^{11} bits/day
Information storage density:	In the near term, for a 40 track/inch by 2×10^4 bits/linear inch recorder = $8 \times 10^5/\text{in}^2$. Considerably higher storage densities are desirable.
Bit error rate:	1 part in 10^7 for random errors (not burst)
Data processed per day:	5×10^{11} maximum now; expected to increase by factor of 10 by 1981



HARRIS

ELECTRO-OPTICS

6-1

SECTION VI

CONCLUSIONS AND RECOMMENDATIONS



SECTION VI

CONCLUSIONS AND RECOMMENDATIONS

The key accomplishments of the DIGIMEM program phase can be summarized as follows:

ACTIVITY

I. THE DIGIMEM BREADBOARD

- Designed, fabricated, and tested critical breadboard components
 - Floppy disk film transport
 - Electronically-agile photodetector array
 - Data wander tracking subsystem
 - Control electronics
- Designed and fabricated an optical spot recording breadboard
- Recorded 8-bit data bursts (ASCII-coded characters) on SO-173 film at 1 Mb/s data rate
- Achieved 50×10^6 bits/in² spot packing density (2.0 μ spots on 3.5 μ m centers)
- Read 8-bit data bursts in parallel format with electronically-agile array
- Achieved 1 Mb/s readout rate

II. DATA BASE MANAGEMENT INVESTIGATIONS

- Visited key data processors and end-users within the NASA community
 - The Johnson Space Center



- The Goddard Space Flight Center
- The Marshall Space Flight Center
- The EROS Data Center (civilian repository for NASA remote sensing data)
- Summarized and evaluated user needs
- Determined potential applications of DIGIMEM technology for NASA
 - On-line, high-density, recorder/reproducer
 - Random access archival optical MSS for LANDSAT and aerial reconnaissance data
 - Archival document storage and retrieval system

Based on the results of the DIGIMEM study, we conclude that:

- Direct digital optical spot recording is a feasible baseline technology for the development of very high capacity archival mass storage systems.
- There is a well-defined need within NASA, other government facilities, and in the private business sector for high-speed, high-density and cost-effective mass stores.
- The development of DIGIMEM technology should proceed in parallel with relevant systems architecture and data base management activities.
- The components and subsystems required for the implementation of a DIGIMEM archival mass storage system exists or can be engineered using existing technology.



HARRIS

ELECTRO-OPTICS

6-4

Our recommendation is for a continuing technology development program based on the DIGIMEM concept. The goal of this effort should be to bring on line in the early 1980's a fully operational archival optical mass storage system. We suggest a three phase program to begin in FY-78. A synopsis of our proposed 5-year development plan is as follows:

A. ENGINEERING PLAN

Phase I

- Engineering technology phase (1 year)
 - Data Base Management/user and technology surveys
 - Critical components evaluation
 - Trade-off and systems architecture studies
 - System definition

Phase II

- Exploratory development (2 years)
 - Design and fabrication of a brassboard model
 - Test and evaluation experiments
 - Engineering prototype specification

Phase III

- Production of an operational engineering model (2 years)
 - Final design and fabrication
 - Engineering test and evaluation
 - Delivery/integration
 - User operational test and evaluation



HARRIS

ELECTRO-OPTICS

6-5/6

B. DATA BASE MANAGEMENT SUPPORT PLAN

Phase I

- Complete investigation of end-user/facility requirements
- Perform comparative analysis/trade-off studies
- Develop data base management applications concepts and methodology

Phase II

- Design preliminary data base management application software in support of brassboard activity
- Implement preliminary software package to prove design concepts
- Complete final design specifications of prototype production software

Phase III

- Design and implement prototype production software
- Unit test
- Integrate and system test

The two part plan is consistent with our position that technology development and an end-user/data base management requirements definition be pursued in parallel. Our plan is discussed in greater detail in Volume III, "Considerations for the Development of an Archival Optical Mass Memory System."



HARRIS

ELECTRO-OPTICS

A-1/2

APPENDIX A

THE WRITE CONTROL ELECTRONICS

ORIGINAL PAGE IS
OF POOR QUALITY

D

C

B

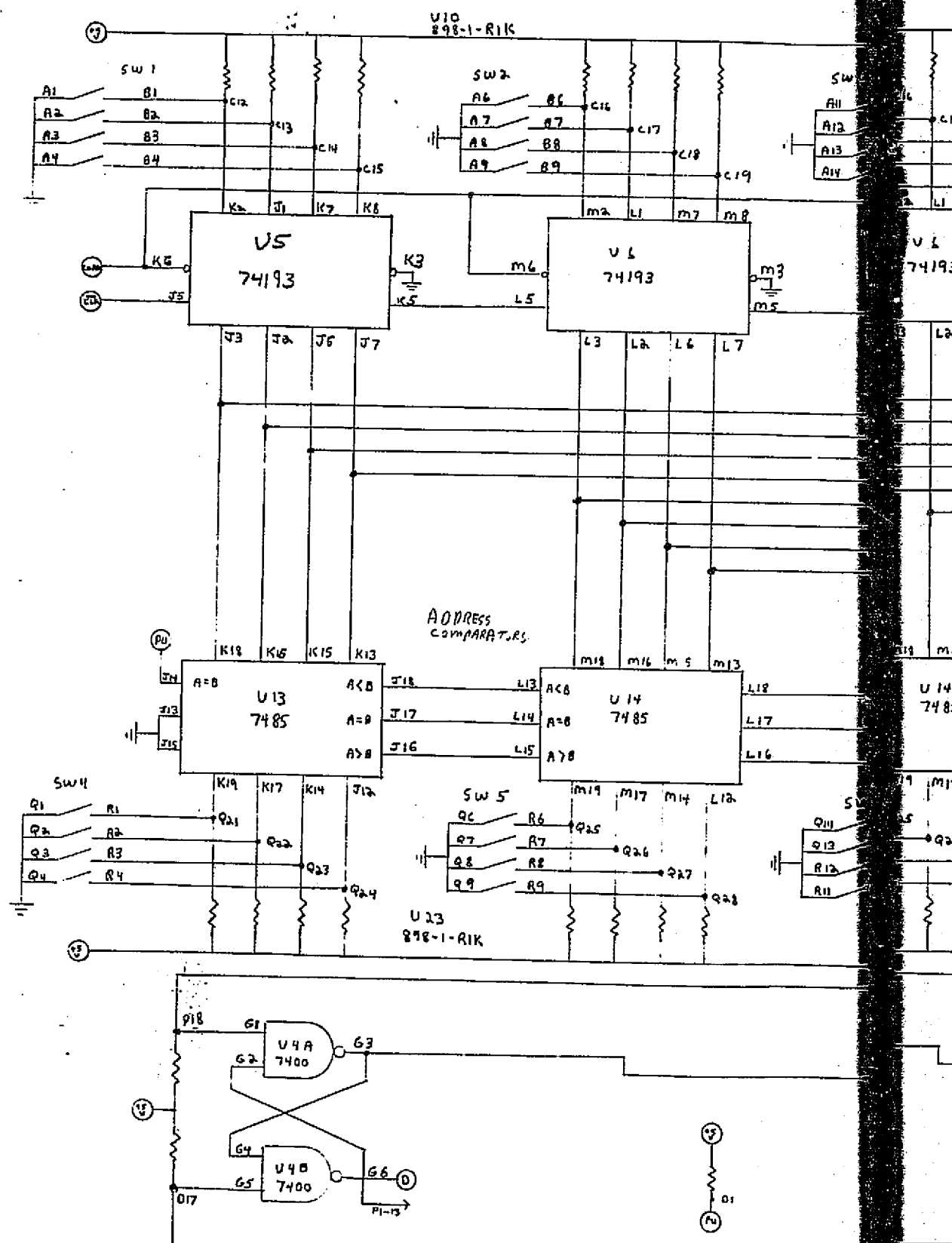
A

U & BLUE PRINT PAPER CO CLEARPRINT TONGUE

4

3

ADDRESS COUNTERS



FOLDOUT FRAME

4

3

REVISIONS						
ZONE	LTR	DESCRIPTION			DATE	APPROVED
		CHNG BY	CHK BY	ECO NO.		

COUNTERS

ORIGINAL PAGE IS
OF POOR QUALITY

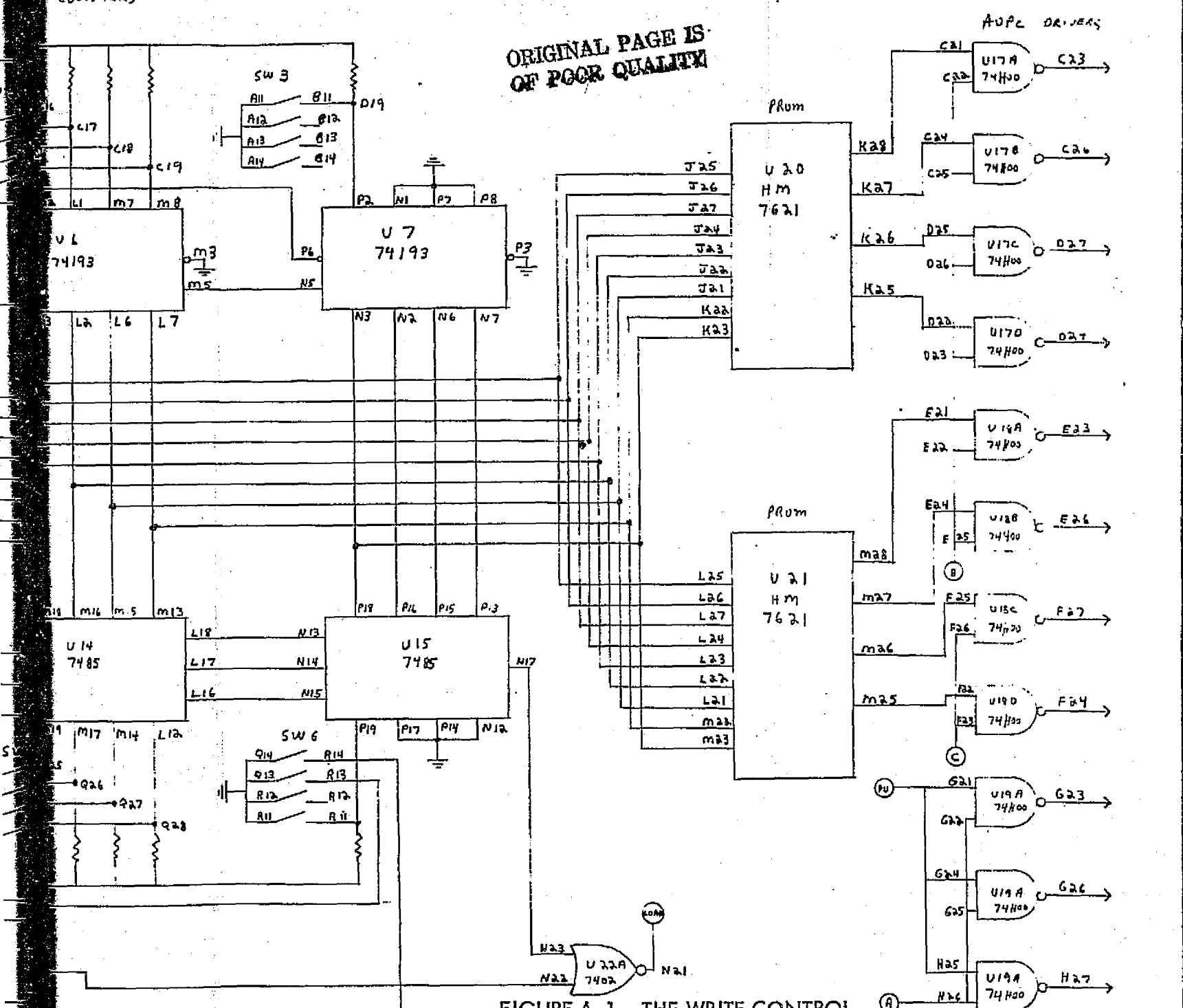



FIGURE A-1. THE WRITE CONTROL ELECTRONICS, PART 1

CONTRACT NO.		DWN BY DET		CHG BY		 HARRIS ELECTRONIC SYSTEMS DIVISION		Melbourne, Florida 32901	
DASH NO.		NEXT ASSY		USED ON		ENGINEER Gerald E. Angle		TITLE WRITE CONTROL ELECTRONICS (ADDRESS COUNTERS AND COMPARATORS, PROMS, AOPC DRIVERS)	
APPLICATION ABBREVIATIONS PER MIL-STD-12 LOGIC SYMBOLS PER MIL-STD-806 ELECTRICAL AND ELECTRONIC DIAGRAM PER USAS ELECTRONIC DIAGRAM PER USAS Y32.2 ELECTRICAL AND ELECTRONIC REFERENCE						PACKED INSTRUCTIONS Gerald E. Angle		SIZE CODE IDENT NO 91417	
APPROVAL APPROVAL						CODE IDENT NO 81		REV	
SCALE						SHEET 1 of 2			

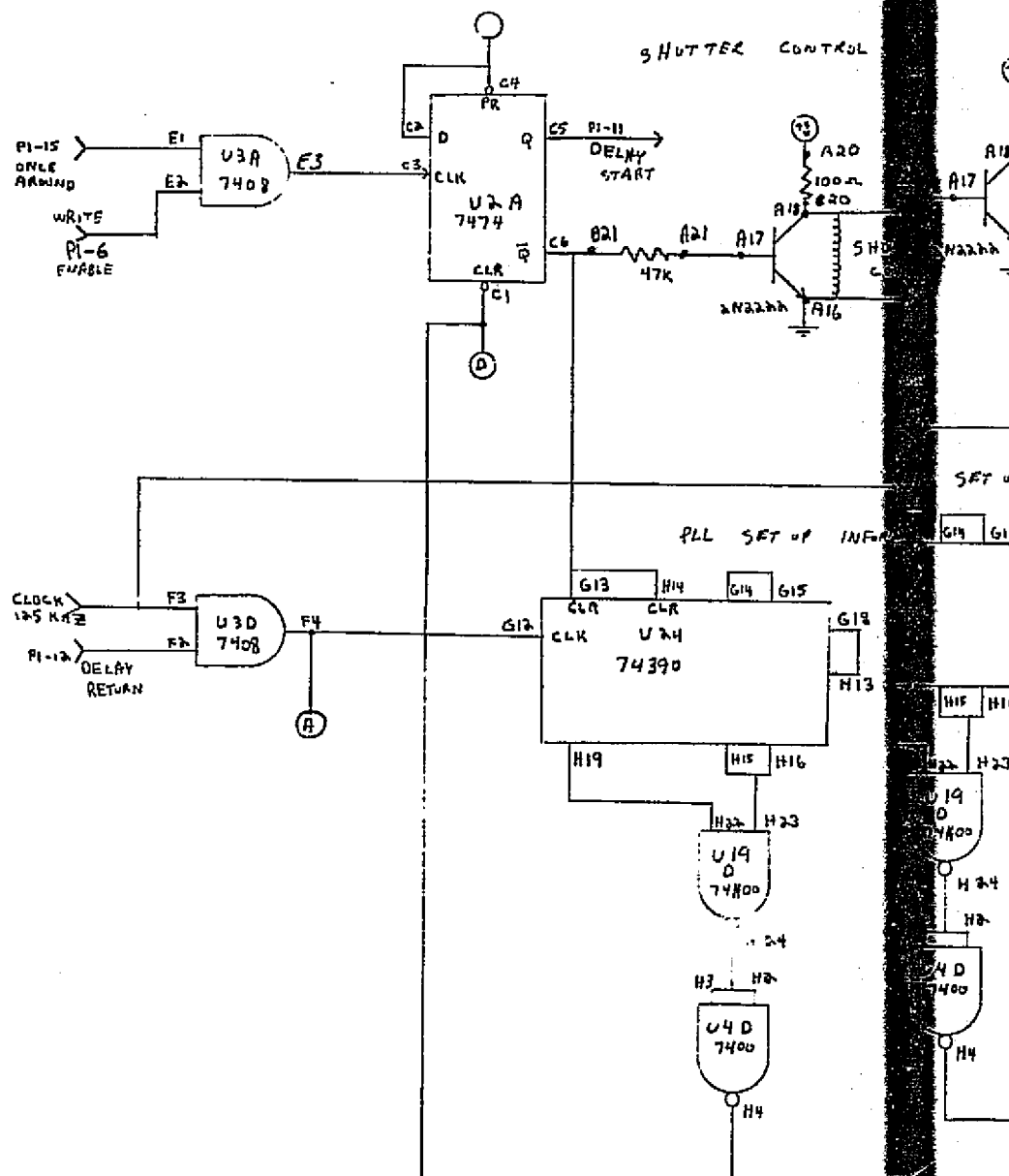
ORIGINAL PAGE IS
OF POOR QUALITY

D

C

B

A

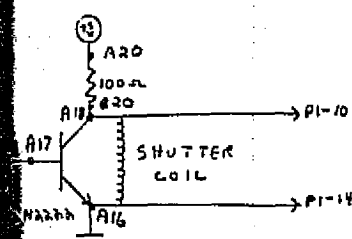


FOLDOUT FRAME

REVISIONS				
ZONE	LTR	DESCRIPTION		DATE
		CHNG BY	CHK BY	ECO NO.

ORIGINAL PAGE IS
OF POOR QUALITY

FE CONTROL



SET UP INFORMATION

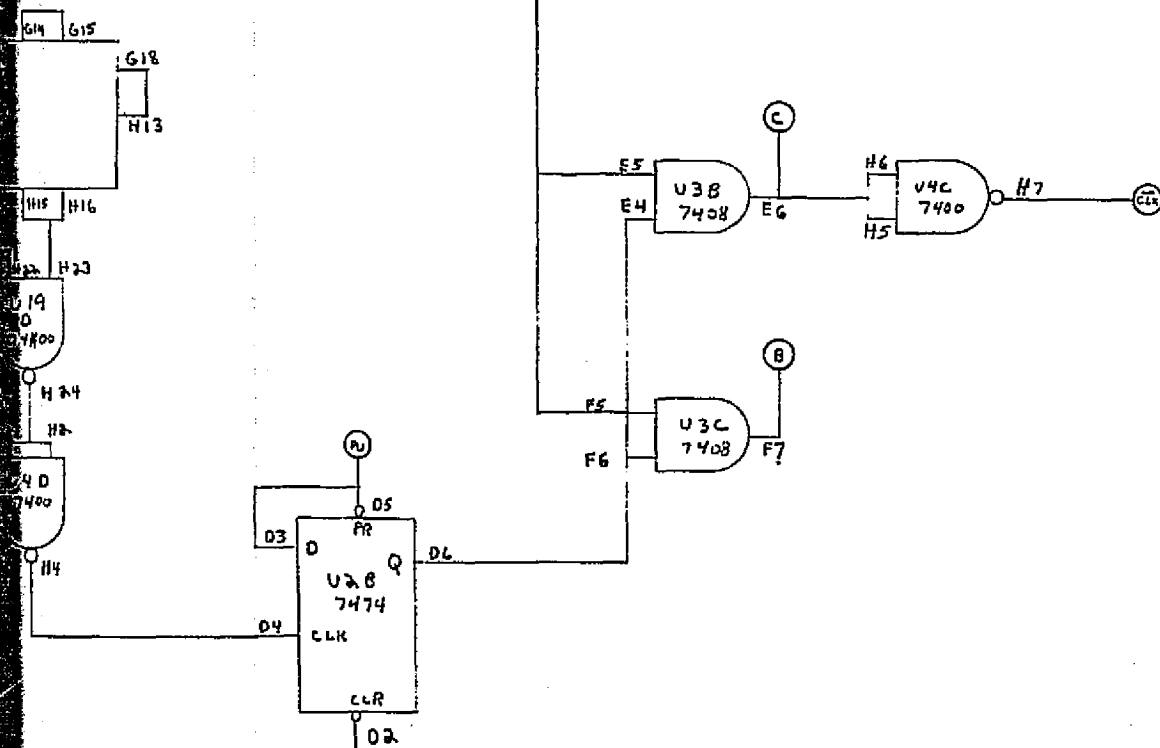
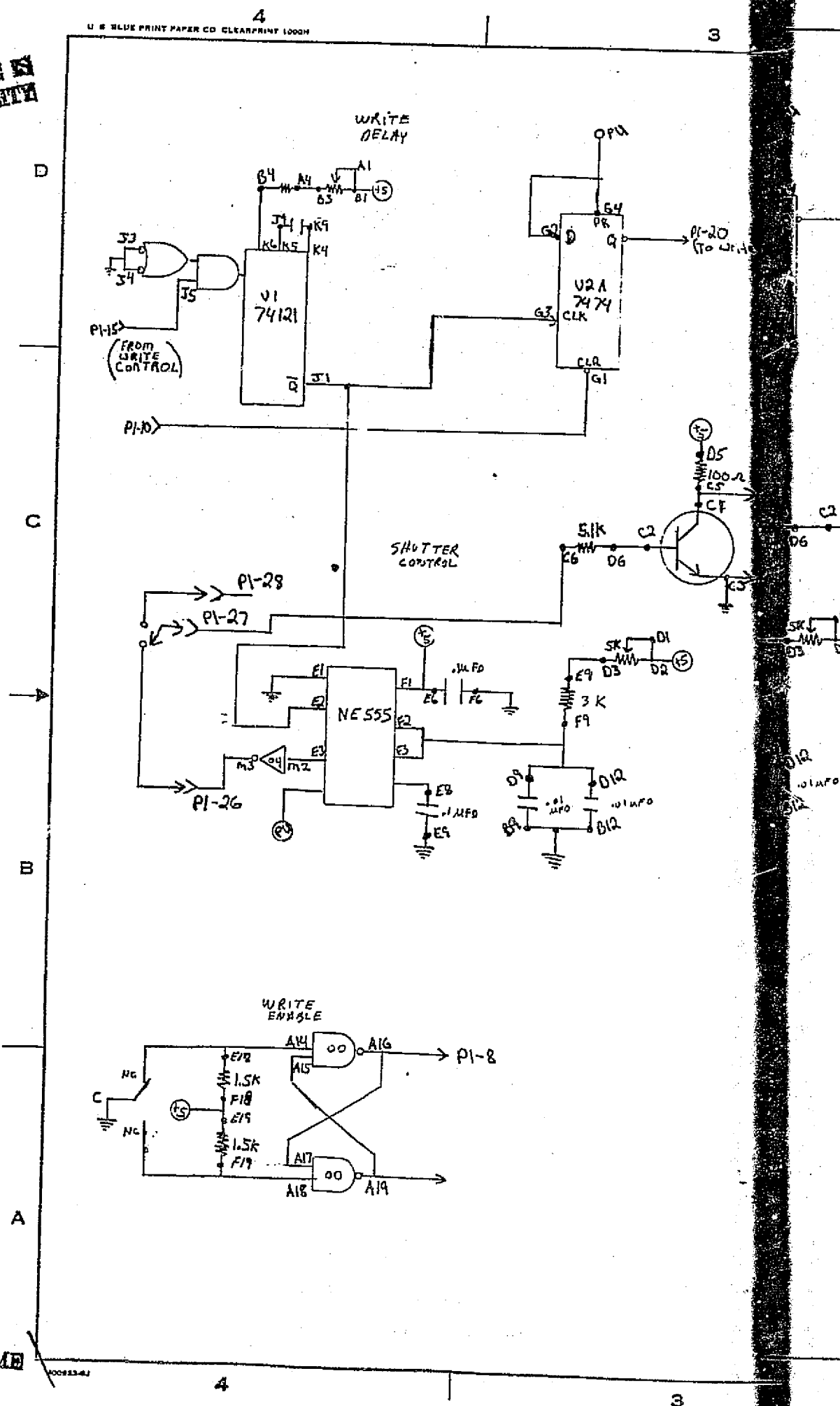


FIGURE A-2. THE WRITE CONTROL
ELECTRONICS, PART 2

FOLDOUT FRAME

CONTRACT NO.			HARRIS ELECTRONIC SYSTEMS DIVISION		Melbourne, Florida 32901	
DASH NO.			NEXT ASSY		USED ON	
APPLICATION			ENGINEER		TITLE	
ABBREVIATIONS PER MIL STD-12			DESIGNED BY		WRITE CONTROL ELECTRONICS	
LOGIC SYMBOLS PER MIL STD 806			CHECKED BY		(SHUTTER CONTROL, PHASE LOCKED LOOP)	
ELECTRICAL AND ELECTRONIC DIAGRAM PER USAS			APPROVAL		SIZE	
ELECTRONIC DIAGRAM PER USAS Y322			APPROVAL		CODE IDENT NO.	
ELECTRICAL AND ELECTRONIC REFERENCE			APPROVAL		91417	
			APPROVAL		REV	
			APPROVAL		B 1	
			APPROVAL		SHEET 2 of 2	

FOLDOUT FRAME



3

2

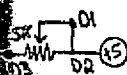
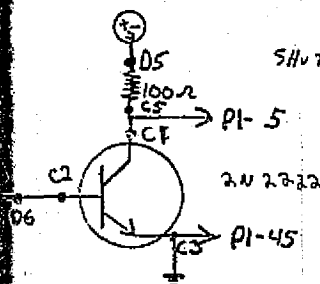
1



P1-26
(To Write Control)

ORIGINAL PAGE IS
OF POOR QUALITY

SHUTTER CONTROL



012
012AFO
012

FIGURE A-3. THE WRITE CONTROL
ELECTRONICS, PART 3

FOLDOUT FRAME

			CONTRACT NO.		HARRIS Melbourne, Florida 32901	
			DESIGNED BY M. R. J. J.		TITLE WRITE CONTROL ELECTRONICS (SHUTTER CONTROL, WRITE DELAY, WRITE ENABLE)	
			ENGINEER D. R. J. J.		SIZE 91417	
			APPROVAL D. R. J. J.		CODE IDENT NO 02	
			APPROVAL		REV	
			APPROVAL		SHEET	
			SCALE		1 OF 1	

3

2

1



HARRIS

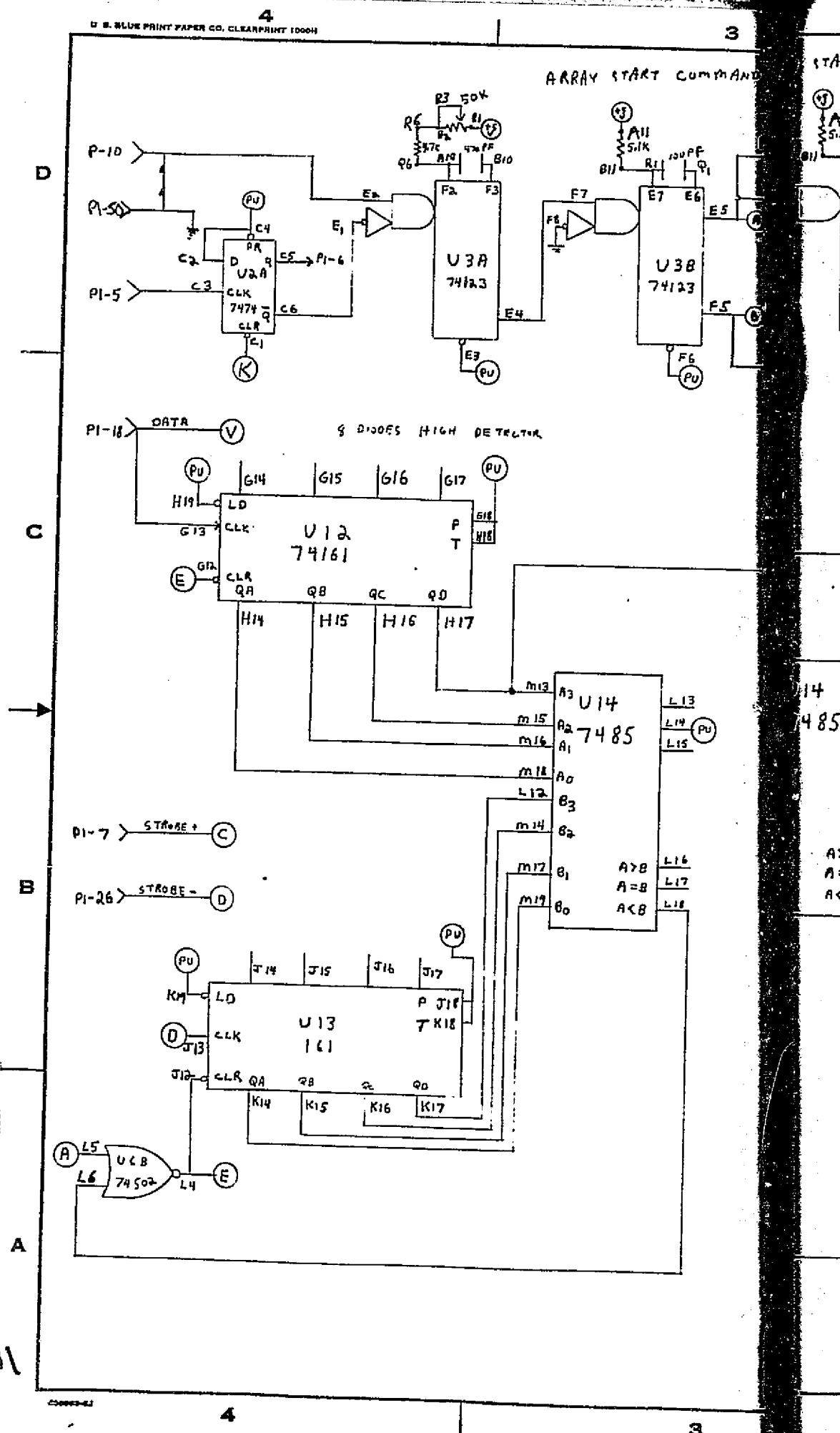
ELECTRO-OPTICS

B-1/2

APPENDIX B

THE READOUT CONTROL ELECTRONICS


~~FOUO - FRANK~~



REVISIONS

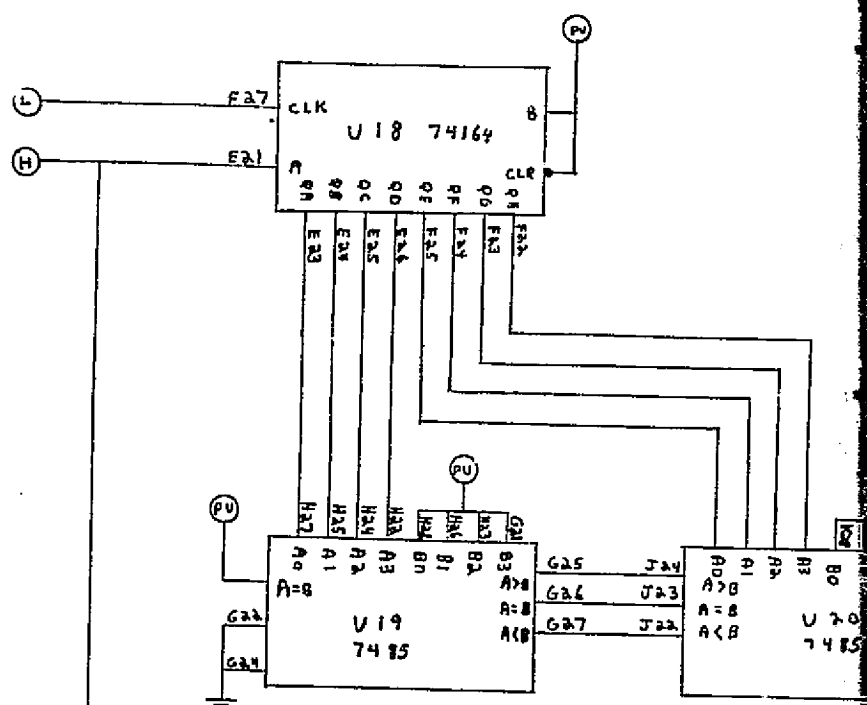
4 DIODES TO ONE BIT CONVERTER



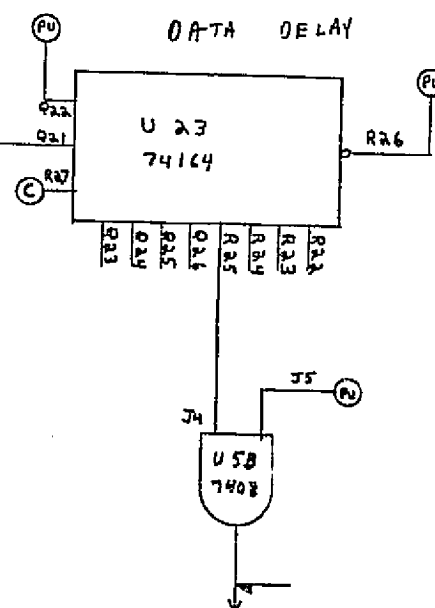
		CONTRACT NO.			HARRIS		Melbourne, Florida 32901	
		DATE 1 SEP	CHECK		ELECTRONIC SYSTEMS DIVISION			
DATE NOV	NEXT ASSY	USED ON		ENGINEER CON T E M A L B		TITLE READ CONTROL ELECTRONICS		
APPLICATION				PROJECT OFFICER <i>Paul Redden</i>		ARRAY SMART COMMAND, "8 DIODES HIGH"		
ABBREVIATIONS PER MIL-STD-12				APPROVAL		SIZE		CODE IDENT NO.
LOGIC SYMBOLS PER MIL-STD-806						91417		AI
ELECTRICAL AND ELECTRONIC DIAGRAM PER USAS								REV
ELECTRONIC DIAGRAM PER USAS Y32.2				APPROVAL		SCALE		SHEET 1 OF 2
ELECTRICAL AND ELECTRONIC REFERENCE								

ORIGINAL PAGE IS
OF POOR QUALITY

START PATTERN DETECTOR

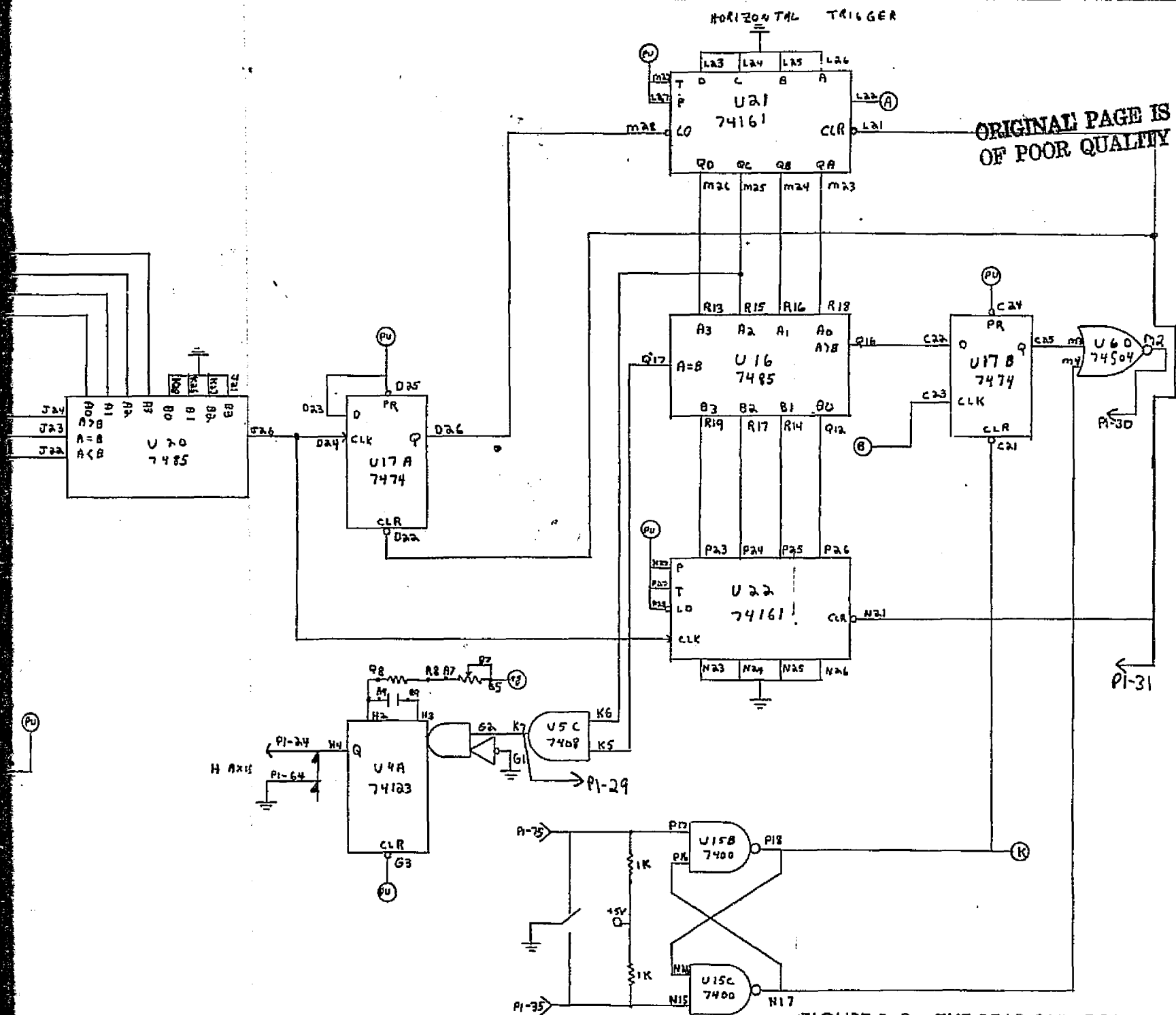


DATA DELAY



FOLDOUT FRAME

REVISIONS					
ZONE	LTR	DESCRIPTION			DATE
		CHG BY	CHK BY	ECO NO.	

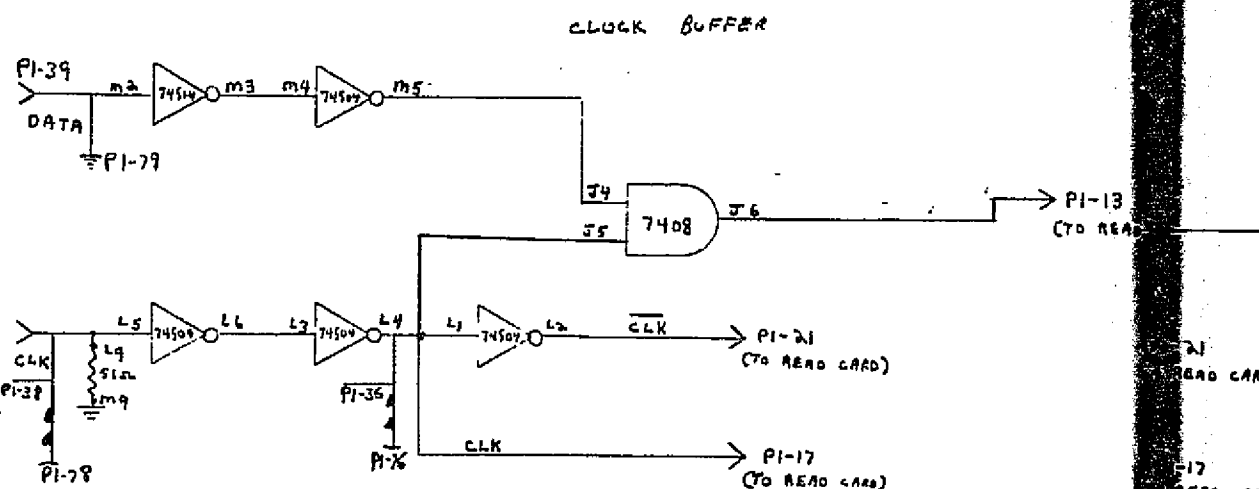


FOLDOUT FRAME 2

FIGURE B-2. THE READOUT CONTROL ELECTRONICS, PART 2

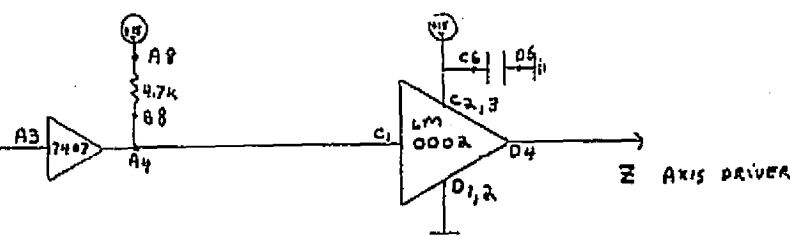
CONTRACT NO.		HARRIS		Melbourne, Florida 32901	
DES BY		CHK BY			
DATE		DATE			
DASH NO.		NEXT ASSY		USED ON	
APPLICATION		TITLE		READ CONTROL ELECTRONICS	
ABBREVIATIONS PER MIL-STD-12		SIZE		CODE IDENT NO	
LOGIC SYMBOLS PER MIL-STD-806		91417		A-1	
ELECTRICAL AND ELECTRONIC DIAGRAM PER USAS		SCALE		REV	
ELECTRONIC DIAGRAM PER USAS Y32.2		SHEET 2 OF 2			
ELECTRICAL AND ELECTRONIC REFERENCE					

MULDOUT FRAME



REVISIONS						
ZONE	LTR	DESCRIPTION			DATE	APPROVED
		CHNG BY	CHE BY	ECO NO.		

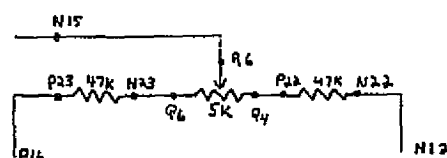
ORIGINAL PAGE IS
OF POOR QUALITY



PI-13
(TO READ CARD)

PI-17
(READ CARD)

PI-17
(READ CARD)



OFFSET NETWORK FOR V AXIS
FOR PLACEMENT SEE BELOW

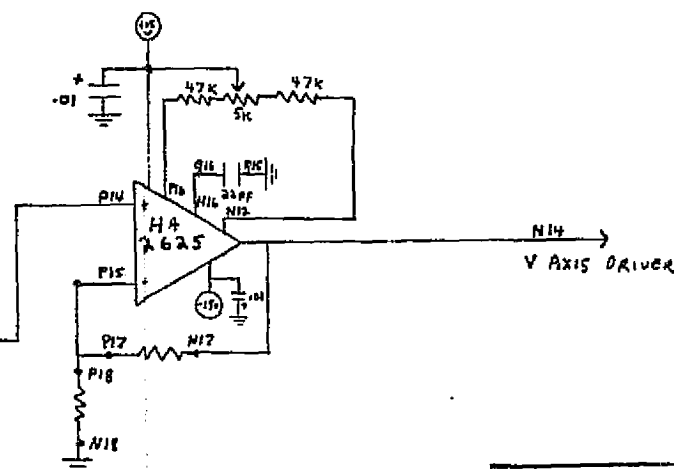


FIGURE B-3. THE READOUT CONTROL
ELECTRONICS, PART 3

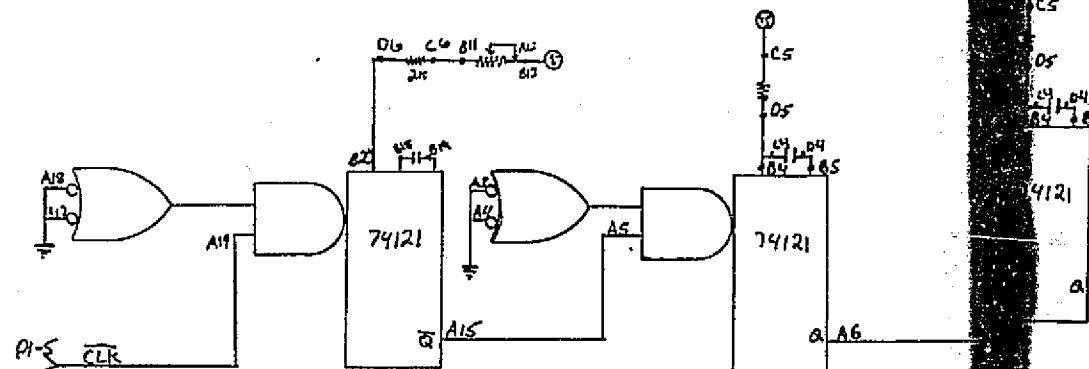
COLDOUT **FIG. A-11** **2**

CONTRACT NO.		HARRIS ELECTRONIC SYSTEMS DIVISION Melbourne, Florida 32901	
DES BY		CHK BY	
ENGINEER SM - 4046		TITLE READ CONTROL ELECTRONICS (D/A CARD AND DRIVERS; CLOCK BUFFER)	
APPROVAL		SIZE	CODE IDENT NO.
APPROVAL		91417	A2
APPROVAL		SCALE	SHEET 1 of 1

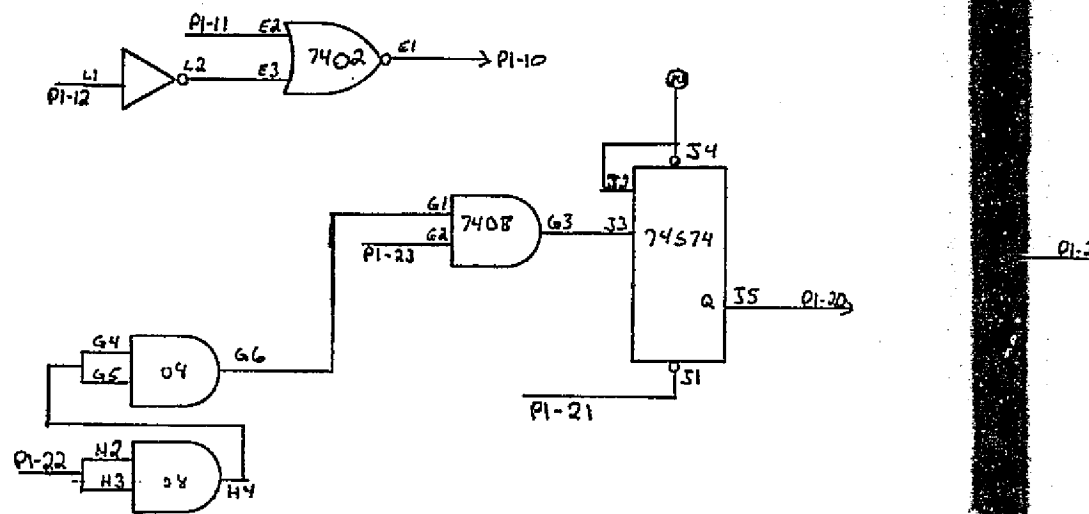
APPLICATION
ABBREVIATIONS PER MIL-STD-12
LOGIC SYMBOLS PER MIL-STD-806
ELECTRICAL AND ELECTRONIC DIAGRAM PER USAS
ELECTRONIC DIAGRAM PER USAS Y32.2
ELECTRICAL AND ELECTRONIC REFERENCE

ORIGINAL PAGE IS
OF POOR QUALITY

D

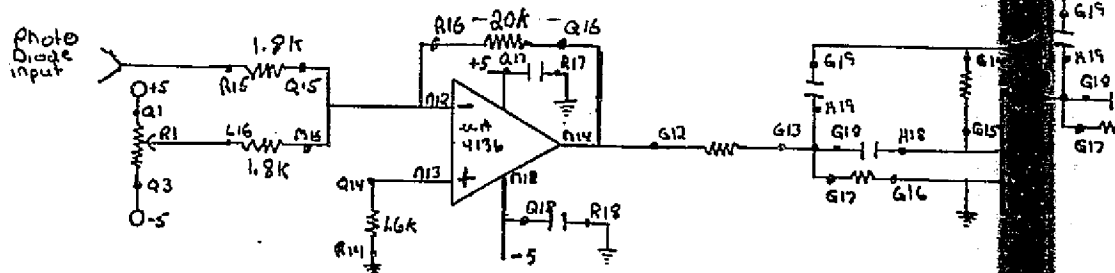


C



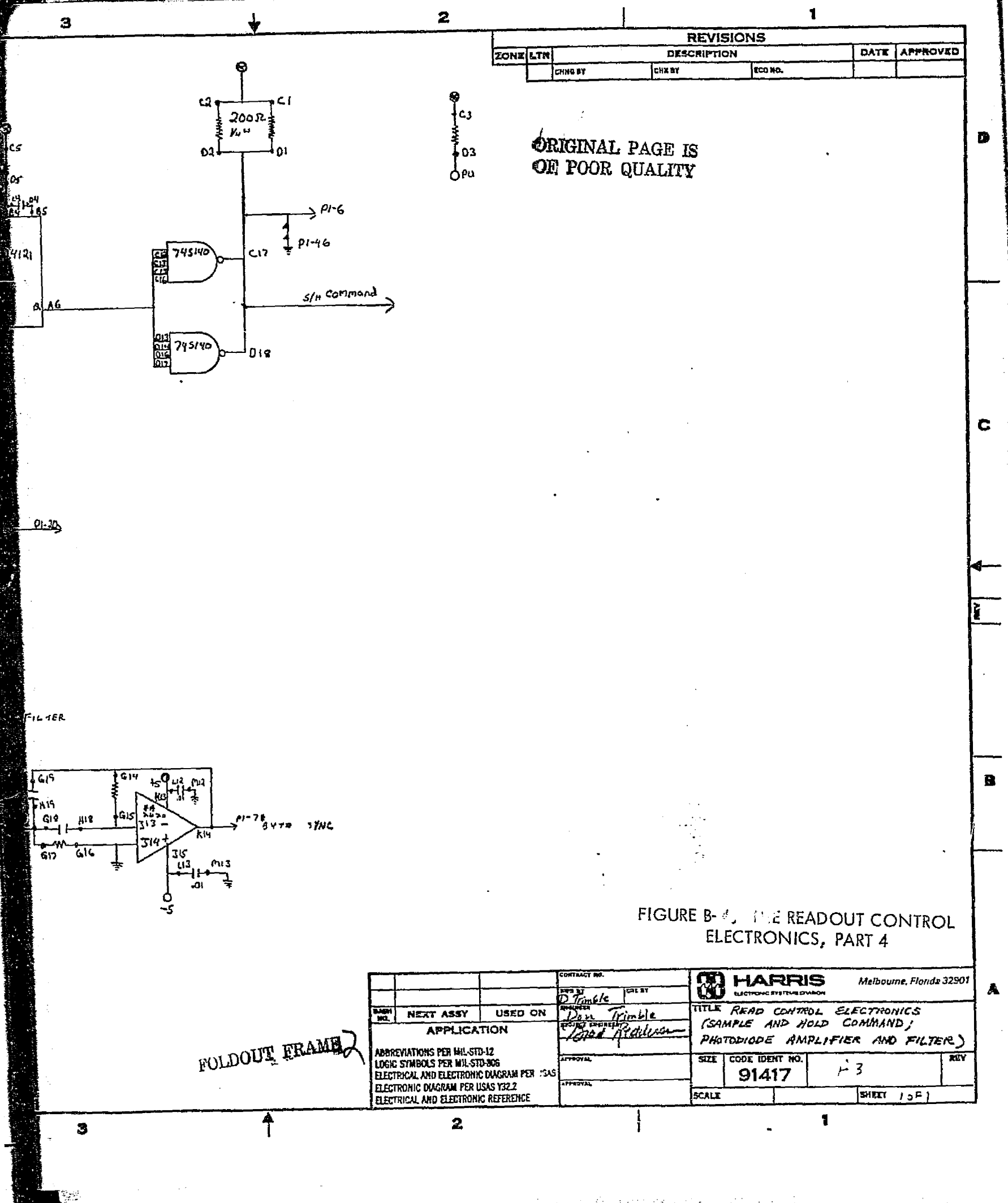
B

PHOTO DIODE AMPLIFIER AND FILTER



A

FOLDOUT FRAME



REVISIONS				
ZONE	LTN	DESCRIPTION	DATE	APPROVED
CHNG BY	CHK BY	ECO NO.		

FIGURE B-4. THE READOUT CONTROL ELECTRONICS, PART 4

CONTRACT NO.		HARRIS ELECTRONIC SYSTEMS DIVISION Melbourne, Florida 32901	
DES BY <i>D. Trimble</i>	CHK BY	TITLE READ CONTROL ELECTRONICS (SAMPLE AND HOLD COMMAND; PHOTODIODE AMPLIFIER AND FILTER)	
DESIGNED BY <i>Don Trimble</i>	TESTED BY <i>John Anderson</i>	SIZE	CODE IDENT NO. 91417
APPROVAL	APPROVAL	SCALE	SHEET 1 of 1

FOLDOUT FRAME